

# Covalent Functionalization of Silicon Nitride Surfaces for Anti-biofouling and Bioselective Capture

## **Thesis committee**

### **Thesis supervisors**

Prof. dr. C. J. M. van Rijn

Professor of Microsystem and NanoTechnology for Agrofood and Health  
Wageningen University

Prof. dr. J. T. Zuilhof

Professor of Organic Chemistry  
Wageningen University

### **Thesis co-supervisor**

Dr. ir. J. M. J. Paulusse

External staff member, Laboratory of Organic Chemistry  
Wageningen University

### **Other members**

Prof. dr. E. F. Leonard

Columbia University, New York, USA

Prof. dr. W. T. S. Huck

Radboud University, Nijmegen, The Netherlands

Prof. dr. ir. R. G. H. Lammertink

University of Twente, The Netherlands

Prof. dr. ir. R. M. Boom

Wageningen University, The Netherlands

This research was conducted under the auspices of the graduate school VLAG



# Covalent Functionalization of Silicon Nitride Surfaces for Anti-biofouling and Bioselective Capture

Nguyễn Thúy Ái

## **Thesis**

submitted in fulfillment of the requirements for the degree of doctor  
at Wageningen University

by the authority of the Rector Magnificus

Prof.dr. M. J. Kropff,

in the presence of the

Thesis Committee appointed by the Academic Board

to be defended in public

on Tuesday 4 October 2011

at 11 a.m. in the Aula.

Nguyễn Thúy Ái

Covalent Functionalization of Silicon Nitride Surfaces for Anti-biofouling and  
Bioselective Capture

Thesis, Wageningen University, Wageningen, The Netherlands (2011)

With references, with summaries in English, Dutch and Vietnamese

ISBN: 978-94-6173-008-4

*To those who dare to dream, all doors are open.  
For my family and for Jacob*



## Contents

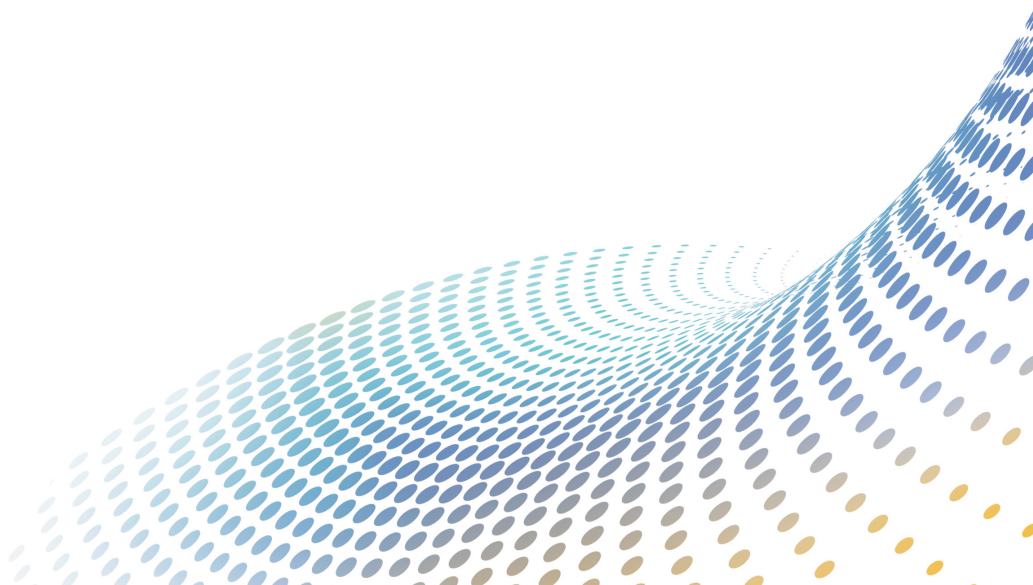
<b>Chapter 1</b>	General Introduction .....	1
<b>Chapter 2</b>	Protein-Repellent Silicon Nitride Surfaces:..... UV-Induced Formation of Oligo(ethylene oxide) Monolayers	23
<b>Chapter 3</b>	Stable Protein-Repellent Zwitterionic Polymer Brushes ..... Grafted from Silicon Nitride	45
<b>Chapter 4</b>	Rapid Microsieve-Based Microbial Diagnostics .....	65
<b>Chapter 5</b>	Bioconjugation of Protein-Repellent Zwitterionic Polymer ..... Brushes Grafted from Silicon Nitride	85
<b>Chapter 6</b>	General Discussion.....	105
<b>Appendices</b>	.....	113
<b>Summary</b>	.....	127
<b>Samenvatting</b>	.....	129
<b>Tóm tắt</b>	.....	131
<b>Curriculum Vitae</b>	.....	133
<b>List of Publications</b>	.....	135
<b>Overview of Completed Training Activities</b>	.....	137
<b>Acknowledgment</b>	.....	139





## General Introduction

The aim of this thesis is to develop adequate covalent functionalization techniques for silicon nitride surfaces, in particular for silicon nitride microsieves to be applied in analytical microfluidic systems. Approaches to minimize fouling issues in membrane microfiltration, as well as the selective capture of microorganisms in diagnostics are discussed.



## Surfaces Phenomena in Microdevices

Miniaturization of microfluidic systems and components holds a great promise for advanced analysis techniques. The main reason is that this allows numerous experiments to be performed rapidly and in parallel, while requiring only small sample volumes and minimal consumption of reagents at the same time. When scaling down system dimensions the surface-to-bulk ratio will increase, hence surface effects – such as viscous friction, capillary forces and diffusion – will become more pertinent and will increasingly dominate performance.<sup>1</sup> Control of surface chemistry properties, such as hydrophilicity, hydrophobicity and protein repellence therefore become more important. For example, to enter a 1 micron-sized hydrophobic capillary water needs to be supplied at a typical pressure of ~3 bar, whereas 300 bar is needed for an analogous 10-nm capillary. Surface phenomena are therefore the critical matter in operation of microdevices.<sup>2</sup>

The importance of surfaces in miniature systems has resulted in enormous exploration of methods that can regulate surface characteristics, in order to improve the performance of devices as well as to minimize problems that derive from interfacial interactions between surfaces and materials.<sup>3</sup> Particularly, minimization of biofouling of fluidic components plays a crucial role in microfluidic devices. Fouling changes surface properties and at a further stage might even clog the small microfluidic channels itself. A number of approaches to tailor functionality of the surface for anti-biofouling and biorecognition to improve the performance of microfluidic components have been presented.<sup>4-7</sup>

This chapter discusses biofouling issues on the surface of specific silicon nitride micro-engineered membranes. Recent approaches to tailor the functionality of the device surfaces for anti-biofouling and biorecognition are presented.

## Silicon Nitride Surfaces

Silicon nitride ( $\text{Si}_3\text{N}_4$ ) is an important structural material in micro-electro-mechanical systems (MEMS) technology.<sup>8, 9</sup> The material offers many outstanding features, such as superior mechanical strength, wear resistance, chemical inertness in acidic and alkaline media, biocompatibility and micromachining reliability.<sup>8-11</sup> It is often used as an insulator and chemical barrier in the manufacturing of integrated circuits.<sup>12</sup> Silicon nitride thin films are typically formed by chemical vapor deposition (CVD),<sup>13</sup> or one of its variants: low pressure chemical vapor deposition (LPCVD)<sup>14, 15</sup> or plasma-enhanced chemical vapor deposition (PECVD).<sup>11, 16-18</sup> Stoichiometric silicon nitride ( $\text{Si}_3\text{N}_4$ ) films are excellent insulators, displaying extreme physical and chemical resistance. However, a thick layer (> 500 nm) of this stoichiometric configuration of  $\text{Si}_3\text{N}_4$  may contain excess surface



stress, which negatively affects its micromechanical properties.<sup>19</sup> Alternatively, silicon-rich silicon nitride coatings ( $\text{Si}_x\text{N}_4$ ,  $x > 3$ ), with an amorphous structure, exhibit very low residual stresses and form homogeneous layers.<sup>11, 18</sup> Long cantilevers for atomic force microscopy,<sup>20, 21</sup> and large free-standing membranes<sup>11, 22-25</sup> are often made of thin silicon-rich silicon nitride films thanks to the possibility to construct extreme aspect ratio structures.

## Microsieves – Micro-Engineered Membranes

Membranes are indispensable elements in nature as well as in today's modern industrial society. Membrane technology has developed since the 18<sup>th</sup> century in many aspects of daily life and scientific research.<sup>26, 27</sup> Nowadays, membranes play a key factor in many fields, particularly in water treatment, chemical purification, gas separation, medical devices (artificial organs, drug delivery, tissue engineering), and food processing (beer clarification and milk filtration).<sup>26-30</sup> Membrane technology has evolved and expanded drastically over the last decades. Various types of membranes are now commercially available and widely used for microfiltration and ultrafiltration on the industrial scale. However, their applications are limited by intrinsic characteristics of the membrane materials used. For instance, the use of polymeric membranes is often restricted by their limited chemical resistance and inferior thermal stability. Moreover, they are easily damaged at high pressures.<sup>30</sup> Ceramic membranes have proven more advantageous, owing to their high chemical resistance, in combination with their high thermal stability. However, they are not extensively used due to high production cost and relatively poor control over pore-size distribution.<sup>31</sup>

In 1994, a novel micro-engineered membrane (microsieve) was introduced in microfiltration technology. The microsieve is a new generation of advanced inorganic membranes fabricated by photolithography and silicon micromachining technology.<sup>22-24</sup> These membranes are made of a thin layer of silicon-rich silicon nitride, deposited by LPCVD, with thicknesses ranging from 100-1000 nm. The microsieve has a very well-defined pore size and shape, and an extremely homogeneous pore-size distribution with high porosity (Figure 1). The microsieve inherits the outstanding features of silicon nitride, such as high thermal stability, chemical inertness, and mechanical strength. In comparison with other types of membranes, a  $\text{Si}_x\text{N}_4$ -based microsieve fulfills most of the critical requirements of microfiltration membranes such as high porosity, well-defined, uniformly distributed pores, and a thin membrane layer, as well as chemical resistance.<sup>23-25</sup> As a result, microsieves have the ideal combination of high flux performance with low trans-membrane pressure and excellent size-selectivity (Figure 2).<sup>25, 32-34</sup>

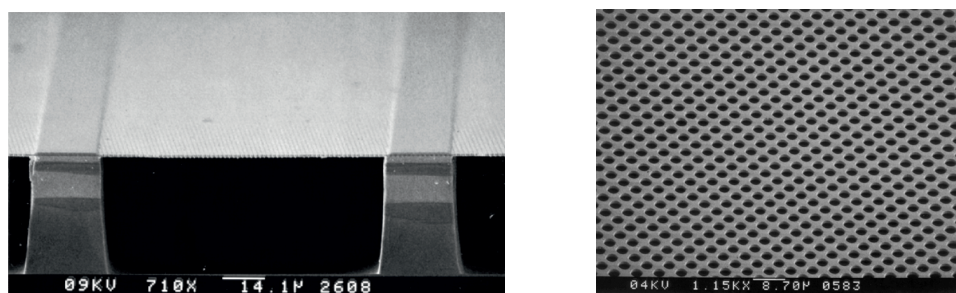


**Figure 1.** SEM images of a cross-section of a microsieve, showing the freestanding membrane on silicon supports (left); top-view showing the homogenous pore size and high porosity (right).<sup>34</sup>

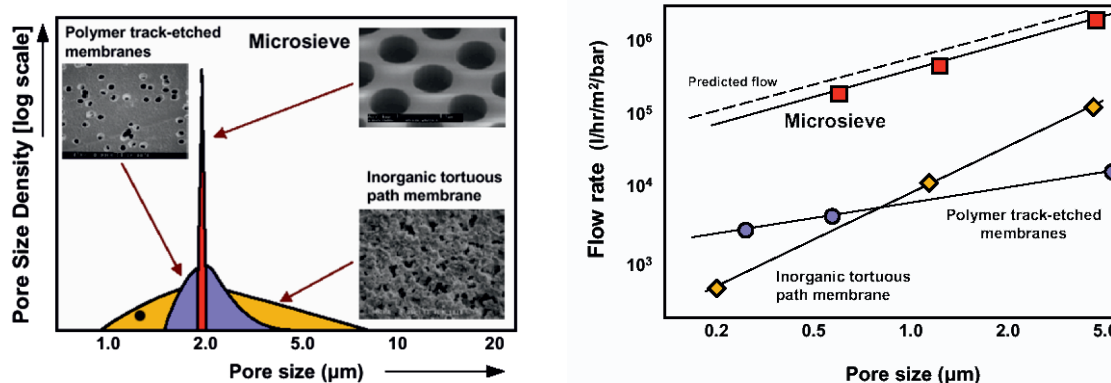


**Figure 2.** Pore-size distribution (left) and clear water flux of various microfiltration membrane filters (right).<sup>35</sup>

## Biofouling in Microfiltration

As any other conventional membrane, microsieves also face fouling issues, keeping them from being used to their full potential. Fouling is the deposition of retained foulants such as particles, cells, colloids, macromolecules or proteins at the membrane surface or inside the pores on the pore walls. The aggregation of these foulants leads to the formation of a cake layer on top of the membrane surface, blocking the passage of smaller elements (Figure 3).<sup>6</sup> Consequently, adsorption of these foulants, especially proteins and cells, initiates surface contamination, and facilitates microorganism growth. As a result, the permeability is diminished either temporarily or permanently, thereby dramatically affecting the overall performance of the filtration process. Fouling is one of the main problems in membrane filtration processes – both technically and economically – as it causes an increase in membrane resistance, affecting the filtration process both qualitatively, as well as quantitatively. This leads to high energy demands and process interruption. Antifouling is therefore of critical importance to maintain the efficiency of membrane filtration. Hence, it has been a subject of many academic studies<sup>6, 36-38</sup> and industrial research projects.

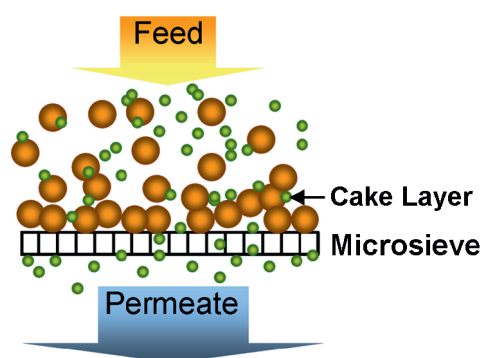


**Figure 3.** Cake-layer formation during microfiltration.

Approaches to prevent fouling of membranes vary from mechanical methods (applying an external force to remove the cake layer),<sup>37, 39, 40</sup> via biological methods (using bacteriophages or enzymes to disrupt the biofilm)<sup>41</sup> to chemical methods (using chemicals such as acids, bases or surfactants to clean the membrane surface).<sup>42</sup> The most commonly employed method is the use of mechanical forces, which are applied either continuously or periodically onto membrane surfaces during the filtration process. Several prevailing techniques are cross-flow,<sup>34, 39, 43</sup> vibratory filtration,<sup>37, 44-48</sup> back-pulse,<sup>40, 49</sup> sonic irradiation<sup>50, 51</sup> or a combination of these techniques.

However, applying external forces only removes the reversible fouling layer from the membrane surface. In the case that a membrane becomes permanently fouled, application of external forces typically does not restore the initial flux, i.e., the foulants bind irreversibly to the membrane surface. In order to minimize permanent fouling, modification of the membrane surface is considered a feasible approach to minimize or even eliminate fouling issues. Coatings that repel biological substances, such as cells and proteins, from membrane surfaces have been studied extensively over the past couple of decades. Proposed biorepelling coatings range from inorganic materials, e.g., photocatalytic antibacterial/antiviral  $\text{TiO}_2$ <sup>52</sup> and  $\text{Ag}$ <sup>53</sup> particles, to polymeric coatings, such as poly(ethylene glycol)<sup>54</sup> and zwitterionic polymers.<sup>6, 36, 38</sup>

### Coatings to Prevent Biofouling

Organic coatings to prevent biofouling of surfaces have been explored for several decades.<sup>6, 38</sup> Self-assembled organic monolayers of oligo(ethylene oxide) immobilized on gold surfaces via alkanethiols, reported by Whitesides and co-workers in 1991,<sup>55</sup> brought about a number of fundamental studies on coatings for preventing biofouling.<sup>38, 56</sup> The understanding of the mechanism of protein adsorption on solid surfaces and the principles of good antifouling coatings was deepened by many simulation studies on the behavior of these coatings in solution.<sup>57-62</sup> The exploration of protein-repellent monolayers has

covered many aspects, such as chemical composition,<sup>63</sup> density,<sup>64</sup> stability,<sup>65, 66</sup> thickness of the coatings<sup>67</sup> on substrates such as gold,<sup>68-70</sup> glass<sup>71</sup> and semiconductor materials.<sup>72, 73</sup> Complex media and actual biological samples were used to challenge their performance, showing the potential of these coatings for their practical application.<sup>74-76</sup>

The adsorption of proteins onto solid surfaces depends on the interfacial energy between the surface and the aqueous medium.<sup>77, 78</sup> The principle of anti-biofouling coatings is based on reducing interfacial energies with water, and weakening intermolecular interactions with biomolecules.<sup>38</sup> In terms of interfacial energy, proteins adsorb more readily onto hydrophobic surfaces – characterized by low surface energies – than on hydrophilic surface, as this adsorption process reduces the interfacial energy between the hydrophobic surface and water. Such adsorbed biomolecules are easily removed from the surface by external forces (e.g., high-energy water jet<sup>79</sup> or cleaning) owing to the low surface energy. Hence, hydrophobic surfaces, for instance polydimethylsiloxane (PDMS) and polytetrafluoroethylene (PTFE), are known as good fouling-release surfaces. In comparison, hydrophilic surfaces with high surface energies display only low interfacial energies with water, and as a result it is not favorable for proteins, which are amphiphilic, to adsorb onto the surface, resulting in protein-repelling behavior. The relationship between the substrates with different surface tensions and their degree of biofouling retention is described in Figure 4.

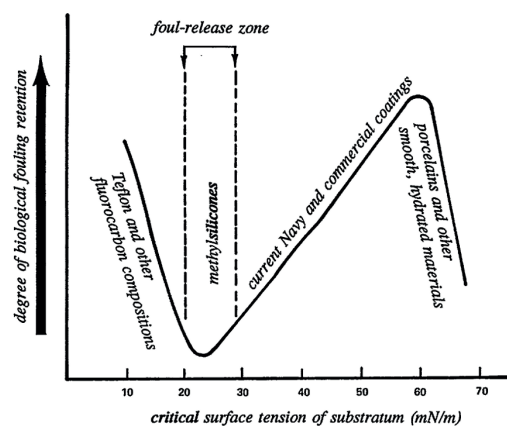


**Figure 4.** A descriptive plot of the generally observed strength of biological adhesion to substrates of different initial critical surface tensions.<sup>77</sup>

Whitesides and coworkers defined four general criteria for protein-repellent surfaces; such surfaces are (i) hydrophilic, (ii) electrically neutral, (iii) hydrogen bond acceptors, and (iv) not hydrogen bond donors.<sup>59</sup> Later it was hypothesized that molecules, which are excluded from the protein-water interface (kosmotropes) affect the repellence of proteins from surfaces to which they are attached.<sup>80</sup> Thus, protein-repellent surfaces often contain polar groups, such as ethylene oxides or zwitterions (Table 1).

**Table 1.** Common protein-resistant monolayers and their related kosmotropes.<sup>80</sup>

Protein-resistant monolayer	Structurally similar kosmotrope	
	Name	Molecular formula
HS(CH <sub>2</sub> ) <sub>11</sub> (EG) <sub>6</sub> OH	PEG	HO(CH <sub>2</sub> CH <sub>2</sub> O) <sub>n</sub> H
HS(CH <sub>2</sub> ) <sub>11</sub> O(Man)	Mannitol	HOCH <sub>2</sub> (CH(OH)) <sub>4</sub> CH <sub>2</sub> OH
HS(CH <sub>2</sub> ) <sub>10</sub> C(O)N(CH <sub>3</sub> )CH <sub>2</sub> (CH(OCH <sub>3</sub> )) <sub>4</sub> CH <sub>2</sub> OCH <sub>3</sub>		
HS(CH <sub>2</sub> ) <sub>11</sub> N(CH <sub>3</sub> ) <sub>3</sub> <sup>+</sup> Cl <sup>-</sup> /HS(CH <sub>2</sub> ) <sub>11</sub> SO <sub>3</sub> <sup>-</sup> Na <sup>+</sup> (1:1)	Taurine	H <sub>3</sub> N <sup>+</sup> (CH <sub>2</sub> ) <sub>2</sub> SO <sub>3</sub> <sup>-</sup>
HS(CH <sub>2</sub> ) <sub>11</sub> N(CH <sub>3</sub> ) <sub>2</sub> <sup>+</sup> CH <sub>2</sub> CH <sub>2</sub> SO <sub>3</sub> <sup>-</sup>	Taurine	H <sub>3</sub> N <sup>+</sup> (CH <sub>2</sub> ) <sub>2</sub> SO <sub>3</sub> <sup>-</sup>
HS(CH <sub>2</sub> ) <sub>15</sub> C(O)Pip(Nac)	DMA	CH <sub>3</sub> C(O)N(CH <sub>3</sub> ) <sub>2</sub>
HS(CH <sub>2</sub> ) <sub>11</sub> N(CH <sub>3</sub> ) <sub>2</sub> <sup>+</sup> CH <sub>2</sub> CO <sub>2</sub> <sup>-</sup>	Betaine	(CH <sub>3</sub> ) <sub>3</sub> N <sup>+</sup> CH <sub>2</sub> CO <sub>2</sub> <sup>-</sup>
HS(CH <sub>2</sub> ) <sub>11</sub> O(Malt)	Maltose	Glc-α(1,4)-Glc
HS(CH <sub>2</sub> ) <sub>15</sub> C(O)N(CH <sub>3</sub> )CH <sub>2</sub> C(O)) <sub>3</sub> N(CH <sub>3</sub> ) <sub>2</sub>	DMA	CH <sub>3</sub> C(O)N(CH <sub>3</sub> ) <sub>2</sub>
HS(CH <sub>2</sub> ) <sub>11</sub> N(CH <sub>3</sub> ) <sub>2</sub> <sup>+</sup> CH <sub>2</sub> CH <sub>2</sub> CH <sub>2</sub> SO <sub>3</sub> <sup>-</sup>	Taurine	H <sub>3</sub> N <sup>+</sup> (CH <sub>2</sub> ) <sub>2</sub> SO <sub>3</sub> <sup>-</sup>
HS(CH <sub>2</sub> ) <sub>10</sub> C(O)N(CH <sub>3</sub> )CH <sub>2</sub> CH <sub>2</sub> N(CH <sub>3</sub> )P(O)(N(CH <sub>3</sub> ) <sub>2</sub> ) <sub>2</sub>	HMPA	O=P(N(CH <sub>3</sub> ) <sub>2</sub> ) <sub>3</sub>
HS(CH <sub>2</sub> ) <sub>11</sub> (S(O)CH <sub>2</sub> CH <sub>2</sub> CH <sub>2</sub> ) <sub>3</sub> S(O)CH <sub>3</sub>	DMSO	O=S(CH <sub>3</sub> ) <sub>2</sub>

Antifouling coatings in microfiltration mainly target hydrophilic surfaces, because these surfaces not only prevent the initial attachment of the fouling organisms, but also improve the wettability of the membrane surface in the early stages of the filtration process.

Poly- and oligo(ethylene oxide) have been widely employed for several decades to reduce nonspecific binding of proteins.<sup>57, 65, 67, 81</sup> A hydration layer is formed surrounding the ethylene oxide chains as a result of hydrogen bonding between water molecules and ether moieties.<sup>82</sup> This hydration layer at the interface contributes greatly to the reduction of the interfacial surface energy with water, thereby reducing interactions between proteins and the surface.<sup>62</sup> Protein resistance of poly- or oligo(ethylene oxide) coated to various substrates was demonstrated by experimental studies<sup>64, 67, 81, 83-87</sup> and corroborated by simulations.<sup>61, 62</sup>

However, Qin *et al.* recently reported the auto-oxidation of ethylene oxide chains upon prolonged exposure in aqueous solution, resulting in cleavage of ethylene oxide units and formation of aldehyde-terminated chains.<sup>88</sup> This leads to deterioration of the protein-repellent nature of ethylene oxide coatings. Moreover, poly(ethylene oxide) coatings lose their protein resistance at 37 °C,<sup>89, 90</sup> which is a critical temperature for many biomedical applications. Furthermore it was also reported that poly(ethylene oxide) can cause auto-immune responses after implantation of coated prostheses.<sup>91</sup>

Recently, zwitterionic polymer brush coatings have emerged as a superior alternative to poly(ethylene oxide) coatings.<sup>59, 80, 92, 93</sup> Zwitterionic polymers display minimized adhesion of proteins due to a more strongly bound hydration layer induced by electrostatic ionic solvation in addition to hydrogen-bonding interactions. The electrostatic interactions between water molecules and dipoles present in the zwitterionic polymers make these polymers better “water-bearers”.<sup>94</sup> Moreover, these interactions are more stable at

physiologically relevant temperatures (4 - 37 °C) than the hydrogen-bonding interactions along an ethylene oxide chain.<sup>74</sup> As a result the number of studies on zwitterionic polymer brushes such as sulfobetaine-based,<sup>66, 94, 95</sup> carboxybetaine-based<sup>74, 93, 96</sup> and phosphorylcholine-based zwitterionic polymers<sup>97</sup> for protein repellence in biocomplex media is rapidly increasing.<sup>59, 98-100</sup>

## Application of Microsieves in Microbial Detection

Microsieves are more than just a filtration membrane, they have also been employed as capturing devices for microorganisms, which are caught on the microsieve whose pore-size is smaller than the microorganisms.<sup>23</sup> This approach is expected to enable a high sample throughput in comparison with known detection techniques such as agar plating and antibody-based detection microarrays. Indeed, agar plating allows for detection of a large variety of microorganisms. This approach, however, remains both time-consuming and laborious, involving procedures such as (selective) bacterial enrichment or plating prior to analysis, followed by direct counting of the colonies or using common fluorescence-based detection assays, which typically require at least 100-1000 bacterial cells per analysis.<sup>101-103</sup> Recently, the pioneering of antibody-based biosensors has substantially improved the development of a novel generation of diagnostic devices.<sup>104, 105</sup> However, direct detection of microorganisms with these techniques still faces limitations with respect to sensitivity and applicability. Detection by antibody-based planar microarrays<sup>106, 107</sup> is limited by mass transfer, in particular the diffusion of cells towards surfaces, as well as adequate affinity because the cells have to overcome fluid forces before they can reach the sensor surface where they are captured.<sup>108</sup> Bead-based microarrays<sup>109</sup> have proven particularly versatile and sensitive in multiplexed detection. However, the sensitivity of this technique depends on the reliability of washing steps based on filtration, which may suffer from clogging, leaking and nonspecific adsorption.<sup>109-111</sup>

In comparison with these common techniques, the use of microsieves as a detection device not only overcomes the limitation of cell diffusion towards the surface, but may also eliminate the complex washing and collection steps required in bead-based microarrays. The use of microsieves in microbiology thus exhibits high potential as a rapid and sensitive detection method, with the promise to significantly improve the detection efficiency in crude biological samples. In practice, the system is hampered by fouling issues and nonspecific adsorption of undesired components from crude biological samples. A strategy to improve upon this situation is the use of microsieves whose pore-size is larger than the microorganism of interest, in combination with antibodies



immobilized on the microsieves surface (Figure 5). In this manner, the antibody can play a role as “gate keeper” to capture bacteria present in the solution, while many other components of the crude sample can still easily pass through the microsieve.<sup>112</sup>

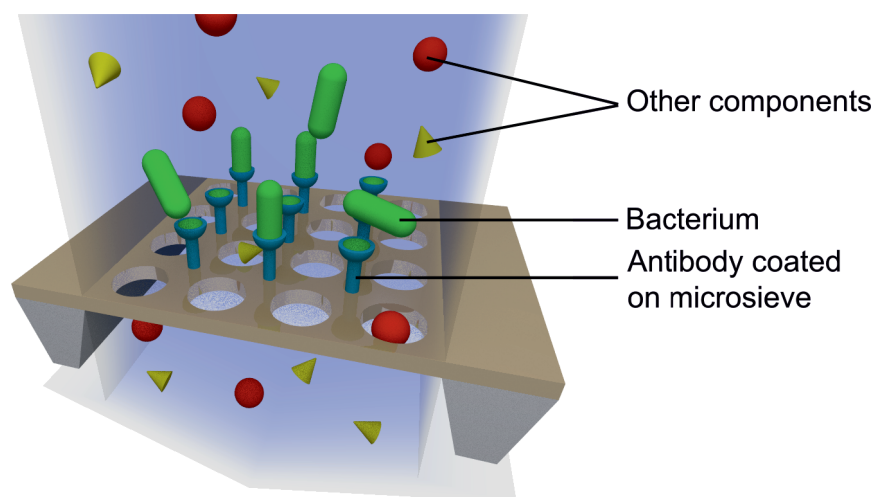


**Figure 5.** Biofunctionalized microsieves in microbial detection application.

### Biofunctionalization on Protein-Repellent Coatings

The capture efficiency of microorganisms in complex media, e.g., milk or blood, with antibody-based capture devices, such as microarrays and microsieves, is lower than that in (phosphate-buffered saline) PBS solution due to competing nonspecific adsorption of proteins present in the medium. Achieving a low degree of nonspecific binding in sensing devices is thus of the utmost importance for highly selective and sensitive microbial detection. Therefore, many groups have investigated the incorporation of protein-repellent coatings into biorecognition layers to achieve a detecting layer that simultaneously repels proteins.<sup>113-116</sup> Immobilization of antibodies is often achieved via *N*-hydroxysuccinimide (NHS) active ester moieties attached onto protein-repellent coatings. Attempts have been made to incorporate biorecognizing molecules into poly(ethylene oxide) or zwitterionic polymers.<sup>115, 117, 118</sup> The attachment of immunoglobulin proteins on poly(ethylene oxide) layer for this purpose was reported to yield a sensitive detection layer while repelling proteins.<sup>116</sup> Immobilization of antibodies on the zwitterionic polycarboxy-betaine films was achieved by activation of some carboxylic acid groups with NHS moieties, as reported by Brault *et al.*<sup>114</sup> and Gao *et al.*<sup>115</sup> The reported data showed significant improvement of the detection of biomarkers in undiluted blood samples without using blocking solution. Another approach to biofunctionalize zwitterionic polymers was introduced by the group of Kitano and co-workers, in which a second polymer containing NHS moieties was grown on top of the zwitterionic polymer brushes, through which the

sugar molecules were attached.<sup>119</sup> These early studies demonstrate the feasibility of the biorecognition layer, which repels and detects proteins simultaneously, as well as its substantial potential in practical applications.

## Approaches for Surface Modification

A common method to attach functional molecules on silicon-based materials through chemical bond formation is the use of organosilane compounds containing functional groups to react with the silanol groups on substrates obtained after surface oxidization. Si-O-Si-C linkages between the organosilane compounds and oxidized substrates are formed, yielding functional monolayers (Figure 6). The main advantage of this method is a wide range of organosilane compounds bearing various functional groups is commercially available. In addition, the ease of application of this surface modification technique accounts for its common use in surface modification. However, Si-O-Si-C<sup>116, 119</sup> and Si-O-C<sup>114, 115</sup> linkages have been reported to hydrolyze in slightly basic media.<sup>120, 121</sup> This may result in severe detachment of functional coatings and limits its long-term use.

Recently, the covalent attachment of organic monolayers onto silicon,<sup>122, 123</sup> silicon nitride<sup>66, 73, 124, 125</sup> and silicon carbide<sup>126</sup> substrates via Si-C and N-C linkages has received significant attention. The attachment of functional monolayers may be achieved either by thermal or photochemical reaction. Stable and high-quality monolayers prepared by these approaches allow for a variety of (bio)chemical surface modifications (Figure 6).<sup>127, 128</sup> These monolayers were demonstrated to possess significant stability in both acidic and basic media.<sup>121, 129</sup> In this thesis, the attachment of such functional monolayers is employed to develop and study coatings on Si<sub>x</sub>N<sub>4</sub> in order to improve the surface properties of microsieves.

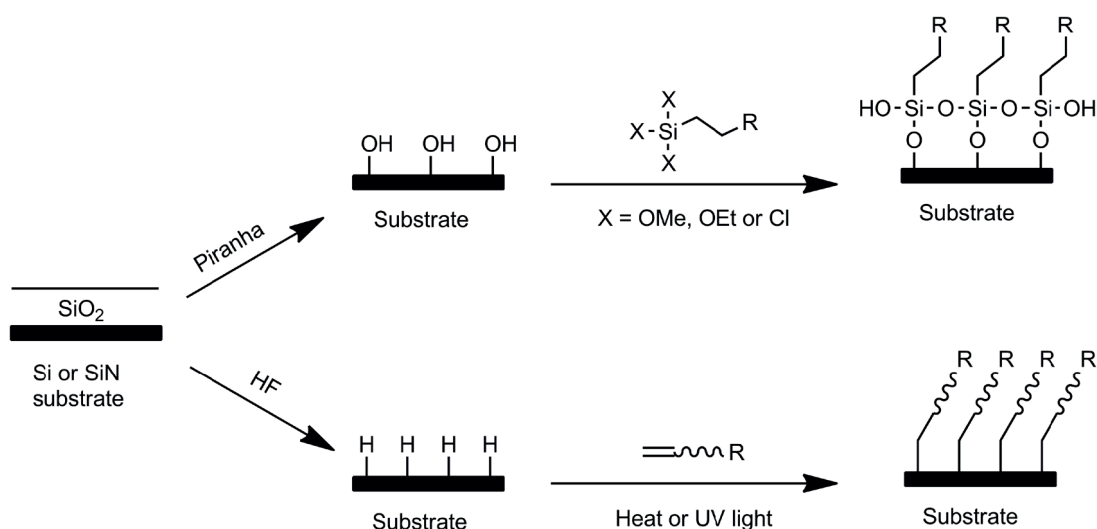


**Figure 6.** Covalent functionalization for silicon-based substrates.



## Surface-Initiated Atom Transfer Radical Polymerization

Surface-initiated atom transfer radical polymerization (SI-ATRP) is a controlled radical polymerization technique that enables the growth of well-defined polymers in a simple and relatively inexpensive manner.<sup>130</sup> SI-ATRP is one of the most effective and most widely used methods to engineer the surface characteristics. It allows scientists to form complex, well-defined nanoscale architectures of specific polymers by precisely controlling the reaction conditions. Assembling polymers in such a manner can be used to tailor various types of polymers with different functionalities. Recently, SI-ATRP has been exploited to control interactions between surfaces and biological elements such as proteins and microorganisms.<sup>59, 119</sup> Antifouling layers formed using SI-ATRP on a variety of surfaces for application in biochips and biosensors have been studied extensively over the recent years. The growth of ethylene oxide and zwitterionic brushes from gold,<sup>75, 92, 99, 131-134</sup> silicon<sup>96</sup> and also polymeric<sup>63</sup> surfaces via SI-ATRP has been investigated extensively.<sup>130, 135</sup> The controlled growth of copolymers and block-copolymers with mixtures of functional monomers was employed to generate hybrid coatings including hydrophobic and hydrophilic polymers, and protein-repellent and bioselective capture coatings.<sup>38, 119</sup> In this thesis, SI-ATRP is employed to growth zwitterionic polymers on  $\text{Si}_x\text{N}_4$  for protein-repellence purposes.

## Outline of this Thesis

Considering the substantial impact of microsieves in the field of microfiltration, the work described in this thesis explores and optimizes the surface properties of microsieves, for biological applications. As mentioned above, their practical use is hampered by fouling issues, which currently prevents microsieves to be used to their full potential. In order to deal with fouling issues, as well as to enable widespread application of microsieves, this thesis initially focuses on functionalization of silicon nitride ( $\text{Si}_x\text{N}_4$ ) surfaces.

The use of oligo(ethylene oxide) (EO) monolayers grafted on  $\text{Si}_x\text{N}_4$  surfaces via UV-induced photochemical reaction to repel protein adsorption is presented in *Chapter 2*. The protein-repellent performance was evaluated in fibrinogen (FIB) and bovine serum albumin (BSA) solution. Furthermore, the stability of the EO-modified surface was examined in PBS solution for 1 week.

The development of protein-repellent zwitterionic polymer brushes grafted from  $\text{Si}_x\text{N}_4$  surfaces is described in *Chapter 3*. The surface-initiated polymerization was studied in detail, and the protein-repelling properties of the polymer-coated surfaces were investigated.

In *Chapter 4* the use of microsieves with antibodies immobilized on the surface and with pore sizes larger than the microorganisms was investigated for bioselective capture from crude biological matrices. Subsequently, the detection platform was improved by grafting antibodies onto a protein-repellent zwitterionic polymer to recognize microorganisms and simultaneously prevent nonspecific adsorption of proteins. This improvement is discussed in *Chapter 5*.

Finally, the most important achievements are summarized and placed into a wider context in *Chapter 6*. In addition, recommendations for further research are discussed.

## References

- (1) Kakaç, S.; Kosoy, B.; Li, D.; Pramuanjaroenikij, A., *Microfluidics Based Microsystems: Fundamentals and Applications*. Springer Science+Business Media B.V.: Dordrecht, 2010.
- (2) Sobolev, V. D.; Churaev, N. V.; Velarde, M. G.; Zorin, Z. M., Surface Tension and Dynamic Contact Angle of Water in Thin Quartz Capillaries. *J. Colloid Interface Sci.* **2000**, *222*, 51-54.
- (3) Prakash, S.; Karacor, M. B.; Banerjee, S., Surface modification in microsystems and nanosystems. *Surf. Sci. Rep.* **2009**, *64*, 233-254.
- (4) Rühle, J.; Biesalski, M., Biocompatibility of Microsystems. In *Comprehensive Microsystems*, Yogesh, G.; Osamu, T.; Hans, Z., Eds. Elsevier: Oxford, 2008; pp 107-130.
- (5) Vong, T.; ter Maat, J.; van Beek, T. A.; van Lagen, B.; Giesbers, M.; van Hest, J. C. M.; Zuilhof, H., Site-Specific Immobilization of DNA in Glass Microchannels via Photolithography. *Langmuir* **2009**, *25*, 13952-13958.
- (6) Rana, D.; Matsuura, T., Surface Modifications for Antifouling Membranes. *Chem. Rev.* **2010**, *110*, 2448-2471.
- (7) Banerjee, I.; Pangule, R. C.; Kane, R. S., Antifouling Coatings: Recent Developments in the Design of Surfaces That Prevent Fouling by Proteins, Bacteria, and Marine Organisms. *Adv. Mater.* **2011**, *23*, 690-718.
- (8) Kazinczi, R.; Mollinger, J. R.; Bossche, A. In *Reliability of silicon nitride as structural material in MEMS*, Proceedings of the SPIE—Materials and Device Characterization in Micromachining II, Vladimirsky, Y.; Friedrich, C. R., Eds. 1999; pp 174-183.
- (9) Chuang, W. H.; Luger, T.; Fetting, R. K.; Ghodssi, R., Characterization of mechanical properties of silicon nitride thin films for space applications. In *Micro- and Nanosystems*, LaVan, D. A.; Ayon, A. A.; Madou, M. J.; McNie, M. E.; Prasad, S. V., Eds. Materials Research Society: Warrendale, 2004; Vol. 782, pp 193-198.
- (10) Voskerician, G.; Shive, M. S.; Shawgo, R. S.; Recum, H. v.; Anderson, J. M.; Cima, M. J.; Langer, R., Biocompatibility and biofouling of MEMS drug delivery devices. *Biomaterials* **2003**, *24*, 1959-1967.
- (11) Wei, J.; Ong, P. L.; Tay, F. E. H.; Iliescu, C., A new fabrication method of low stress PECVD SiN<sub>x</sub> layers for biomedical applications. *Thin Solid Films* **2008**, *516*, 5181-5188.

- (12) Bermudez, V. M.; Perkins, F. K., Preparation and properties of clean Si<sub>3</sub>N<sub>4</sub> surfaces. *Appl. Surf. Sci.* **2004**, *235*, 406-419.
- (13) Andersen, K. N.; Svendsen, W. E.; Stimpel-Lindner, T.; Sulima, T.; Baumgartner, H., Annealing and deposition effects of the chemical composition of silicon-rich nitride. *Appl. Surf. Sci.* **2005**, *243*, 401-408.
- (14) Patel, N. S.; Rajadhyaksha, A.; Boone, J. D., Supervisory control of LPCVD silicon nitride. *IEEE Trans. Semicond. Manuf.* **2005**, *18*, 584-591.
- (15) Resnik, D.; Aljancic, U.; Vrtacnik, D.; Mozek, M.; Amon, S., Mechanical stress in thin film microstructures on silicon substrate. *Vacuum* **2005**, *80*, 236-240.
- (16) Sleenckx, E.; Schaekers, M.; Shi, X.; Kunnen, E.; Degroote, B.; Jurczak, M.; de ten Broeck, M. D.; Augendre, E., Optimization of low temperature silicon nitride processes for improvement of device performance. *Microelectron. Reliab.* **2005**, *45*, 865-868.
- (17) Rahman, H. U.; Gentle, A.; Gauja, E.; Ramer, R., Characterisation of Dielectric Properties of PECVD Silicon Nitride for RF MEMS Applications. In *Multitopic Conference, 2008. INMIC 2008. IEEE International* IEEE: Karachi, 2008; pp 91-96.
- (18) Ciprian, I.; Tay, F. E. H.; Wei, J., Low stress PECVD—SiN<sub>x</sub> layers at high deposition rates using high power and high frequency for MEMS applications. *J. Micromech. Microeng.* **2006**, *16*, 869.
- (19) Ashruf, C. M. A.; French, P. J.; deBoer, C.; Sarro, P. M. In *Strain effects in multi-layers*, Micromachining and Microfabrication Process Technology III, SPIE: 1997; pp 149-159.
- (20) Nam, H. J.; Kim, Y. S.; Lee, C. S.; Jin, W. H.; Jang, S. S.; Cho, I. J.; Bu, J. U.; Choi, W. B.; Choi, S. W., Silicon nitride cantilever array integrated with silicon heaters and piezoelectric detectors for probe-based data storage. *Sensors and Actuators a-Physical* **2007**, *134*, 329-333.
- (21) Jeong, S. Y.; Ahn, S. H.; Lee, D. S.; Jin, W. H.; Jang, S. S.; Cho, I. J.; Kim, Y. S.; Nam, H. J.; Lee, C. S. In *Fabrication and simulation of silicon nitride cantilever for low power nano-data-storage*, International Mechanical Engineering Congress and Exposition 2007 Vol 11 Pt a and Pt B: Micro and Nano Systems, 2008; pp 611-615.
- (22) van Rijn, C. J. M.; Veldhuis, G. J.; Kuiper, S., Nanosieves with microsystem technology for microfiltration applications. *Nanotechnology* **1998**, *9*, 343-345.
- (23) van Rijn, C. J. M., *Nano and Micro Engineered Membrane Technology*. Elsevier: Amsterdam, The Netherlands, 2004.
- (24) Kuiper, S.; van Wolferen, H.; van Rijn, C.; Nijdam, W.; Krijnen, G.; Elwenspoek, M., Fabrication of microsieves with sub-micron pore size by laser interference lithography. *J. Micromech. Microeng.* **2001**, *11*, 33-37.
- (25) Kuiper, S.; Brink, R.; Nijdam, W.; Krijnen, G. J. M.; Elwenspoek, M. C., Ceramic microsieves: influence of perforation shape and distribution on flow resistance and membrane strength. *J. Membr. Sci.* **2002**, *196*, 149-157.

- (26) Cui, Z. F.; Muralidhara, H. S., *Membrane technology: a practical guide to membrane technology and applications in food and bioprocessing*. Elsevier/Butterworth-Heinemann: Oxford, UK, 2010.
- (27) Baker, R. W., *Membrane technology and applications*. 2nd ed.; Wiley: Chichester, UK, 2004.
- (28) Stamatialis, D. F.; Papenburg, B. J.; Girones, M.; Saiful, S.; Bettahalli, S. N. M.; Schmitmeier, S.; Wessling, M., Medical applications of membranes: Drug delivery, artificial organs and tissue engineering. *J. Membr. Sci.* **2008**, *308*, 1-34.
- (29) Sereewatthanawut, I.; Boam, A. T.; Livingston, A. G., Polymeric membrane nanofiltration and its application to separations in the chemical industries. *Macromol. Symp.* **2008**, *264*, 184-188.
- (30) Dunleavy, M., Polymeric membranes. A review of applications. *Med. Device Technol.* **1996**, *7*, 14-6, 18-21.
- (31) Chan, K. K.; Brownstein, A. M., Ceramic Membranes - Growth Prospect and Opportunities *Am. Ceram. Soc. Bull.* **1991**, *70*, 703-707.
- (32) Girones, M.; Borneman, Z.; Lammertink, R. G. H.; Wessling, M., The role of wetting on the water flux performance of microsieve membranes. *J. Membr. Sci.* **2005**, *259*, 55-64.
- (33) Brans, G.; Kromkamp, J.; Pek, N.; Gielen, J.; Heck, J.; van Rijn, C. J. M.; van der Sman, R. G. M.; Schroën, C. G. P. H.; Boom, R. M., Evaluation of microsieve membrane design. *J. Membr. Sci.* **2006**, *278*, 344-348.
- (34) Kuiper, S.; van Rijn, C. J. M.; Nijdam, W.; Elwenspoek, M. C., Development and applications of very high flux microfiltration membranes. *J. Membr. Sci.* **1998**, *150*, 1-8.
- (35) van Rijn, C. J. M., Chapter 7. In *Nano and Micro Engineered Membrane Technology*, Elsevier: Amsterdam, The Netherlands, 2004; p 170.
- (36) Mansouri, J.; Harrisson, S.; Chen, V., Strategies for controlling biofouling in membrane filtration systems: challenges and opportunities. *J. Mater. Chem.* **2010**, *20*, 4567-4586.
- (37) Kyllönen, H. M.; Pirkonen, P.; Nyström, M., Membrane filtration enhanced by ultrasound: a review. *Desalination* **2005**, *181*, 319-335.
- (38) Krishnan, S.; Weinman, C. J.; Ober, C. K., Advances in polymers for anti-biofouling surfaces. *J. Mater. Chem.* **2008**, *18*, 3405-3413.
- (39) Wu, R. M.; Li, K. J., Increasing Filtrate Flux of Cross-Flow Filtration with Side Stream. *Sep. Sci. Technol.* **2010**, *45*, 975-981.
- (40) Kuberkar, V.; Czekaj, P.; Davis, R., Flux enhancement for membrane filtration of bacterial suspensions using high-frequency backpulsing. *Biotechnol. Bioeng.* **1998**, *60*, 77-87.
- (41) Xiong, Y. H.; Liu, Y., Biological control of microbial attachment: a promising alternative for mitigating membrane biofouling. *Appl. Microbiol. Biotechnol.* **2010**, *86*, 825-837.
- (42) Madaeni, S. S.; Tavakolian, H. R.; Rahimpour, F., Cleaning Optimization of Microfiltration Membrane Employed for Milk Sterilization. *Sep. Sci. Technol.* **2011**, *46*, 571-580.

- (43) Teng, M.-Y.; Lin, S.-H.; Wu, C.-Y.; Juang, R.-S., Factors affecting selective rejection of proteins within a binary mixture during cross-flow ultrafiltration. *J. Membr. Sci.* **2006**, *281*, 103-110.
- (44) Shi, W.; Benjamin, M. M., Fouling of RO membranes in a vibratory shear enhanced filtration process (VSEP) system. *J. Membr. Sci.* **2009**, *331*, 11-20.
- (45) Shi, W.; Benjamin, M. M., Membrane interactions with NOM and an adsorbent in a vibratory shear enhanced filtration process (VSEP) system. *J. Membr. Sci.* **2008**, *312*, 23-33.
- (46) Petala, M. D.; Zouboulis, A. I., Vibratory shear enhanced processing membrane filtration applied for the removal of natural organic matter from surface waters. *J. Membr. Sci.* **2006**, *269*, 1-14.
- (47) Vane, L. M.; Alvarez, F. R.; Giroux, E. L., Reduction of concentration polarization in pervaporation using vibrating membrane module. *J. Membr. Sci.* **1999**, *153*, 233-241.
- (48) Vane, L. M.; Alvarez, F. R., Full-scale vibrating pervaporation membrane unit: VOC removal from water and surfactant solutions. *J. Membr. Sci.* **2002**, *202*, 177-193.
- (49) Girones, M.; Bolhuis-Versteeg, L.; Lammertink, R.; Wessling, M., Flux stabilization of silicon nitride microsieves by backpulsing and surface modification with PEG moieties. *J. Colloid Interface Sci.* **2006**, *299*, 831-840.
- (50) Muthukumaran, S.; Kentish, S. E.; Ashokkumar, M.; Stevens, G. W., Mechanisms for the ultrasonic enhancement of dairy whey ultrafiltration. *J. Membr. Sci.* **2005**, *258*, 106-114.
- (51) Hawkes, J. J.; Limaye, M. S.; Coakley, W. T., Filtration of bacteria and yeast by ultrasound-enhanced sedimentation. *J. Appl. Microbiol.* **1997**, *82*, 39-47.
- (52) Zhang, Q.; Peng, H.; Zhang, Z., Antibacteria and Detoxification Function of Polystyrene/TiO<sub>2</sub> Nanocomposites. *J. Dispersion Sci. Technol.* **2007**, *28*, 937 - 941.
- (53) Song, W. H.; Ryu, H. S.; Hong, S. H., Antibacterial properties of Ag (or Pt)-containing calcium phosphate coating formed by micro-arc oxidation. *J. Biomed. Mater. Res. A* **2009**, *88A*, 246-254.
- (54) Veronese, F. M., Peptide and protein PEGylation: a review of problems and solutions. *Biomaterials* **2001**, *22*, 405-417.
- (55) Prime, K. L.; Whitesides, G. M., Self-Assembled Organic Monolayers - Model Systems for Studying Adsorption of Proteins at Surfaces. *Science* **1991**, *252*, 1164-1167.
- (56) Ramsden, J. J., Puzzles and Paradoxes in Protein Adsorption. *Chem. Soc. Rev.* **1995**, *24*, 73-78.
- (57) Norde, W., Surface modifications to influence adhesion of biological cells and adsorption of globular proteins. In *Surface Chemistry in Biomedical and Environmental Science*, Blitz, J.; Gun'ko, V.; Norde, W., Eds. Springer Netherlands: 2006; pp 159-176.
- (58) Norde, W., Adsorption of proteins from solution at the solid-liquid interface. *Adv. Colloid Interface Sci.* **1986**, *25*, 267-340.

- (59) Holmlin, R. E.; Chen, X.; Chapman, R. G.; Takayama, S.; Whitesides, G. M., Zwitterionic SAMs that Resist Nonspecific Adsorption of Protein from Aqueous Buffer. *Langmuir* **2001**, *17*, 2841-2850.
- (60) Tosaka, R.; Yamamoto, H.; Ohdomari, I.; Watanabe, T., Adsorption Mechanism of Ribosomal Protein L2 onto a Silica Surface: A Molecular Dynamics Simulation Study. *Langmuir* **2010**, *26*, 9950-9955.
- (61) Zheng, J.; Li, L. Y.; Chen, S. F.; Jiang, S. Y., Molecular simulation study of water interactions with oligo (ethylene glycol)-terminated alkanethiol self-assembled monolayers. *Langmuir* **2004**, *20*, 8931-8938.
- (62) Zheng, J.; Li, L. Y.; Tsao, H. K.; Sheng, Y. J.; Chen, S. F.; Jiang, S. Y., Strong repulsive forces between protein and oligo (ethylene glycol) self-assembled monolayers: A molecular simulation study. *Biophys. J.* **2005**, *89*, 158-166.
- (63) Zhou, M.; Liu, H.; Kilduff, J. E.; Langer, R.; Anderson, D. G.; Belfort, G., High-Throughput Membrane Surface Modification to Control NOM Fouling. *Environ. Sci. Technol.* **2009**, *43*, 3865-3871.
- (64) Sofia, S. J.; Premnath, V.; Merrill, E. W., Poly(ethylene oxide) grafted to silicon surfaces: Grafting density and protein adsorption. *Macromolecules* **1998**, *31*, 5059-5070.
- (65) Roosjen, A.; de Vries, J.; van der Mei, H. C.; Norde, W.; Busscher, H. J., Stability and effectiveness against bacterial adhesion of poly(ethylene oxide) coatings in biological fluids. *J. Biomed. Mater. Res. Part B Appl. Biomater.* **2005**, *73B*, 347-354.
- (66) Nguyen, A. T.; Baggerman, J.; Paulusse, J. M. J.; van Rijn, C. J. M.; Zuilhof, H., Stable Protein-Repellent Zwitterionic Polymer Brushes Grafted from Silicon Nitride. *Langmuir* **2011**, *27*, 2587-2594.
- (67) Roosjen, A.; van der Mei, H. C.; Busscher, H. J.; Norde, W., Microbial adhesion to poly(ethylene oxide) brushes: Influence of polymer chain length and temperature. *Langmuir* **2004**, *20*, 10949-10955.
- (68) Chan, Y. H. M.; Schweiss, R.; Werner, C.; Grunze, M., Electrokinetic characterization of oligo- and poly(ethylene glycol)-terminated self-assembled monolayers on gold and glass surfaces. *Langmuir* **2003**, *19*, 7380-7385.
- (69) Unsworth, L. D.; Sheardown, H.; Brash, J. L., Protein resistance of surfaces prepared by sorption of end-thiolated poly(ethylene glycol) to gold: Effect of surface chain density. *Langmuir* **2005**, *21*, 1036-1041.
- (70) Vanderah, D. J.; Pham, C. P.; Springer, S. K.; Silin, V.; Meuse, C. W., Characterization of a series of self-assembled monolayers of alkylated 1-thiaoligo (ethylene oxides)<sub>(4-8)</sub> on Gold. *Langmuir* **2000**, *16*, 6527-6532.
- (71) Lee, S. W.; Laibinis, P. E., Protein-resistant coatings for glass and metal oxide surfaces derived from oligo(ethylene glycol)-terminated alkyltrichlorosilanes. *Biomaterials* **1998**, *19*, 1669-1675.



- (72) Rosso, M.; Nguyen, A. T.; de Jong, E.; Baggerman, J.; Paulusse, J. M. J.; Giesbers, M.; Fokkink, R. G.; Norde, W.; Schroën, K.; van Rijn, C. J. M.; Zuilhof, H., Protein-Repellent Silicon Nitride Surfaces: UV-Induced Formation of Oligoethylene Oxide Monolayers. *ACS Appl. Mater. Interfaces* **2011**, *3*, 697-704.
- (73) Rosso, M.; Giesbers, M.; Arafat, A.; Schroën, K.; Zuilhof, H., Covalently Attached Organic Monolayers on SiC and Si<sub>x</sub>N<sub>4</sub> Surfaces: Formation Using UV Light at Room Temperature. *Langmuir* **2009**, *25*, 2172-2180.
- (74) Yang, W.; Xue, H.; Li, W.; Zhang, J.; Jiang, S., Pursuing "Zero" Protein Adsorption of Poly(carboxybetaine) from Undiluted Blood Serum and Plasma. *Langmuir* **2009**, *25*, 11911-11916.
- (75) Rodriguez Emmenegger, C.; Brynda, E.; Riedel, T.; Sedlakova, Z.; Houska, M.; Alles, A. B., Interaction of Blood Plasma with Antifouling Surfaces. *Langmuir* **2009**, *25*, 6328-6333.
- (76) Norde, W.; Gage, D., Interaction of bovine serum albumin and human blood plasma with PEO-tethered surfaces: Influence of PEO chain length, grafting density, and temperature. *Langmuir* **2004**, *20*, 4162-4167.
- (77) Baier, R. E., Surface behaviour of biomaterials: The theta surface for biocompatibility. *J. Mater. Sci.-Mater. Med.* **2006**, *17*, 1057-1062.
- (78) Magin, C. M.; Cooper, S. P.; Brennan, A. B., Non-toxic antifouling strategies. *Mater. Today* **2010**, *13*, 36-44.
- (79) Park, D.; Weinman, C. J.; Finlay, J. A.; Fletcher, B. R.; Paik, M. Y.; Sundaram, H. S.; Dimitriou, M. D.; Sohn, K. E.; Callow, M. E.; Callow, J. A.; Handlin, D. L.; Willis, C. L.; Fischer, D. A.; Kramer, E. J.; Ober, C. K., Amphiphilic Surface Active Triblock Copolymers with Mixed Hydrophobic and Hydrophilic Side Chains for Tuned Marine Fouling-Release Properties. *Langmuir* **2010**, *26*, 9772-9781.
- (80) Kane, R. S.; Deschatelets, P.; Whitesides, G. M., Kosmotropes Form the Basis of Protein-Resistant Surfaces. *Langmuir* **2003**, *19*, 2388-2391.
- (81) Roosjen, A.; Kaper, H. J.; van der Mei, H. C.; Norde, W.; Busscher, H. J., Inhibition of adhesion of yeasts and bacteria by poly(ethylene oxide)-brushes on glass in a parallel plate flow chamber. *Microbiology* **2003**, *149*, 3239-3246.
- (82) Chen, S.; Li, L.; Zhao, C.; Zheng, J., Surface hydration: Principles and applications toward low-fouling/nonfouling biomaterials. *Polymer* **2010**, *51*, 5283-5293.
- (83) Harder, P.; Grunze, M.; Dahint, R.; Whitesides, G. M.; Laibinis, P. E., Molecular conformation in oligo(ethylene glycol)-terminated self-assembled monolayers on gold and silver surfaces determines their ability to resist protein adsorption. *J. Phys. Chem. B* **1998**, *102*, 426-436.
- (84) Palegrosdemange, C.; Simon, E. S.; Prime, K. L.; Whitesides, G. M., Formation of Self-Assembled Monolayers by Chemisorption of Derivatives of Oligo(Ethylene Glycol) of Structure HS(CH<sub>2</sub>)<sub>11</sub>(OCH<sub>2</sub>CH<sub>2</sub>)<sub>m</sub>OH on Gold. *J. Am. Chem. Soc.* **1991**, *113*, 12-20.

- (85) Schlapak, R.; Pammer, P.; Armitage, D.; Zhu, R.; Hinterdorfer, P.; Vaupel, M.; Fruhwirth, T.; Howorka, S., Glass surfaces grafted with high-density poly(ethylene glycol) as substrates for DNA oligonucleotide microarrays. *Langmuir* **2006**, *22*, 277-285.
- (86) Sharma, S.; Johnson, R. W.; Desai, T. A., Evaluation of the stability of nonfouling ultrathin poly(ethylene glycol) films for silicon-based microdevices. *Langmuir* **2004**, *20*, 348-356.
- (87) Zolk, M.; Eisert, F.; Pipper, J.; Herrwerth, S.; Eck, W.; Buck, M.; Grunze, M., Solvation of oligo(ethylene glycol)-terminated self-assembled monolayers studied by vibrational sum frequency spectroscopy. *Langmuir* **2000**, *16*, 5849-5852.
- (88) Qin, G.; Cai, C., Oxidative degradation of oligo(ethylene glycol)-terminated monolayers. *Chem. Commun.* **2009**, 5112-4.
- (89) Leckband, D.; Sheth, S.; Halperin, A., Grafted poly(ethylene oxide) brushes as nonfouling surface coatings. *J. Biomater. Sci., Polym. Ed.* **1999**, *10*, 1125-1147.
- (90) Li, L. Y.; Chen, S. F.; Jiang, S. Y., Protein interactions with oligo(ethylene glycol) (OEG) self-assembled monolayers: OEG stability, surface packing density and protein adsorption. *J. Biomater. Sci.-Polym. Ed.* **2007**, *18*, 1415-1427.
- (91) Knop, K.; Hoogenboom, R.; Fischer, D.; Schubert, U. S., Poly(ethylene glycol) in Drug Delivery: Pros and Cons as Well as Potential Alternatives. *Angew. Chem. Int. Ed.* **2010**, *49*, 6288-6308.
- (92) Jiang, S.; Cao, Z., Ultralow-Fouling, Functionalizable, and Hydrolyzable Zwitterionic Materials and Their Derivatives for Biological Applications. *Adv. Mater.* **2010**, *22*, 920-932.
- (93) Kitano, H.; Tada, S.; Mori, T.; Takaha, K.; Gemmei-Ide, M.; Tanaka, M.; Fukuda, M.; Yokoyama, Y., Correlation between the structure of water in the vicinity of carboxybetaine polymers and their blood-compatibility. *Langmuir* **2005**, *21*, 11932-11940.
- (94) Chang, Y.; Liao, S.-C.; Higuchi, A.; Ruaan, R.-C.; Chu, C.-W.; Chen, W.-Y., A Highly Stable Nonbiofouling Surface with Well-Packed Grafted Zwitterionic Polysulfobetaine for Plasma Protein Repulsion. *Langmuir* **2008**, *24*, 5453-5458.
- (95) Zhao, Y.-H.; Wee, K.-H.; Bai, R., Highly hydrophilic and low-protein-fouling polypropylene membrane prepared by surface modification with sulfobetaine-based zwitterionic polymer through a combined surface polymerization method. *J. Membr. Sci.* **2010**, *362*, 326-333.
- (96) Zhang, Z.; Chao, T.; Chen, S.; Jiang, S., Superlow Fouling Sulfobetaine and Carboxybetaine Polymers on Glass Slides. *Langmuir* **2006**, *22*, 10072-10077.
- (97) Feng, W.; Zhu, S. P.; Ishihara, K.; Brash, J. L., Adsorption of fibrinogen and lysozyme on silicon grafted with poly(2-methacryloyloxyethyl phosphorylcholine) via surface-initiated atom transfer radical polymerization. *Langmuir* **2005**, *21*, 5980-5987.
- (98) He, Y.; Hower, J.; Chen, S.; Bernards, M. T.; Chang, Y.; Jiang, S., Molecular Simulation Studies of Protein Interactions with Zwitterionic Phosphorylcholine Self-Assembled Monolayers in the Presence of Water. *Langmuir* **2008**, *24*, 10358-10364.



- (99) Ladd, J.; Zhang, Z.; Chen, S.; Hower, J. C.; Jiang, S., Zwitterionic Polymers Exhibiting High Resistance to Nonspecific Protein Adsorption from Human Serum and Plasma. *Biomacromolecules* **2008**, *9*, 1357-1361.
- (100) Zhao, C.; Li, L.; Zheng, J., Achieving Highly Effective Nonfouling Performance for Surface-Grafted Poly(HPMA) via Atom-Transfer Radical Polymerization. *Langmuir* **2010**, *26*, 17375-17382.
- (101) Valentin-Bon, I. E.; Brackett, R. E.; Seo, K. H.; Hammack, T. S.; Andrews, W. H., Preenrichment versus direct selective agar plating for the detection of Salmonella enteritidis in shell eggs. *J. Food Prot.* **2003**, *66*, 1670-1674.
- (102) Kiess, A. S.; Parker, H. M.; McDaniel, C. D., Evaluation of different selective media and culturing techniques for the quantification of Campylobacter ssp from broiler litter. *Poultry Science* **2010**, *89*, 1755-1762.
- (103) Hajmeer, M. N.; Fung, D. Y. C.; Marsden, J. L.; Milliken, G. A., Effects of preparation method, age, and plating technique of thin agar layer media on recovery of Escherichia coli O157 : H7 injured by sodium chloride. *J. Microbiol. Methods* **2001**, *47*, 249-253.
- (104) Byrne, B.; Stack, E.; Gilmartin, N.; O’Kennedy, R., Antibody-Based Sensors: Principles, Problems and Potential for Detection of Pathogens and Associated Toxins. *Sensors* **2009**, *9*, 4407-4445.
- (105) North, J. R., Immunosensors: Antibody-based biosensors. *Trends Biotechnol.* **1985**, *3*, 180-186.
- (106) Angenendt, P.; Glökler, J.; Sobek, J.; Lehrach, H.; Cahill, D. J., Next generation of protein microarray support materials:: Evaluation for protein and antibody microarray applications. *J. Chromatogr. A* **2003**, *1009*, 97-104.
- (107) Rusmini, F.; Zhong, Z.; Feijen, J., Protein Immobilization Strategies for Protein Biochips. *Biomacromolecules* **2007**, *8*, 1775-1789.
- (108) Skottrup, P. D.; Nicolaisen, M.; Justesen, A. F., Towards on-site pathogen detection using antibody-based sensors. *Biosens. Bioelectron.* **2008**, *24*, 339-348.
- (109) Barbee, K. D.; Hsiao, A. P.; Roller, E. E.; Huang, X. H., Multiplexed protein detection using antibody-conjugated microbead arrays in a microfabricated electrophoretic device. *Lab Chip* **2010**, *10*, 3084-3093.
- (110) Templin, M. F.; Stoll, D.; Bachmann, J.; Joos, T. O., Protein microarrays and multiplexed sandwich immunoassays: What beats the beads? *Comb. Chem. High Throughput Screen* **2004**, *7*, 223-229.
- (111) Opalka, D.; Lachman, C. E.; MacMullen, S. A.; Jansen, K. U.; Smith, J. F.; Chirmule, N.; Esser, M. T., Simultaneous Quantitation of Antibodies to Neutralizing Epitopes on Virus-Like Particles for Human Papillomavirus Types 6, 11, 16, and 18 by a Multiplexed Luminex Assay. *Clin. Diagn. Lab. Immunol.* **2003**, *10*, 108-115.
- (112) Nguyen, A. T.; van Doorn, R.; Baggerman, J.; Paulusse, J. M. J.; Zuilhof, H.; Klerks, M.; van Rijn, C. J. M., Rapid Microsieve-Based Microbial Diagnostics. *(in preparation)* **2011**.

- (113) Heuts, J.; Salber, J.; Goldyn, A. M.; Janser, R.; Moller, M.; Klee, D., Bio-functionalized star PEG-coated PVDF surfaces for cytocompatibility-improved implant Components. *J. Biomed. Mater. Res. A* **2010**, 92A, 1538-1551.
- (114) Brault, N. D.; Gao, C.; Xue, H.; Pilarik, M.; Homola, J.; Jiang, S.; Yu, Q., Ultra-low fouling and functionalizable zwitterionic coatings grafted onto SiO<sub>2</sub> via a biomimetic adhesive group for sensing and detection in complex media. *Biosens. Bioelectron.* **2010**, 25, 2276-2282.
- (115) Gao, C.; Li, G.; Xue, H.; Yang, W.; Zhang, F.; Jiang, S., Functionalizable and ultra-low fouling zwitterionic surfaces via adhesive mussel mimetic linkages. *Biomaterials* **2010**, 31, 1486-1492.
- (116) Yao, Y.; Ma, Y.-Z.; Qin, M.; Ma, X.-J.; Wang, C.; Feng, X.-Z., NHS-ester functionalized poly(PEGMA) brushes on silicon surface for covalent protein immobilization. *Colloids Surf., B* **2008**, 66, 233-239.
- (117) Weimer, B. C.; Walsh, M. K.; Wang, X. W., Influence of a poly-ethylene glycol spacer on antigen capture by immobilized antibodies. *J. Biochem. Bioph. Methods* **2000**, 45, 211-219.
- (118) Kitano, H.; Nagaoka, K.; Tada, S.; Gemmei-Ide, M., Structure of water in the vicinity of amphoteric polymers as revealed by Raman spectroscopy. *J. Colloid Interface Sci.* **2007**, 313, 461-468.
- (119) Kitano, H.; Suzuki, H.; Matsuura, K.; Ohno, K., Molecular Recognition at the Exterior Surface of a Zwitterionic Telomer Brush. *Langmuir* **2010**, 26, 6767-6774.
- (120) Menawat, A.; Jr, J. H.; Siriwardane, R., Control of surface energy of glass by surface reactions: Contact angle and stability. *J. Colloid Interface Sci.* **1984**, 101, 110-119.
- (121) Sano, H.; Maeda, H.; Ichii, T.; Murase, K.; Noda, K.; Matsushige, K.; Sugimura, H., Alkyl and Alkoxy Monolayers Directly Attached to Silicon: Chemical Durability in Aqueous Solutions. *Langmuir* **2009**, 25, 5516-5525.
- (122) de Smet, L. C. P. M.; Pukin, A. V.; Sun, Q.-Y.; Eves, B. J.; Lopinski, G. P.; Visser, G. M.; Zuilhof, H.; Sudhölter, E. J. R., Visible-light attachment of SiC linked functionalized organic monolayers on silicon surfaces. *Appl. Surf. Sci.* **2005**, 252, 24-30.
- (123) Stewart, M. P.; Buriak, J. M., Photopatterned hydrosilylation on porous silicon. *Angew. Chem. Int. Ed.* **1998**, 37, 3257-3260.
- (124) Coffinier, Y.; Boukherroub, R.; Wallart, X.; Nys, J. P.; Durand, J. O.; Stievenard, D.; Grandidier, B., Covalent functionalization of silicon nitride surfaces by semicarbazide group. *Surf. Sci.* **2007**, 601, 5492-5498.
- (125) Arafat, A.; Schroën, K.; de Smet, L. C. P. M.; Sudhölter, E. J. R.; Zuilhof, H., Tailor-made functionalization of silicon nitride surfaces. *J. Am. Chem. Soc.* **2004**, 126, 8600-8601.
- (126) Qin, G.; Zhang, R.; Makarenko, B.; Kumar, A.; Rabalais, W.; Lopez Romero, J. M.; Rico, R.; Cai, C., Highly stable, protein resistant thin films on SiC-modified silicon substrates. *Chem. Commun.* **2010**, 46, 3289-3291.

- (127) Rosso, M.; Giesbers, M.; Schroën, K.; Zuilhof, H., Controlled Oxidation, Biofunctionalization, and Patterning of Alkyl Monolayers on Silicon and Silicon Nitride Surfaces using Plasma Treatment. *Langmuir* **2009**, *26*, 866-872.
- (128) Stavis, C.; Clare, T. L.; Butler, J. E.; Radadia, A. D.; Carr, R.; Zeng, H.; King, W. P.; Carlisle, J. A.; Aksimentiev, A.; Bashir, R.; Hamers, R. J., Surface functionalization of thin-film diamond for highly stable and selective biological interfaces. *Proc. Natl. Acad. Sci. U.S.A.* **2011**, *108*, 983-988.
- (129) Scheres, L.; Arafat, A.; Zuilhof, H., Self-assembly of high-quality covalently bound organic monolayers onto silicon. *Langmuir* **2007**, *23*, 8343-8346.
- (130) Matyjaszewski, K.; Xia, J., Atom Transfer Radical Polymerization. *Chem. Rev.* **2001**, *101*, 2921-2990.
- (131) Chang, Y.; Chen, W.-Y.; Yandi, W.; Shih, Y.-J.; Chu, W.-L.; Liu, Y.-L.; Chu, C.-W.; Ruaan, R.-C.; Higuchi, A., Dual-Thermoresponsive Phase Behavior of Blood Compatible Zwitterionic Copolymers Containing Nonionic Poly(N-isopropyl acrylamide). *Biomacromolecules* **2009**, *10*, 2092-2100.
- (132) Chang, Y.; Shu, S.-H.; Shih, Y.-J.; Chu, C.-W.; Ruaan, R.-C.; Chen, W.-Y., Hemocompatible Mixed-Charge Copolymer Brushes of Pseudozwitterionic Surfaces Resistant to Nonspecific Plasma Protein Fouling. *Langmuir* **2009**, *26*, 3522-3530.
- (133) Cheng, N.; Brown, A. A.; Azzaroni, O.; Huck, W. T. S., Thickness-Dependent Properties of Polyzwitterionic Brushes. *Macromolecules* **2008**, *41*, 6317-6321.
- (134) Omar, A.; Andrew, A. B.; Huck, W. T. S., UCST Wetting Transitions of Polyzwitterionic Brushes Driven by Self-Association. *Angew. Chem. Int. Ed.* **2006**, *45*, 1770-1774.
- (135) Ohno, K.; Kayama, Y.; Ladmiral, V.; Fukuda, T.; Tsujii, Y., A Versatile Method of Initiator Fixation for Surface-Initiated Living Radical Polymerization on Polymeric Substrates. *Macromolecules* **2010**, *43*, 5569-5574.



## Protein-Repellent Silicon Nitride Surfaces: UV-Induced Formation of Oligo(ethylene oxide) Monolayers

The robust covalent attachment of short oligo(ethylene oxide)-terminated alkenes ( $\text{CH}_3\text{O}(\text{CH}_2\text{CH}_2\text{O})_3(\text{CH}_2)_9(\text{CH}=\text{CH}_2)$  [EO<sub>3</sub>] and  $\text{CH}_3\text{O}(\text{CH}_2\text{CH}_2\text{O})_6(\text{CH}_2)_9(\text{CH}=\text{CH}_2)$  [EO<sub>6</sub>]) by the reaction of alkenes onto silicon-rich silicon nitride ( $\text{Si}_x\text{N}_4$ ,  $x>3$ ) surfaces at room temperature using UV light was presented. Reflectometry was used to monitor in situ the nonspecific adsorption of bovine serum albumin (BSA) and fibrinogen (FIB) onto oligo(ethylene oxide) coated  $\text{Si}_x\text{N}_4$  surfaces ( $\text{EO}_n\text{-Si}_x\text{N}_4$ ,  $x>3$ ) in comparison with plasma-oxidized  $\text{Si}_x\text{N}_4$  surfaces ( $\text{SiO}_y\text{-Si}_x\text{N}_4$ ) and hexadecyl-coated  $\text{Si}_x\text{N}_4$  surfaces ( $\text{C}_{16}\text{-Si}_x\text{N}_4$ ). A significant reduction in protein adsorption on  $\text{EO}_n\text{-Si}_x\text{N}_4$  surfaces was achieved. Prolonged exposure of the modified surfaces to PBS solution for 1 week or alkaline condition for 2 h resulted in only minor degradation of the ethylene oxide moieties while no oxidation of the  $\text{Si}_x\text{N}_4$  substrates was observed.

This chapter has been published as:

Rosso, M.; Nguyen, A.T.; De Jong, E.; Baggerman, J.; Paulusse, J.M.J.; Giesbers, M.; Fokkink, R.G.; Norde, W.; Schroën, K.; Van Rijn, C.J.M.; Zuilhof, H. *ACS Appl. Mater. Interfaces* **2011**, 3, 697–704

## 1. Introduction

Silicon nitride ( $\text{Si}_x\text{N}_4$ ,  $x \geq 3$ ) is widely used as insulator for microelectronics and microsystem devices.<sup>1</sup> Films of this material inhibit diffusion of water, oxygen and sodium ions and are widely used as passivation layers in integrated circuits.<sup>2</sup>  $\text{Si}_x\text{N}_4$  is not only popular because of its superior physical robustness and chemical inertness<sup>3</sup> but also because it provides a good alternative to silicon dioxide<sup>4</sup> in microelectronic and membrane applications.<sup>5-7</sup>

Biocompatibility is an important issue for the use of  $\text{Si}_x\text{N}_4$  films as coatings for biosensors or filtration membranes. In particular, the performance of microfabricated filtration membranes (microsieves) is dramatically affected by nonspecific adsorption of protein (aggregates)<sup>8-10</sup> on surfaces during filtration. In the process of surface fouling, the adsorption of the first protein layer is a decisive step that usually initiates surface contamination, creating suitable conditions for the subsequent adsorption of more protein aggregates,<sup>10</sup> as well as cells, bacteria, and other microorganisms.<sup>11</sup>

Increasing the hydrophilicity of  $\text{Si}_x\text{N}_4$  surfaces partially solves the problem of protein adsorption. Indeed, hydrophilic membranes are less subject to fouling and have a longer operational life.<sup>12-14</sup> For instance, an air-based plasma treatment that superficially oxidizes the silicon nitride surfaces, can improve the wettability and performance of membranes. However, the hydrophilic properties of oxidized surfaces are only temporary.<sup>15</sup>

Widely used alternative solutions to reduce protein adsorption onto surfaces include self-assembled monolayers (SAMS) of ethylene oxide (EO) oligomers. This approach has been applied to polymers,<sup>16-21</sup> gold and silver,<sup>22-30</sup> glass and other oxides,<sup>31-39</sup> and etched silicon surfaces.<sup>19, 40-44</sup> The application to silicon nitride would require a method for the robust attachment of such EO-based materials. Several studies reported on the specific modification of AFM tips<sup>45-50</sup> with poly(ethylene oxide) chains, for applications in which only a few attached chains sufficed. Some work has been carried out on the attachment of long poly(ethylene oxide) chains on oxidized silicon nitride,<sup>51</sup> but these irregular coatings were not stable in water. Organosilane compounds have been used to graft poly(ethylene oxide) methacrylate<sup>52</sup> onto oxidized silicon nitride, giving layers with some protein-repellent properties, but the obtained layers were not stable under aqueous or alkaline conditions, most likely because of the hydrolysis of Si-O bonds.<sup>51, 53</sup> Another report on organosilane-based monolayers of linear oligo(ethylene oxide) molecules [3 - 12 ethylene oxide (EO) units] on oxidized silicon nitride substrates<sup>54</sup> also mentioned good thermal stability, but details on their hydrolytic stability or protein repellence were not given. Recently, we have shown that it is possible to covalently attach an organic monolayer

onto a silicon nitride<sup>55, 56</sup> or silicon carbide<sup>57</sup> surface, using conditions similar to those used for the thermal hydrosilylation of silicon surfaces.<sup>58-61</sup> Stable and high-quality monolayers were obtained with several simple alkenes, as well as esters, allowing further (bio)chemical surface modifications. However, the employed reaction conditions were not suitable for attachment of oligo(ethylene oxide) because of thermal degradation of ethylene oxide moieties.<sup>62</sup> Very recently, it was demonstrated that the modification of SiO<sub>2</sub>, Si<sub>x</sub>N<sub>4</sub> and SiC can also be initiated by UV light at room temperature using less compound and a simpler experimental setup.<sup>63-65</sup> This method allows monolayer formation from labile and/or more expensive alkenes.

In the current paper, we report on the use of this photochemical method to attach oligo(ethylene oxide)-terminated monolayers onto silicon-rich silicon nitride surfaces in a single-step procedure. In particular, methoxy-tri(ethylene oxide) undec-1-ene (CH<sub>3</sub>O(CH<sub>2</sub>CH<sub>2</sub>O)<sub>3</sub>(CH<sub>2</sub>)<sub>9</sub>CH=CH<sub>2</sub>), and methoxy-hexa(ethylene oxide) undec-1-ene (CH<sub>3</sub>O(CH<sub>2</sub>CH<sub>2</sub>O)<sub>6</sub>(CH<sub>2</sub>)<sub>9</sub>CH=CH<sub>2</sub>) were synthesized and grafted onto etched silicon-rich silicon nitride (Si<sub>x</sub>N<sub>4</sub>) surfaces, to yield monolayers abbreviated as EO<sub>3</sub> and EO<sub>6</sub> layers, respectively. The obtained monolayers were characterized by X-ray photoelectron spectroscopy (XPS), static water contact angle measurements, X-ray reflectivity, and atomic force microscopy (AFM). Subsequently, the protein-repelling properties of the surfaces were investigated by studying the adsorption of bovine serum albumin (BSA) and fibrinogen (FIB) from solution, both in situ by reflectometry and ex situ by static water contact angle measurement. In each case, the antifouling properties of modified surfaces were compared to those of SiO<sub>y</sub>-Si<sub>x</sub>N<sub>4</sub> and C<sub>16</sub>-Si<sub>x</sub>N<sub>4</sub> surfaces to reveal the potential of EO<sub>3</sub> and EO<sub>6</sub> monolayers. The stability of modified surfaces in aqueous solutions plays an important role for their future implementation in filtration and microfluidic devices. Therefore, the stability of the EO<sub>6</sub>-modified surfaces in PBS solutions was investigated as well.

## 2. Experimental Section

### 2.1. Materials

Bovine serum albumin (fraction V, min 96% lyophilized powder) and fibrinogen (fraction I from pig plasma, 78% in protein) were purchased from Sigma. Sodium phosphate dibasic (analytical grade, Acros), potassium dihydrogenophosphate (ACS grade, Merck), potassium chloride (pro analysis, Merck) and sodium chloride (puriss., Riedel-de-Haën) were used to prepare the PBS solution. The synthesis of EO<sub>3</sub> and EO<sub>6</sub> is described in Appendix 1.



## 2.2. Silicon Nitride Surface Modification

Silicon-rich silicon nitride samples (LPCVD  $\text{Si}_x\text{N}_4$ ,  $x > 3$ ) on Si (100), thickness of 147 nm, obtained from Lionix B.V., The Netherlands, with sizes of  $1 \times 1 \text{ cm}^2$  for XPS or  $4 \times 0.75 \text{ cm}^2$  for reflectometry were cleaned by sonication in acetone, followed by oxidation in air-based plasma for 10 min and in pure oxygen (99.999%) for another 5 min. The oxidized samples were then etched with a 2.5% aqueous solution of HF for 2 min and dried in a nitrogen flow. They were then immediately dipped into argon-saturated neat alkenes in a quartz flask. After 30 more min under argon flow, a UV pen lamp (254 nm, low pressure mercury vapor, double bore lamp from Jelight Cie, California) with the output intensity of  $9 \text{ mW.cm}^{-2}$  was placed 4 mm above the  $\text{Si}_x\text{N}_4$  surface and the sample was irradiated for 24 h. Afterward, samples were removed and rinsed several times with ethyl acetate, ethanol and dichloromethane, and sonicated in the same solvents. Reference hydrophilic surfaces were plasma-treated for only 10 min. Angle-resolved XPS revealed that such plasma-treated surfaces presented a thin hydrophilic layer of silicon oxy-nitride (atomic composition of the first 10 nm: 40%  $\text{Si}_{2p}$ , 30%  $\text{N}_{1s}$ , 20%  $\text{O}_{1s}$ , 10%  $\text{C}_{1s}$ , values obtained from XPS  $\pm 5\%$ ).

## 2.3. Static Water Contact Angle Measurements

The wetting properties of modified surfaces were characterized by automated static water contact angle measurements performed using an Erma Contact Angle Meter G-1 (volume of the drop of demineralized water =  $3.5 \text{ }\mu\text{L}$ ). For stability measurements, samples were dipped in PBS for a defined time and then rinsed thoroughly with pure water, acetone and finally with petroleum ether before measuring contact angle. After that, the samples were immersed again in fresh PBS. Stability for different times was determined sequentially on the same samples. For the stability in alkaline condition, the samples were immersed in NaOH solution (0.1mM, pH 10) at room temperature for 2 h, subsequently rinsed thoroughly with pure water, acetone, and finally with petroleum ether before measuring contact angle. In both studies, 3 samples were employed, the reported data are average values.

## 2.4. X-ray Photoelectron Spectroscopy (XPS)

The XPS analysis of surfaces was performed using a JPS-9200 Photoelectron Spectrometer (JEOL, Japan). The high-resolution spectra were obtained under UHV conditions using monochromatic Al  $K\alpha$  X-ray radiation at 12 kV and 25 mA, using an analyzer pass energy of 10 eV. High-resolution spectra were corrected with a linear background before fitting.



## 2.5. X-ray Reflectivity

X-ray reflectivity measurements were performed on a Panalytical X'Pert Pro diffractometer using nickel-filtered Cu K $\alpha$  radiation (tube settings 50 kV and 40 mA). The data were collected using a fixed divergence slit 1/32°, and a parallel plate collimator on the diffracted beam side. The layer thickness was calculated from the interference fringes.

## 2.6. Atomic Force Microscopy (AFM)

Images were obtained with an MFP-3D AFM from Asylum Research (Santa Barbara, CA). Imaging was performed in AC mode in air using OMCL-AC240 silicon cantilevers (Olympus Corporation, Japan). The root-mean-square (rms) roughness was calculated from the fluctuations of the surface height around the average height in the image. In this way the rms value describes the topography of the surface. The rms is the standard deviation, i.e., the square root of the variance, of the Z-values within the image, according to:  $\text{rms} = \sqrt{(\sum(Z_i)^2/n)}$

## 2.7. Reflectometry

In a typical reflectometer (Figure 1), a monochromatic linearly polarized light beam (He-Ne laser; 632.8 nm) passes a 45° glass prism. This beam arrives at the interface with an angle of incidence of 66° for the solvent/substrate interface. After reflection at the interface and refraction in the prism the beam is split into its p- and s-polarized components relative to the plane of incidence by means of a beam splitter. Both components are separately detected by two photodiodes and the ratio between the intensity of the parallel and perpendicular components is the output signal S ( $S = I_p/I_s$ ) (the output signal given by the detection box is  $10 \times S$ ). It is combined with a stagnation point flow cell, allowing the introduction of PBS solution or protein solutions, to study homogeneous adsorption on surfaces in diffusion-controlled conditions.<sup>66</sup>

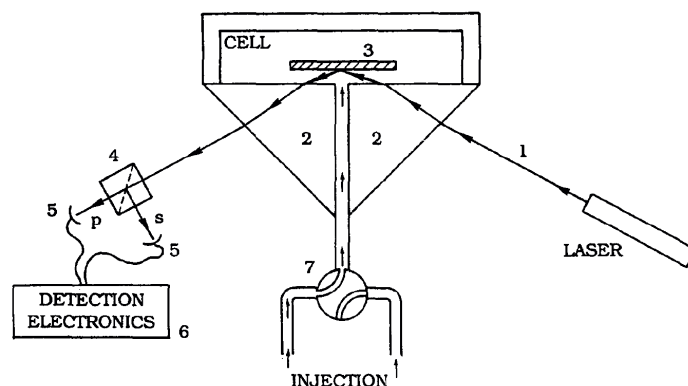


**Figure 1.** Schematic representation of the fixed angle reflectometer: 1) laser beam, 2) glass prism, 3) sample, 4) beam splitter, 5) photodiodes.<sup>66</sup>

Strips of  $\text{Si}_x\text{N}_4$ -coated silicon wafer (typical size of  $4 \times 0.75 \text{ cm}^2$ ) were modified with alkenes on one end (about half of the sample length), whereas the other end was used to hold the strip in the measuring cell of the reflectometer. The BSA solutions ( $0.1 \text{ g.L}^{-1}$ ) were freshly prepared in PBS solution (pH 6.7, ionic strength 0.08 M) and settled for one hour at room temperature before use in measurement. Due to a lower solubility in water, FIB solutions were prepared differently. First, PBS solution at pH 6.7 with a higher ionic strength of 0.16 M was prepared. The desired amount of FIB was added and the solution was gently shaken at 80 rpm at room temperature during 15 min to obtain a clear protein solution. Finally, the solution was diluted with water to obtain  $0.1 \text{ g.L}^{-1}$  of FIB in PBS solution at pH 6.7 with ionic strength 0.08 M. All reflectometry experiments were performed at  $23^\circ\text{C}$ . Before measurements were taken, surfaces were incubated 1 h in PBS solution to avoid artifacts due to initial surface wetting, which caused a baseline drift. After placing the samples in the reflectometer, the PBS solution was injected until the output signal was nearly constant: fluctuations of less than 1% over 5 min were considered satisfactory. Each experiment involved at least one adsorption phase, in which protein solutions were injected onto the surface, and one subsequent desorption phase, in which only PBS solution was injected. Details of the calculation of adsorbed protein amount are given in Appendix 2. Each experiment was repeated at least 3 times, and the reported data are average values.

## 3. Results and Discussion

### 3.1. Silicon Nitride Surface Modification with $\text{EO}_3$ and $\text{EO}_6$

Silicon nitride was functionalized in a one-step photochemical procedure as described in the Experimental Section. Hydrogen-terminated  $\text{Si}_x\text{N}_4$  surfaces were obtained by etching with HF, and the surfaces were subsequently employed in the photochemical attachment of  $\text{CH}_3\text{O}(\text{CH}_2\text{CH}_2\text{O})_3(\text{CH}_2)_9\text{CH}=\text{CH}_2$  [ $\text{EO}_3$ ] and  $\text{CH}_3\text{O}(\text{CH}_2\text{CH}_2\text{O})_6(\text{CH}_2)_9\text{CH}=\text{CH}_2$  [ $\text{EO}_6$ ]. Under UV irradiation, the double bonds readily react with silicon atoms on the hydrogen-terminated surface resulting in Si-C linkages. The resultant UV-modified  $\text{Si}_x\text{N}_4$  surfaces with covalently attached  $\text{EO}_3$  and  $\text{EO}_6$  monolayers exhibited very reproducible static water contact angles of  $64^\circ$  and  $58^\circ$  ( $\pm 1^\circ$ ), respectively, in agreement with previous reports on similar monolayers on other surfaces. Water contact angles of  $\text{EO}_3$ -modified  $\text{Si}_x\text{N}_4$  surfaces ( $64 \pm 1^\circ$ ) are identical to those measured for  $\text{EO}_3$  monolayers obtained with thiols on gold and silver,<sup>30</sup> but lower values were obtained for  $\text{EO}_3$  monolayers obtained by reaction of alkenes with hydrogen-terminated silicon ( $58 \pm 1^\circ$ ).<sup>40, 44</sup> In general, substrates coated with  $\text{EO}_3$  monolayers display water contact angle values smaller than 11-methoxyundecene thiol monolayers on gold surfaces

( $\sim 84^\circ$ ),<sup>28, 67</sup> suggesting that internal ether bonds of the ethylene oxide moieties are always partially exposed. EO<sub>6</sub> coatings on Si<sub>x</sub>N<sub>4</sub> were even more hydrophilic, with a contact angle of  $58 \pm 1^\circ$ , which is between the values of  $66^\circ$  and  $49^\circ$  ( $\pm 1^\circ$ ) observed for EO<sub>6</sub> monolayers on gold<sup>29</sup> and silicon<sup>40</sup> surfaces, respectively. The hydrophilic character of modified surfaces correlates with the disorder and the packing density of oligo(ethylene oxide) monolayers, exposing polar internal C-O bonds to the outer environment. It can thus be concluded that EO<sub>3</sub> monolayers on Si<sub>x</sub>N<sub>4</sub> are comparable to thiol monolayers on gold or silver, while EO<sub>6</sub> monolayers on Si<sub>x</sub>N<sub>4</sub> are slightly less densely packed.

It was attempted to measure this difference in density and the resulting thickness by X-ray reflectivity measurements. The thus obtained thicknesses for both types of monolayers is  $2.6 \pm 0.2$  nm, which would correspond to 95% and 70% of the length of extended EO<sub>3</sub> and EO<sub>6</sub> molecules, respectively. However, beside the 0.2 nm uncertainty associated with the reflectivity measurement, the initial roughness of bare amorphous Si<sub>x</sub>N<sub>4</sub> surfaces obtained by AFM ( $0.45 \pm 0.05$  nm for all surfaces used; see Table 1) yields an uncertainty of 0.6 nm. This makes these thicknesses obtained by X-ray reflectivity inconclusive to identify EO<sub>3</sub> and EO<sub>6</sub> monolayer, and thus hampers a direct comparison with reported values for EO<sub>3</sub> and EO<sub>6</sub> monolayers on gold surfaces ( $2.0 \pm 0.2$  and  $2.8 \pm 0.2$  nm,<sup>28</sup> respectively).

**Table 1.** RMS roughness measured by AFM on oxidized Si<sub>x</sub>N<sub>4</sub> and on EO<sub>n</sub>-coated Si<sub>x</sub>N<sub>4</sub>, before and after exposure to protein solution [Values are  $\pm 0.05$  nm].

Samples	Before adsorption (nm)	After BSA adsorption (nm)	Before adsorption (nm)	After FIB adsorption (nm)
Oxidized Si <sub>x</sub> N <sub>4</sub>	0.48	0.81	0.49	0.80
Si <sub>x</sub> N <sub>4</sub> -EO <sub>3</sub>	0.49	0.57	n.d.	n.d.
Si <sub>x</sub> N <sub>4</sub> -EO <sub>6</sub>	0.45	0.52	0.40	0.44

The C<sub>1s</sub> regions of the XPS data measured on EO<sub>3</sub> and EO<sub>6</sub> monolayers (Figure 2) display the two characteristic peaks corresponding to carbon of the hydrocarbon chains (C-C at 285.0 eV) and oxygen-bound carbon (C-O at 286.8 eV). After fitting the high-resolution spectra, the measured (C-C)/(C-O) ratios of 1.30 (EO<sub>3</sub> coatings) and 0.77 (EO<sub>6</sub> coatings) are close to the theoretical stoichiometry values of 1.25 (10/8) and 0.71 (10/14), showing the intact attachment of the EO alkenes. Similar attachment experiments at elevated temperatures lead to cleavage of the EO moieties, showing the necessity of this mild attachment with light.

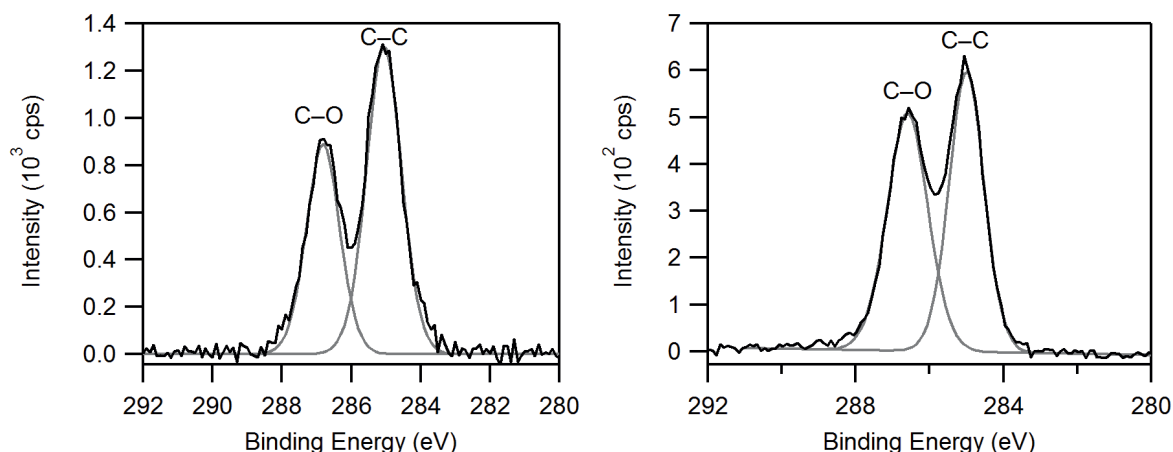


**Figure 2.** XPS narrow-scan spectra of  $C_{1s}$  region of  $Si_xN_4$  ( $x \approx 4$ ) surfaces coated with ethylene oxide-containing monolayers:  $EO_3$  (left) and  $EO_6$  (right).

The AFM images of coated substrates (Figure 3) show a typical clean  $Si_xN_4$  surface after oxidation (left), and two analogous surfaces coated with  $EO_3$  (center) and  $EO_6$  (right) monolayers. Images and profile traces appear identical before and after modification, still displaying the structure of the initial  $Si_xN_4$  substrate, with only marginal sample-to-sample variation.

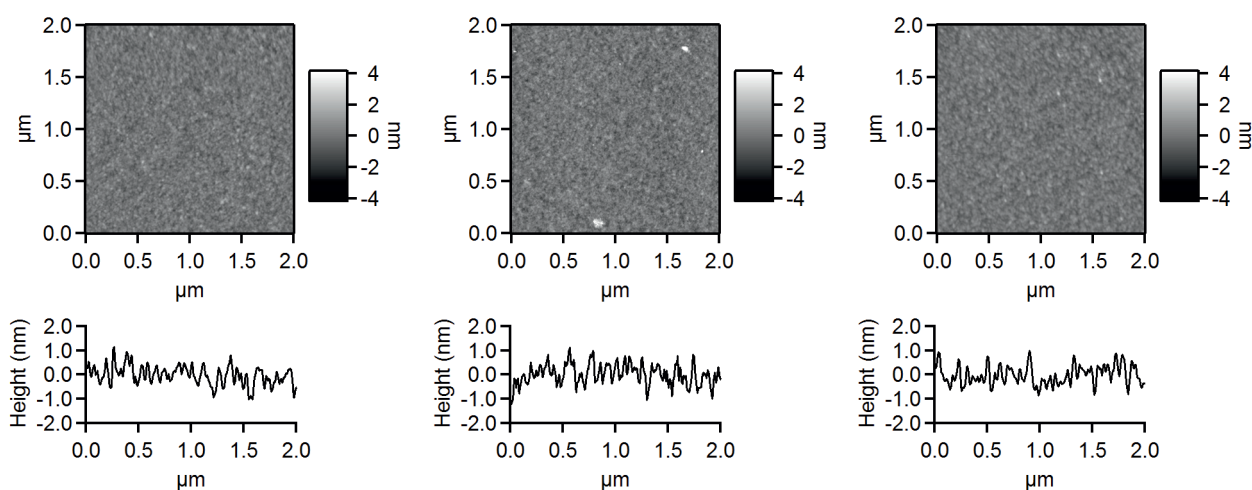


**Figure 3.** AFM images of oxidized (left),  $EO_3$ -coated (center), and  $EO_6$ -coated (right)  $Si_xN_4$  surfaces and corresponding profile traces.

From these characterizations (water contact angle, XPS, AFM and X-ray reflectivity) it can be concluded that by using UV irradiation homogeneous  $EO_3$  and  $EO_6$  monolayers on silicon nitride surfaces are obtained reproducibly. Moreover these monolayers display comparable features as observed earlier for such monolayers on silicon and gold surfaces. However, the higher stability of these coatings on  $Si_xN_4$  makes them preferred for applications where long-term stability of surfaces is required.<sup>55, 56, 64</sup>

### 3.2. Protein Adsorption onto Modified $\text{Si}_x\text{N}_4$ Surfaces

In contrast to all the *ex situ* techniques used to monitor protein adsorption onto surfaces (e.g., contact angle, AFM, XPS, ellipsometry, quartz micro balance), reflectometry allows *in situ* observation of protein adsorption without removing the surface from the protein solution and without intermediate cleaning steps. In addition, this allows one to distinguish between reversible and irreversible adsorption during the adsorption and rinsing phases, respectively. Air-based plasma oxidized surfaces ( $\text{SiO}_y\text{-Si}_x\text{N}_4$ ) were used as references in our protein adsorption survey. Other studies have reported protein-repellent behavior by comparison with methyl-terminated surfaces, obtained by formation of alkyl monolayers on silicon<sup>44</sup> or gold surfaces.<sup>28</sup> In fact, such hydrophobic surfaces adsorb significantly more protein in aqueous solution, compared to hydrophilic surfaces, to minimize interfacial tension between coatings and water phase. In comparison, the hydrophilic surfaces, which have a higher surface energy, have a low interfacial energy with water, as a result, it is less favorable for proteins to adsorb on the surfaces, i.e., the surfaces repel proteins.<sup>68</sup> In agreement with these earlier observations, our experimental results showed that the protein adsorption onto hydrophobic hexadecane-coated  $\text{Si}_x\text{N}_4$  surfaces ( $\text{C}_{16}\text{-Si}_x\text{N}_4$ ) is much higher than that of  $\text{SiO}_y\text{-Si}_x\text{N}_4$  surfaces. The adsorption of FIB on  $\text{C}_{16}\text{-Si}_x\text{N}_4$  surfaces was 91% higher than on  $\text{SiO}_y\text{-Si}_x\text{N}_4$  surfaces and 12% higher for BSA. These results show that the adsorption of proteins onto hydrophobic and hydrophilic surfaces differs significantly depending on the type of protein, and in the case of monolayer-modified surfaces will likely vary with the quality of the monolayer. Therefore, the use of hydrophilic  $\text{SiO}_y\text{-Si}_x\text{N}_4$  surfaces as reference allowed us to have a stricter comparison in the efficiency of the protein repellence of hydrophilic EO coatings.

When exposed to protein solutions, the  $\text{SiO}_y\text{-Si}_x\text{N}_4$  surfaces showed a reproducible maximum adsorbed amount of  $1.25 \pm 0.1 \text{ mg.m}^{-2}$  of BSA, and  $3.0 \pm 0.1 \text{ mg.m}^{-2}$  of FIB (Figure 4). There was no desorption during cleaning with PBS solution, showing that the adsorption is almost entirely irreversible. The difference in the maximum adsorbed amounts of FIB and BSA on  $\text{SiO}_y\text{-Si}_x\text{N}_4$  surfaces are partially due to differences in the charges on the proteins. The pI value of FIB is 6.0, which indicates that FIB is nearly neutral at pH 6.7. In contrast, BSA has a pI value of 4.7, showing that BSA is negatively charged in PBS solution. Thus, BSA has difficulties to approach the surface due to repulsive electrostatic forces at the negatively charged  $\text{SiO}_y\text{-Si}_x\text{N}_4$  surfaces (pI = 1.7 - 3.5),<sup>69</sup> leading to a low adsorption rate. Once the protein has attached to the surface, it relaxes toward a (set of) new equilibrium structure(s) to optimize the protein-surface interaction. This normally involves a certain degree of spreading of the protein over the surface, creating more contacts with the surface.<sup>70</sup> As a consequence, it will be less

favorable for the next protein to adhere. This results in a low maximum adsorbed amount of BSA on  $\text{SiO}_x\text{-Si}_x\text{N}_4$ . In comparison, FIB can more easily approach the surface due to the neutrality of the protein under our experimental conditions. Thus, it adsorbs onto the surface with a higher adsorption rate, leading to early full occupation on the surfaces (plateau region). This leaves less space for the protein to spread out on the surface. The data shows that the adsorption can reach the plateau region corresponding to saturated occupation of the surface within 3 min in the case of FIB and 20 min for BSA (Figure 5).

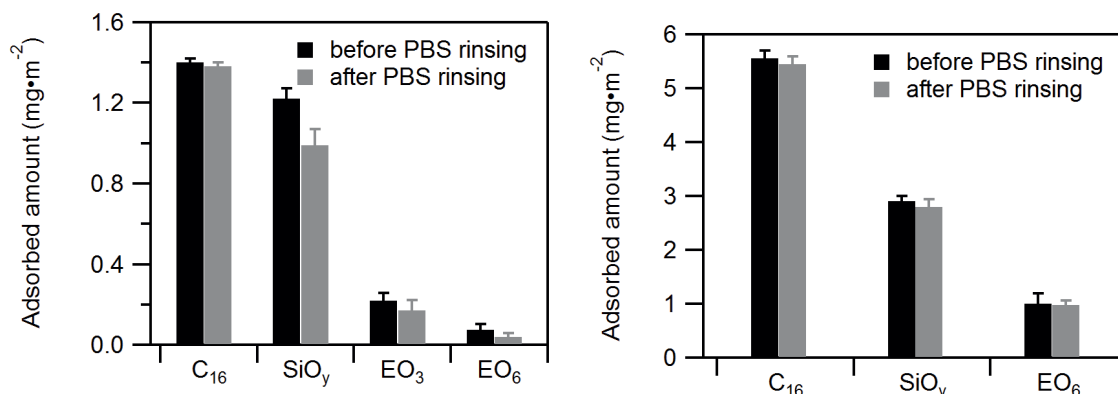


**Figure 4.** Reflectometry data: adsorbed amounts of BSA (left) and FIB (right) onto hexadecane-coated  $\text{Si}_x\text{N}_4$  ( $\text{C}_{16}$ ), plasma-oxidized  $\text{Si}_x\text{N}_4$  ( $\text{SiO}_y$ ) and  $\text{EO}_3/\text{EO}_6$ -coated  $\text{Si}_x\text{N}_4$  surfaces ( $\text{EO}_3$  and  $\text{EO}_6$ ), after subsequent exposure to protein solution and to PBS solution.

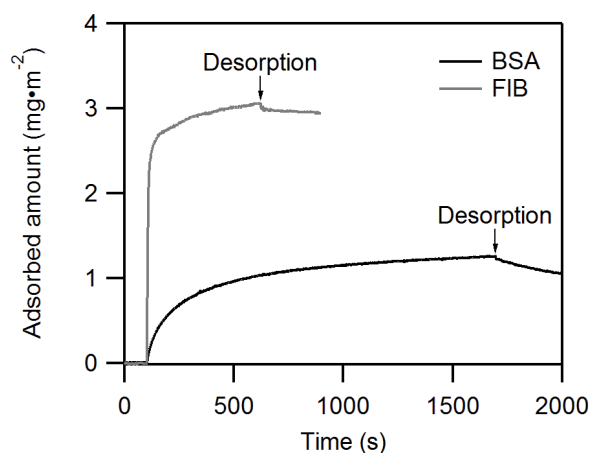


**Figure 5.** Protein adsorption of  $0.1 \text{ g}\cdot\text{L}^{-1}$  BSA and FIB solution onto  $\text{SiO}_y\text{-Si}_3\text{N}_4$  surfaces.

The adsorbed amount of BSA on  $\text{EO}_3\text{-Si}_x\text{N}_4$  was  $0.22 \text{ mg}\cdot\text{m}^{-2}$ , corresponding to 82% repellence compared to  $\text{SiO}_y\text{-Si}_x\text{N}_4$ . Water contact angle measurements on the exposed surfaces revealed similar values, most likely due to the adhesion of small amounts of protein (Figure 6). Remarkably,  $\text{EO}_6\text{-Si}_x\text{N}_4$  surfaces only adsorbed  $0.08 \text{ mg}\cdot\text{m}^{-2}$ , corresponding to 94% repellence. These results demonstrate the important role of the



length of ethylene oxide chain in the repulsion of proteins. Our experimental data is in agreement with the results of Grunze and co-workers on similar work on gold surfaces about protein repellence of  $\text{EO}_n$  coatings,<sup>29</sup> and with several simulation studies on the role of hydration layers in protein repellent coatings.<sup>71-73</sup> A longer chain of ethylene oxide results in a thicker hydrophilic part within the coating, which plays a crucial role in the repellence of proteins. As  $\text{EO}_6\text{-Si}_x\text{N}_4$  coated surfaces gave a better protein repellent property compared to  $\text{EO}_3\text{-Si}_x\text{N}_4$  surfaces, we used  $\text{EO}_6\text{-Si}_x\text{N}_4$  surfaces to study the behavior of ethylene oxide chain with different protein, i.e., FIB and its stability.

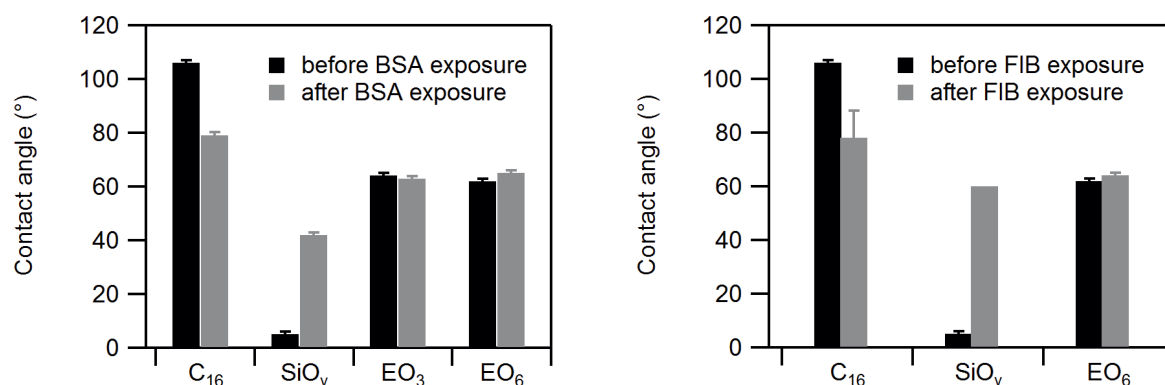


**Figure 6.** Static water contact angles values before and after adsorption of BSA (left) and FIB (right) onto hexadecane-coated  $\text{Si}_x\text{N}_4$  ( $\text{C}_{16}$ ), plasma-oxidized  $\text{Si}_x\text{N}_4$  ( $\text{SiO}_y$ ) and  $\text{EO}_3/\text{EO}_6$ -coated  $\text{Si}_x\text{N}_4$  surfaces ( $\text{EO}_3$  and  $\text{EO}_6$ ), after subsequent exposure to protein solution and to PBS solution.

Higher adsorbed amounts of FIB were observed on  $\text{EO}_6\text{-Si}_x\text{N}_4$  modified surfaces ( $1 \pm 0.05 \text{ mg.m}^{-2}$ ) as compared to BSA, corresponding to 67% repellence by the modified surface, with water contact angle values of these  $\text{EO}_6\text{-Si}_x\text{N}_4$  surfaces that were the same before and after exposure to protein solution. This latter observation can be attributed to similarity in hydrophilicity between  $\text{EO}_n$ -modified surfaces and adsorbed protein layer as explained earlier. The adsorption of FIB on  $\text{C}_{16}\text{-Si}_x\text{N}_4$  and  $\text{SiO}_x\text{-Si}_x\text{N}_4$  surfaces was also considerably higher than BSA,  $5.6 \text{ mg.m}^{-2}$  and  $2.9 \text{ mg.m}^{-2}$  respectively. FIB is a fibrous protein (MW = 340 kDa) with dimensions of about  $9 \times 9 \times 45 \text{ nm}^3$ ,<sup>74</sup> and has a weak internal cohesion. In comparison, BSA is a globular protein (MW = 69 kDa) with dimensions of  $4 \times 4 \times 14 \text{ nm}^3$ ,<sup>75</sup> having a compact structure and stronger cohesion, which is less favorable as compared to FIB for the structural rearrangement when proteins absorb onto a surface.<sup>76</sup> This is supported by DLVO theory, which describes the forces between interacting surfaces through a liquid medium.<sup>77</sup> A calculation of the Van der Waals interactions between proteins (FIB and BSA) and monolayer-modified surfaces indicates that the interaction between FIB and the surface is approximately 4 times greater than the energy of thermal motion, whereas the Van der Waals interaction between BSA

and the surface is only half the energy of thermal motion (see Appendix 3). These results are in agreement with the experimental finding of a higher adsorption rate for FIB as compared to BSA.

In addition, we noticed that the preparation of the FIB solution influenced the total adsorbed amount of protein, whereas its adsorption onto  $\text{SiO}_y\text{-Si}_x\text{N}_4$  surfaces was approximately the same as in the case of FIB solution prepared as described in the Experimental Section. A thick foam layer on top of the protein solution formed during shaking and remained even after settling for one hour at room temperature. As a result, the obtained concentration in bulk solution was likely significantly reduced. Furthermore, this procedure probably causes denaturation of proteins, leading to changes in protein conformation and thus in the adsorption behavior of the proteins onto the surface. Finally, shaking caused the adsorbed amount of FIB onto  $\text{EO}_6\text{-Si}_x\text{N}_4$  surfaces to become irreproducible. In comparison, dissolving FIB gently at higher ionic strength resulted in homogeneous solutions without foam,<sup>78</sup> i.e., a desired amount of FIB was dissolved in high ionic strength PBS solution ( $I = 0.16 \text{ M}$ ), subsequently the solution was diluted with water to obtain  $0.08 \text{ M}$  ionic strength PBS solution, and finally gently shaken (80 rpm) at room temperature for 15 min to obtain homogeneous solution. A very reproducible maximum adsorbed amount was achieved when the protein was dissolved gently.

### 3.3. Stability of Modified $\text{Si}_x\text{N}_4$ Surfaces in Aqueous Media

The stability of antifouling poly(ethylene oxide) coatings immobilized onto silicon substrates via organosilane chemistry has been investigated by several research groups.<sup>53, 79-81</sup> Ethylene oxides are known to degrade upon exposure to water, and an auto-oxidation mechanism has recently been reported by Qin et al.<sup>79</sup> Monolayer degradation is a complex process, which depends on the nature and chemical stability of the monolayer molecules, the type of connection between the modified layer and the substrate, as well as the packing density and ordering of the immobilized molecules. However, prolonged stability studies were not performed. The usefulness of functionalized surfaces hinges for many applications around the stability of that functionalization upon long-term exposure to aqueous solutions. We therefore studied the stability of the  $\text{EO}_6$ -monolayers on silicon nitride surfaces in PBS during 1 week. Static water contact angles were measured daily, and the results are depicted in Figure 7. A slight increase in contact angle ( $\sim 6^\circ$ ) was measured after the first day, but no significant changes were observed during the following days. XPS measurements were performed before and after exposure to PBS. After 7 days in PBS, the wide-scan XPS spectra of modified silicon nitride substrates revealed a decrease in the C/Si ratio from 1.09 to 0.75 ( $31 \pm 3\%$ ). The XPS narrow-scan



of the  $C_{1s}$  region showed a reduction of the C-O signal at 286.7 eV, and a decrease in the C-O/C-C ratio from 1.25 to 0.99 ( $20 \pm 3\%$ ), which corresponds approximately to an average of 1 unit of ethylene oxide being cleaved off (Figure 8 and Figure 9). This cleavage is attributed to auto-oxidation of ethylene oxide moieties.<sup>79, 80</sup> This minor degradation is most likely the reason for the change in contact angle that was observed. Interestingly, in the XPS narrow-scan spectrum of the  $Si_{2p}$  region, no oxidation of the exposed substrates was observed, demonstrating the robustness of the Si-C linkage.

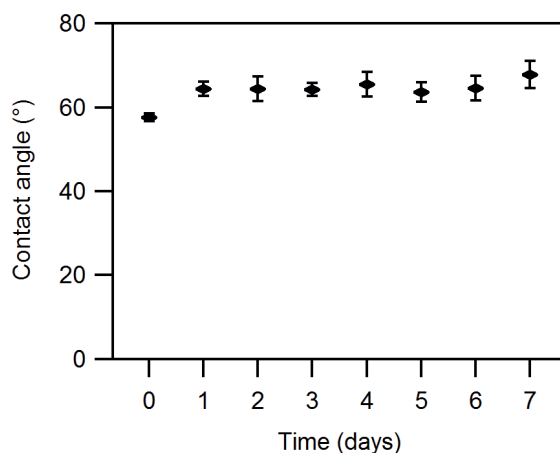


**Figure 7.** Static water contact angle of  $EO_6-Si_3N_4$  surfaces exposed to PBS solution for 1 week.

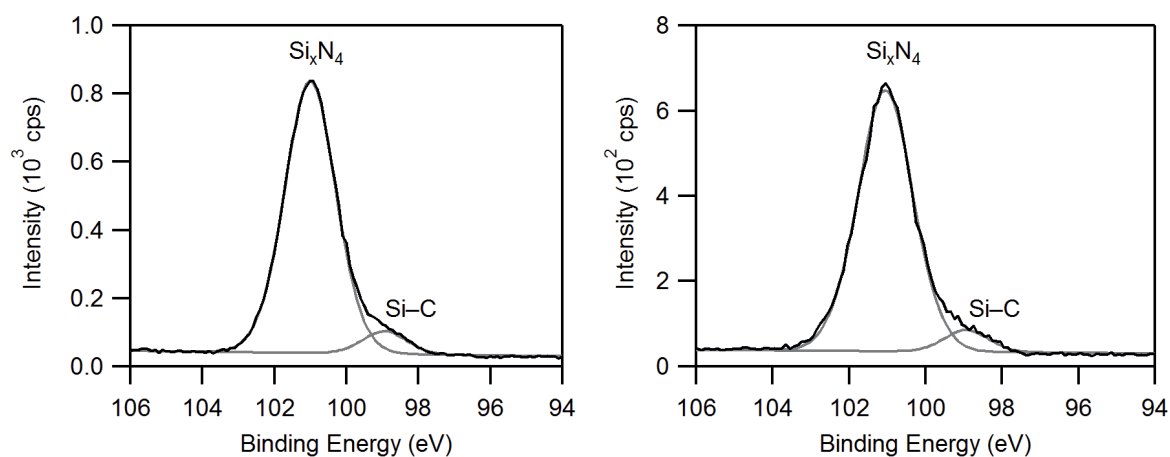


**Figure 8.** XPS narrow-scan spectra of  $Si_{2p}$  region of  $EO_6-Si_3N_4$  surfaces before exposure (left) and after exposure (right) to PBS solution for 1 week.

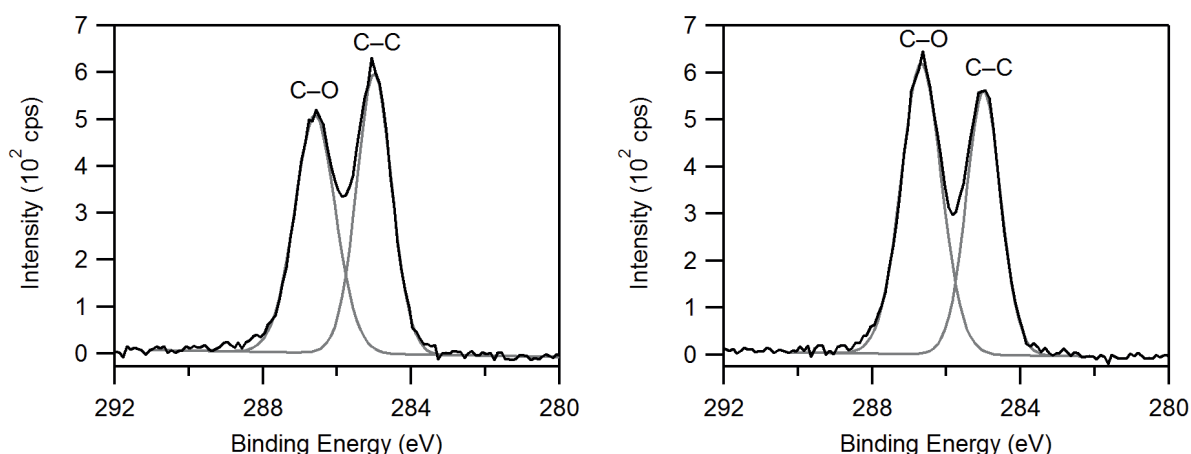


**Figure 9.** XPS narrow-scan spectra of  $C_{1s}$  region of  $EO_6-Si_3N_4$  surfaces before exposure (left) and after exposure (right) to PBS solution for 1 week.

After a week in PBS the majority of the ethylene oxide segments are still intact, and so the monolayer should also still be able to repel proteins. The protein repellency of the exposed  $EO_6$ -coated surfaces was therefore investigated, and reflectometry measurements revealed that the maximum adsorbed amount of BSA on the exposed surface was  $0.44 \pm 0.05 \text{ mg.m}^{-2}$ . In other words, even after exposure of a week to PBS solution, 65% of BSA was still repelled, as compared to plasma-oxidized silicon nitride surfaces.

Recently, Sano et al. reported on the stability of monolayers bound onto Si (111) surfaces via Si-C and Si-O-C bonds in various basic and acidic media during 1 h.<sup>53</sup> The Si-C bound monolayers showed superior stability compared to monolayers bound via Si-O-C linkages. To determine the application potential of the modified surfaces, the stability of the  $EO_6$  modified  $Si_3N_4$  surfaces were further studied in alkaline condition (pH 10) at room temperature for 2 h. Static water contact angle measurements and XPS were used to characterize the surfaces before and after the stability study. No significant change in water contact angle value was observed. The ratio of C/Si derived from the wide-scan XPS spectra changed only to a minor degree, within error of measurement. The narrow-scan XPS spectrum of the  $C_{1s}$  region, however, showed cleavage of 1.5 EO units (on average) from the oligo(ethylene oxide) chain. The narrow-scan XPS spectrum of the  $Si_{2p}$  region did not show a silicon oxide peak at 104 eV (Figure 10). These results indicate that the degradation mainly occurs at the ethylene oxide chain due to auto-oxidation as mentioned before, whereas the Si-C linkage remains intact not only in PBS solution but also under alkaline conditions.

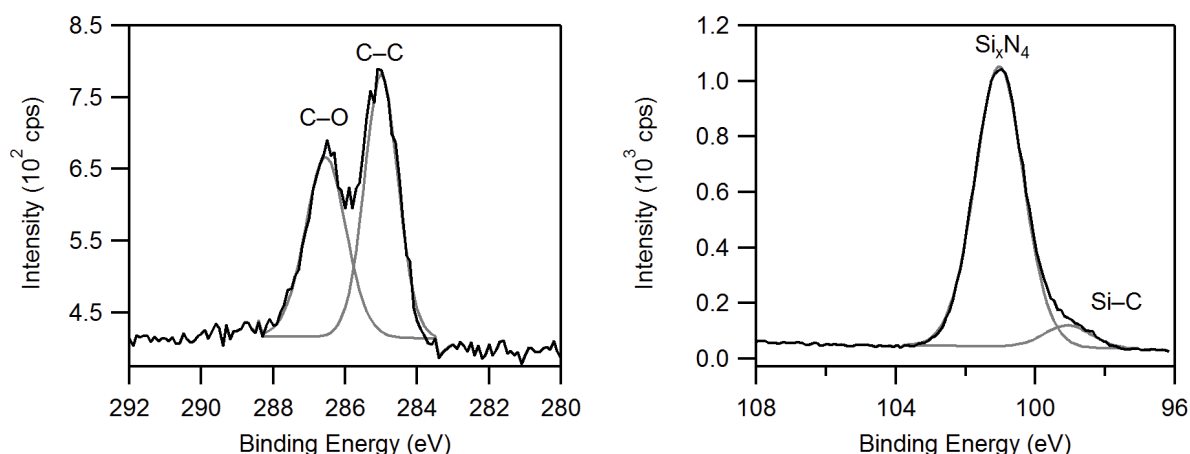


**Figure 10.** Narrow-scan XPS spectra of C<sub>1s</sub> region (left) and Si<sub>2p</sub> region (right) of EO<sub>6</sub>-modified Si<sub>x</sub>N<sub>4</sub> surface after exposure to aqueous NaOH solution (0.1 mM, pH 10) for 2 h.

## 4. Conclusions

For the first time, well-defined monolayers of short oligo(ethylene oxide) chains, CH<sub>3</sub>O(CH<sub>2</sub>CH<sub>2</sub>O)<sub>3</sub>(CH<sub>2</sub>)<sub>11</sub> [EO<sub>3</sub>] and CH<sub>3</sub>O(CH<sub>2</sub>CH<sub>2</sub>O)<sub>6</sub>(CH<sub>2</sub>)<sub>11</sub> [EO<sub>6</sub>] were successfully grafted onto silicon-rich Si<sub>x</sub>N<sub>4</sub> surfaces using a photochemical attachment of 1-alkenes at room temperature.<sup>64</sup> Such EO<sub>n</sub>-modified Si<sub>x</sub>N<sub>4</sub> surfaces displayed excellent protein-repelling behavior. EO<sub>6</sub> monolayers reduced the adsorption of proteins (FIB and BSA) significantly as compared to SiO<sub>y</sub>-Si<sub>x</sub>N<sub>4</sub>. In addition, a strong dependence on the dissolution method of FIB on the adsorption efficiency was found. Investigations into the stability of EO<sub>6</sub>-Si<sub>x</sub>N<sub>4</sub> surfaces revealed minor degradation of the ethylene oxide moieties upon exposure to PBS for 1 week, as well as upon exposure under alkaline conditions (pH 10) for 2 h, whereas no oxidation of the substrate was observed. The inertness of the silicon nitride substrate and the robust Si-C linkage through which the monolayers are coupled provide for highly stable substrates. The excellent antifouling behavior combined with the high stability of these monolayers opens up a wide range of practical applications, such as in reactor walls, biosensors, or lithographically prepared microsieves.

## 5. ACKNOWLEDGMENT

The authors thank Graduate School VLAG and MicroNed (Project no. 6163510395 and no. 6163510587) for financial support.

## 6. REFERENCES

- (1) Patil, L. S.; Pandey, R. K.; Bange, J. P.; Gaikwad, S. A.; Gautam, D. K., Effect of deposition temperature on the chemical properties of thermally deposited silicon nitride films. *Opt. Mater.* **2005**, *27*, 663-670.
- (2) Bermudez, V. M.; Perkins, F. K., Preparation and properties of clean Si<sub>3</sub>N<sub>4</sub> surfaces. *Appl. Surf. Sci.* **2004**, *235*, 406-419.
- (3) Antsiferov, V. N.; Gilev, V. G.; Karmanov, V. I., Infrared spectra and structure of Si<sub>3</sub>N<sub>4</sub>, Si<sub>2</sub>ON<sub>2</sub>, and sialons. *Refract. Ind. Ceram.* **2003**, *44*, 108-114.
- (4) Rathi, V. K.; Gupta, M.; Agnihotri, O. P., The Dependence of Etch Rate of Photo-CVD Silicon-Nitride Films on NH<sub>4</sub>F Content in Buffered HF. *Microelectron. J.* **1995**, *26*, 563.
- (5) Kuiper, S.; van Wolferen, H.; van Rijn, C.; Nijdam, W.; Krijnen, G.; Elwenspoek, M., Fabrication of microsieves with sub-micron pore size by laser interference lithography. *J. Micromech. Microeng.* **2001**, *11*, 33-37.
- (6) van Rijn, C. J. M.; Veldhuis, G. J.; Kuiper, S., Nanosieves with microsystem technology for microfiltration applications. *Nanotechnology* **1998**, *9*, 343-345.
- (7) van Rijn, C. J. M., *Nano and Micro Engineered Membrane Technology*. Elsevier: Amsterdam, The Netherlands, 2004.
- (8) Kuiper, S.; Brink, R.; Nijdam, W.; Krijnen, G. J. M.; Elwenspoek, M. C., Ceramic microsieves: influence of perforation shape and distribution on flow resistance and membrane strength. *J. Membr. Sci.* **2002**, *196*, 149-157.
- (9) Girones, M.; Lammertink, R. G. H.; Wessling, M., Protein aggregate deposition and fouling reduction strategies with high-flux silicon nitride microsieves. *J. Membr. Sci.* **2006**, *273*, 68-76.
- (10) Marshall, A. D.; Munro, P. A.; Tragardh, G., The Effect of Protein Fouling in Microfiltration and Ultrafiltration on Permeate Flux, Protein Retention and Selectivity - a Literature-Review. *Desalination* **1993**, *91*, 65-108.
- (11) Vanloosdrecht, M. C. M.; Lyklema, J.; Norde, W.; Zehnder, A. J. B., Influence of Interfaces on Microbial Activity. *Microbiol. Rev.* **1990**, *54*, 75-87.
- (12) Koehler, J. A.; Ulbricht, M.; Belfort, G., Intermolecular forces between a protein and a hydrophilic modified polysulfone film with relevance to filtration. *Langmuir* **2000**, *16*, 10419-10427.
- (13) Ulbricht, M.; Belfort, G., Surface Modification of Ultrafiltration Membranes by Low-Temperature Plasma .1. Treatment of Polyacrylonitrile. *J. Appl. Polymer Sci.* **1995**, *56*, 325-343.
- (14) Ulbricht, M.; Belfort, G., Surface modification of ultrafiltration membranes by low temperature plasma .2. Graft polymerization onto polyacrylonitrile and polysulfone. *J. Membr. Sci.* **1996**, *111*, 193-215.

- (15) Girones, M.; Borneman, Z.; Lammertink, R. G. H.; Wessling, M., The role of wetting on the water flux performance of microsieve membranes. *J. Membr. Sci.* **2005**, *259*, 55-64.
- (16) Amirgoulova, E. V.; Groll, J.; Heyes, C. D.; Ameringer, T.; Rocker, C.; Moller, M.; Nienhaus, G. U., Biofunctionalized polymer surfaces exhibiting minimal interaction towards immobilized proteins. *ChemPhysChem* **2004**, *5*, 552-555.
- (17) Bosker, W. T. E.; Iakovlev, P. A.; Norde, W.; Cohen Stuart, M. A., BSA adsorption on bimodal PEO brushes. *J. Colloid Interface Sci.* **2005**, *286*, 496-503.
- (18) Bremmell, K. E.; Kingshott, P.; Ademovic, Z.; Winther-Jensen, B.; Griesser, H. J., Colloid probe AFM investigation of interactions between fibrinogen and PEG-like plasma polymer surfaces. *Langmuir* **2006**, *22*, 313-318.
- (19) Cecchet, F.; De Meersman, B.; Demoustier-Champagne, S.; Nysten, B.; Jonas, A. M., One step growth of protein antifouling surfaces: Monolayers of poly(ethylene oxide) (PEO) derivatives on oxidized and hydrogen-passivated silicon surfaces. *Langmuir* **2006**, *22*, 1173-1181.
- (20) Krishnan, S.; Ayothi, R.; Hexemer, A.; Finlay, J. A.; Sohn, K. E.; Perry, R.; Ober, C. K.; Kramer, E. J.; Callow, M. E.; Callow, J. A.; Fischer, D. A., Anti-biofouling properties of comblike block copolymers with amphiphilic side chains. *Langmuir* **2006**, *22*, 5075-5086.
- (21) Lazos, D.; Franzka, S.; Ulbricht, M., Size-selective protein adsorption to polystyrene surfaces by self-assembled grafted poly(ethylene glycols) with varied chain lengths. *Langmuir* **2005**, *21*, 8774-8784.
- (22) Yam, C. M.; Deluge, M.; Tang, D.; Kumar, A.; Cai, C. Z., Preparation, characterization, resistance to protein adsorption, and specific avidin-biotin binding of poly (amidoamine) dendrimers functionalized with oligo(ethylene glycol) on gold. *J. Colloid Interface Sci.* **2006**, *296*, 118-130.
- (23) Vanderah, D. J.; Pham, C. P.; Springer, S. K.; Silin, V.; Meuse, C. W., Characterization of a series of self-assembled monolayers of alkylated 1-thiaoligo (ethylene oxides)<sub>(4-8)</sub> on Gold. *Langmuir* **2000**, *16*, 6527-6532.
- (24) Unsworth, L. D.; Sheardown, H.; Brash, J. L., Protein resistance of surfaces prepared by sorption of end-thiolated poly(ethylene glycol) to gold: Effect of surface chain density. *Langmuir* **2005**, *21*, 1036-1041.
- (25) Seigel, R. R.; Harder, P.; Dahint, R.; Grunze, M.; Josse, F.; Mrksich, M.; Whitesides, G. M., On-line detection of nonspecific protein adsorption at artificial surfaces. *Anal. Chem.* **1997**, *69*, 3321-3328.
- (26) Prime, K. L.; Whitesides, G. M., Adsorption of Proteins onto Surfaces Containing End-Attached Oligo(Ethylene Oxide) - a Model System Using Self-Assembled Monolayers. *J. Am. Chem. Soc.* **1993**, *115*, 10714-10721.
- (27) Prime, K. L.; Whitesides, G. M., Self-Assembled Organic Monolayers - Model Systems for Studying Adsorption of Proteins at Surfaces. *Science* **1991**, *252*, 1164-1167.

- (28) Palegrosdemange, C.; Simon, E. S.; Prime, K. L.; Whitesides, G. M., Formation of Self-Assembled Monolayers by Chemisorption of Derivatives of Oligo(Ethylene Glycol) of Structure  $\text{HS}(\text{CH}_2)_{11}(\text{OCH}_2\text{CH}_2)_m\text{OH}$  on Gold. *J. Am. Chem. Soc.* **1991**, *113*, 12-20.
- (29) Herrwerth, S.; Eck, W.; Reinhardt, S.; Grunze, M., Factors that determine the protein resistance of oligoether self-assembled monolayers - Internal hydrophilicity, terminal hydrophilicity, and lateral packing density. *J. Am. Chem. Soc.* **2003**, *125*, 9359-9366.
- (30) Harder, P.; Grunze, M.; Dahint, R.; Whitesides, G. M.; Laibinis, P. E., Molecular conformation in oligo(ethylene glycol)-terminated self-assembled monolayers on gold and silver surfaces determines their ability to resist protein adsorption. *J. Phys. Chem. B* **1998**, *102*, 426-436.
- (31) Chan, Y. H. M.; Schweiss, R.; Werner, C.; Grunze, M., Electrokinetic characterization of oligo- and poly(ethylene glycol)-terminated self-assembled monolayers on gold and glass surfaces. *Langmuir* **2003**, *19*, 7380-7385.
- (32) Heyes, C. D.; Kobitski, A. Y.; Amirgoulova, E. V.; Nienhaus, G. U., Biocompatible surfaces for specific tethering of individual protein molecules. *J. Phys. Chem. B* **2004**, *108*, 13387-13394.
- (33) Hoffmann, C.; Tovar, G. E. M., Mixed self-assembled monolayers (SAMs) consisting of methoxy-tri(ethylene glycol)-terminated and alkyl-terminated dimethylchlorosilanes control the non-specific adsorption of proteins at oxidic surfaces. *J. Colloid Interface Sci.* **2006**, *295*, 427-435.
- (34) Lee, S. W.; Laibinis, P. E., Protein-resistant coatings for glass and metal oxide surfaces derived from oligo(ethylene glycol)-terminated alkyltrichlorosilanes. *Biomaterials* **1998**, *19*, 1669-1675.
- (35) Ma, H. W.; Li, D. J.; Sheng, X.; Zhao, B.; Chilkoti, A., Protein-resistant polymer coatings on silicon oxide by surface-initiated atom transfer radical polymerization. *Langmuir* **2006**, *22*, 3751-3756.
- (36) Norde, W.; Gage, D., Interaction of bovine serum albumin and human blood plasma with PEO-tethered surfaces: Influence of PEO chain length, grafting density, and temperature. *Langmuir* **2004**, *20*, 4162-4167.
- (37) Roosjen, A.; Kaper, H. J.; van der Mei, H. C.; Norde, W.; Busscher, H. J., Inhibition of adhesion of yeasts and bacteria by poly(ethylene oxide)-brushes on glass in a parallel plate flow chamber. *Microbiology* **2003**, *149*, 3239-3246.
- (38) Roosjen, A.; van der Mei, H. C.; Busscher, H. J.; Norde, W., Microbial adhesion to poly(ethylene oxide) brushes: Influence of polymer chain length and temperature. *Langmuir* **2004**, *20*, 10949-10955.
- (39) Schlapak, R.; Pammer, P.; Armitage, D.; Zhu, R.; Hinterdorfer, P.; Vaupel, M.; Fruhwirth, T.; Howorka, S., Glass surfaces grafted with high-density poly(ethylene glycol) as substrates for DNA oligonucleotide microarrays. *Langmuir* **2006**, *22*, 277-285.

- (40) Yam, C. M.; Lopez-Romero, J. M.; Gu, J. H.; Cai, C. Z., Protein-resistant monolayers prepared by hydrosilylation of  $\alpha$ -oligo(ethylene glycol)- $\omega$ -alkenes on hydrogen-terminated silicon (111) surfaces. *Chem. Commun.* **2004**, 2510-2511.
- (41) Yam, C. M.; Gu, J. H.; Li, S.; Cai, C. Z., Comparison of resistance to protein adsorption and stability of thin films derived from  $\alpha$ -hepta-(ethylene glycol) methyl  $\omega$ -undecenyl ether on H-Si(111) and H-Si(100) surfaces. *J. Colloid Interface Sci.* **2005**, 285, 711-718.
- (42) Bocking, T.; Killan, K. A.; Gaus, K.; Gooding, J. J., Single-step DNA immobilization on antifouling self-assembled monolayers covalently bound to silicon (111). *Langmuir* **2006**, 22, 3494-3496.
- (43) Bocking, T.; Kilian, K. A.; Hanley, T.; Ilyas, S.; Gaus, K.; Gal, M.; Gooding, J. J., Formation of tetra(ethylene oxide) terminated Si-C linked monolayers and their derivatization with glycine: An example of a generic strategy for the immobilization of biomolecules on silicon. *Langmuir* **2005**, 21, 10522-10529.
- (44) Bocking, T.; Gal, M.; Gaus, K.; Gooding, J. J., Evidence for why tri(ethylene oxide) functionalized Si-C linked monolayers on Si(111) have inferior protein antifouling properties relative to the equivalent alkanethiol monolayers assembled on gold. *Aust. J. Chem.* **2005**, 58, 660-663.
- (45) Ebner, A.; Wildling, L.; Kamruzzahan, A. S. M.; Rankl, C.; Wruss, J.; Hahn, C. D.; Holzl, M.; Zhu, R.; Kienberger, F.; Blaas, D.; Hinterdorfer, P.; Gruber, H. J., A new, simple method for linking of antibodies to atomic force microscopy tips. *Bioconjugate Chem.* **2007**, 18, 1176-1184.
- (46) Gabriel, S.; Jerome, C.; Jerome, R.; Fustin, C. A.; Pallandre, A.; Plain, J.; Jonas, A. M.; Duwez, A. S., One-step polymer grafting from silicon nitride SPM probes: From isolated chains to brush regime. *J. Am. Chem. Soc.* **2007**, 129, 8410-8411.
- (47) Gu, C.; Ray, C.; Guo, S.; Akhremitchev, B. B., Single-molecule force Spectroscopy measurements of interactions between C-60 fullerene molecules. *J. Phys. Chem. C* **2007**, 111, 12898-12905.
- (48) Kamruzzahan, A. S. M.; Ebner, A.; Wildling, L.; Kienberger, F.; Riener, C. K.; Hahn, C. D.; Pollheimer, P. D.; Winklehner, P.; Holzl, M.; Lackner, B.; Schorkl, D. M.; Hinterdorfer, P.; Gruber, H. J., Antibody linking to atomic force microscope tips via disulfide bond formation. *Bioconjugate Chem.* **2006**, 17, 1473-1481.
- (49) Riener, C. K.; Kienberger, F.; Hahn, C. D.; Buchinger, G. M.; Egwim, I. O. C.; Haselgrubler, T.; Ebner, A.; Romanin, C.; Klampfl, C.; Lackner, B.; Prinz, H.; Blaas, D.; Hinterdorfer, P.; Gruber, H. J., Heterobifunctional crosslinkers for tethering single ligand molecules to scanning probes. *Anal. Chim. Acta* **2003**, 497, 101-114.
- (50) Wang, T.; Xu, J. J.; Qiu, F.; Zhang, H. D.; Yang, Y. L., Force spectrum of a few chains grafted on an AFM tip: Comparison of the experiment to a self-consistent mean field theory simulation. *Polymer* **2007**, 48, 6170-6179.
- (51) Suo, Z. Y.; Arce, F. T.; Avci, R.; Thielges, K.; Spangler, B., Dendritic structures of poly(ethylene glycol) on silicon nitride and gold surfaces. *Langmuir* **2006**, 22, 3844-3850.



- (52) Girones, M.; Bolhuis-Versteeg, L.; Lammertink, R.; Wessling, M., Flux stabilization of silicon nitride microsieves by backpulsing and surface modification with PEG moieties. *J. Colloid Interface Sci.* **2006**, *299*, 831-840.
- (53) Sano, H.; Maeda, H.; Ichii, T.; Murase, K.; Noda, K.; Matsushige, K.; Sugimura, H., Alkyl and Alkoxy Monolayers Directly Attached to Silicon: Chemical Durability in Aqueous Solutions. *Langmuir* **2009**, *25*, 5516-5525.
- (54) Cerruti, M.; Fissolo, S.; Carraro, C.; Ricciardi, C.; Majumdar, A.; Maboudian, R., Poly(ethylene glycol) monolayer formation and stability on gold and silicon nitride substrates. *Langmuir* **2008**, *24*, 10646-10653.
- (55) Arafat, A.; Giesbers, M.; Rosso, M.; Sudhölter, E. J. R.; Schroën, K.; White, R. G.; Yang, L.; Linford, M. R.; Zuilhof, H., Covalent biofunctionalization of silicon nitride surfaces. *Langmuir* **2007**, *23*, 6233-6244.
- (56) Arafat, A.; Schroën, K.; de Smet, L. C. P. M.; Sudhölter, E. J. R.; Zuilhof, H., Tailor-made functionalization of silicon nitride surfaces. *J. Am. Chem. Soc.* **2004**, *126*, 8600-8601.
- (57) Rosso, M.; Arafat, A.; Schroën, K.; Giesbers, M.; Roper, C. S.; Maboudian, R.; Zuilhof, H., Covalent attachment of organic monolayers to silicon carbide surfaces. *Langmuir* **2008**, *24*, 4007-4012.
- (58) Ciampi, S.; Harper, J. B.; Gooding, J. J., Wet chemical routes to the assembly of organic monolayers on silicon surfaces via the formation of Si-C bonds: surface preparation, passivation and functionalization. *Chem. Soc. Rev.* **2010**, *39*, 2158-2183.
- (59) Scheres, L.; Arafat, A.; Zuilhof, H., Self-assembly of high-quality covalently bound organic monolayers onto silicon. *Langmuir* **2007**, *23*, 8343-8346.
- (60) Scheres, L.; Giesbers, M.; Zuilhof, H., Organic Monolayers onto Oxide-Free Silicon with Improved Surface Coverage: Alkynes versus Alkenes. *Langmuir* **2010**, *26*, 4790-4795.
- (61) Scheres, L.; Giesbers, M.; Zuilhof, H., Self-Assembly of Organic Monolayers onto Hydrogen-Terminated Silicon: 1-Alkynes Are Better Than 1-Alkenes. *Langmuir* **2010**, *26*, 10924-10929.
- (62) Yang, L.; Heatley, F.; Blease, T. G.; Thompson, R. I. G., A study of the mechanism of the oxidative thermal degradation of poly(ethylene oxide) and poly(propylene oxide) using <sup>1</sup>H- and <sup>13</sup>C-NMR. *Eur. Polym. J.* **1996**, *32*, 535-547.
- (63) Qin, G.; Zhang, R.; Makarenko, B.; Kumar, A.; Rabalais, W.; Lopez Romero, J. M.; Rico, R.; Cai, C., Highly stable, protein resistant thin films on SiC-modified silicon substrates. *Chem. Commun.* **2010**, *46*, 3289-3291.
- (64) Rosso, M.; Giesbers, M.; Arafat, A.; Schroën, K.; Zuilhof, H., Covalently Attached Organic Monolayers on SiC and Si<sub>x</sub>N<sub>4</sub> Surfaces: Formation Using UV Light at Room Temperature. *Langmuir* **2009**, *25*, 2172-2180.
- (65) ter Maat, J.; Regeling, R.; Yang, M.; Mullings, M. N.; Bent, S. F.; Zuilhof, H., Photochemical Covalent Attachment of Alkene-Derived Monolayers onto Hydroxyl-Terminated Silica. *Langmuir* **2009**, *25*, 11592-11597.



- (66) Dijt, J. C.; Cohen Stuart, M. A.; Fleer, G. J., Reflectometry as a Tool for Adsorption Studies. *Adv. Colloid Interface Sci.* **1994**, *50*, 79-101.
- (67) Laibinis, P. E.; Bain, C. D.; Nuzzo, R. G.; Whitesides, G. M., Structure and Wetting Properties of  $\omega$ -Alkoxy-N-Alkanethiolate Monolayers on Gold and Silver. *J. Phys. Chem.* **1995**, *99*, 7663-7676.
- (68) Krishnan, S.; Weinman, C. J.; Ober, C. K., Advances in polymers for anti-biofouling surfaces. *J. Mater. Chem.* **2008**, *18*, 3405-3413.
- (69) Kosmulski, M., *Chemical properties of material surfaces*. Marcel Dekker: New York, 2001; p 753.
- (70) Norde, W., Energy and Entropy of Protein Adsorption. *J. Dispersion Sci. Technol.* **1992**, *13*, 363-377.
- (71) He, Y.; Hower, J.; Chen, S.; Bernards, M. T.; Chang, Y.; Jiang, S., Molecular Simulation Studies of Protein Interactions with Zwitterionic Phosphorylcholine Self-Assembled Monolayers in the Presence of Water. *Langmuir* **2008**, *24*, 10358-10364.
- (72) Zheng, J.; Li, L. Y.; Chen, S. F.; Jiang, S. Y., Molecular simulation study of water interactions with oligo (ethylene glycol)-terminated alkanethiol self-assembled monolayers. *Langmuir* **2004**, *20*, 8931-8938.
- (73) Zheng, J.; Li, L. Y.; Tsao, H. K.; Sheng, Y. J.; Chen, S. F.; Jiang, S. Y., Strong repulsive forces between protein and oligo (ethylene glycol) self-assembled monolayers: A molecular simulation study. *Biophys. J.* **2005**, *89*, 158-166.
- (74) Feng, W.; Zhu, S. P.; Ishihara, K.; Brash, J. L., Adsorption of fibrinogen and lysozyme on silicon grafted with poly(2-methacryloyloxyethyl phosphorylcholine) via surface-initiated atom transfer radical polymerization. *Langmuir* **2005**, *21*, 5980-5987.
- (75) Su, T. J.; Lu, J. R.; Thomas, R. K.; Cui, Z. F.; Penfold, J., The conformational structure of bovine serum albumin layers adsorbed at the silica-water interface. *J. Phys. Chem. B* **1998**, *102*, 8100-8108.
- (76) Norde, W., My voyage of discovery to proteins in flatland ...and beyond. *Colloids Surf., B* **2008**, *61*, 1-9.
- (77) Norde, W., *Colloids and interfaces in life sciences*. Dekker: New York, USA, 2003.
- (78) Leavis, P. C.; Rothstein, F., The solubility of fibrinogen in dilute salt solutions. *Arch. Biochem. Biophys.* **1974**, *161*, 671-682.
- (79) Qin, G.; Cai, C., Oxidative degradation of oligo(ethylene glycol)-terminated monolayers. *Chem. Commun.* **2009**, 5112-4.
- (80) Sharma, S.; Johnson, R. W.; Desai, T. A., Evaluation of the stability of nonfouling ultrathin poly(ethylene glycol) films for silicon-based microdevices. *Langmuir* **2004**, *20*, 348-356.
- (81) Sofia, S. J.; Premnath, V.; Merrill, E. W., Poly(ethylene oxide) grafted to silicon surfaces: Grafting density and protein adsorption. *Macromolecules* **1998**, *31*, 5059-5070.



## Stable Protein-Repellent Zwitterionic Polymer Brushes Grafted from Silicon Nitride

Zwitterionic poly(sulfobetaine acrylamide) (SBMAA) brushes were grafted from silicon-rich silicon nitride ( $\text{Si}_x\text{N}_4$ ,  $x>3$ ) surfaces by atom transfer radical polymerization (ATRP) and studied in protein adsorption experiments. Zwitterionic polymer brushes of SBMAA with a thickness of  $\sim 30$  nm were grown from initiator-coated surfaces. Excellent protein repellence ( $>99\%$ ) was observed by reflectometry for these zwitterionic polymer-coated  $\text{Si}_x\text{N}_4$  surfaces during exposure to fibrinogen (FIB) solution ( $0.1 \text{ g.L}^{-1}$ ) as compared to hexadecyl-coated  $\text{Si}_x\text{N}_4$  surfaces ( $\text{C}_{16}\text{-Si}_x\text{N}_4$ ). The zwitterionic polymer brushes show the superior stability in an aqueous solution. After 1 week exposure to phosphate-buffered saline (PBS) solution, the zwitterionic polymer coating remained intact and its thickness was unchanged within experimental error. No hydrolysis was observed for the zwitterionic polymer and the surfaces still repelled 98% FIB as compared to  $\text{C}_{16}\text{-Si}_x\text{N}_4$  surfaces, demonstrating the long-term efficiency of these easily prepared surface coatings

This chapter has been published as:

Nguyen, A. T.; Baggerman, J.; Paulusse, J. M. J.; Van Rijn, C. J. M.; Zuilhof, H., Stable Protein-Repellent Zwitterionic Polymer Brushes Grafted from Silicon Nitride. *Langmuir*, **2011**, 27, 2587-2594.

## 1. Introduction

Protein-resistant coatings are of paramount importance in many biomedical applications such as contact lenses, biosensors, and prostheses. The adhesion of proteins onto exposed areas of these devices may eventually lead to thrombosis, produce false results in diagnostics, or limit the precision of medical instruments.<sup>1-4</sup> Therefore, minimizing the interactions between proteins and the surfaces is a prerequisite for the long-term use thereof.

Over the past decades, poly- and oligo(ethylene oxide) have been widely used to reduce nonspecific binding of proteins.<sup>5-8</sup> The hydration layer surrounding the ethylene oxide chains due to hydrogen bonding is considered to be the reason for the efficient repulsion of proteins. Protein resistance of poly- or oligo(ethylene oxide) coated to various substrates was demonstrated and corroborated by experimental and simulation studies.<sup>5, 6, 9-16</sup> However, the ethylene oxide chains are over time auto-oxidized in aqueous solution, resulting in cleavage of ethylene oxide units and formation of aldehyde-terminated chains.<sup>17</sup> These aldehyde moieties may react with proteins bearing amine groups, resulting in a declination of the protein-repellent nature of the coatings.<sup>17</sup> Moreover, the poly(ethylene oxide) coatings lose their protein resistance at 37 °C,<sup>18</sup> which is a critical temperature for many biomedical applications.

Recently, zwitterionic polymer brush coated surfaces have emerged as a superior alternative to poly(ethylene oxide) coatings.<sup>19</sup> The zwitterionic polymers display minimized adhesion of proteins due to a more strongly bound hydration layer induced by electrostatically ionic solvation in addition to hydrogen-bonding interactions. The electrostatic interactions between water molecules and dipoles present in the zwitterionic polymer chains make these polymers better “water-bearers”. Moreover, these interactions are more stable at body temperature than hydrogen-bonding interactions along an ethylene oxide chain.<sup>20-25</sup>

The growth of zwitterionic polymers from gold,<sup>19, 22, 26-30</sup> silicon,<sup>24</sup> and also polymer<sup>31</sup> surfaces via surface-initiated atom transfer radical polymerization (ATRP) has been reported. ATRP is a controlled radical polymerization technique that enables the formation of well-defined polymers on the surface. It has found widespread applications due to its relative simplicity and versatility.<sup>32, 33</sup> However, coatings on silicon surfaces are typically obtained via silanization resulting in Si-O-Si-C linkages, which are reported to hydrolyze in slightly basic media,<sup>34</sup> and may result in severe detachment of these coatings. Alternative approaches were introduced to immobilize various functional molecules onto silicon<sup>35-37</sup> and silicon nitride<sup>38-40</sup> substrates via Si-C and N-C linkages. These monolayers were demonstrated to possess significant stability in both acidic and basic media.<sup>34, 41</sup> We

recently investigated the stability of hexa(ethylene oxide) methyl  $\omega$ -undecenyl ether coated  $\text{Si}_x\text{N}_4$  surfaces ( $\text{EO}_6\text{-Si}_x\text{N}_4$ ).<sup>42</sup> The initial protein repellence was high (94% for bovine serum albumin), but this value diminished over time (week long exposure to phosphate buffered saline (PBS)). Although no oxidation of the  $\text{Si}_x\text{N}_4$  surface was observed after exposure to PBS solution, auto-oxidation of the ether moieties in the monolayer still occurred,<sup>42</sup> keeping long-term protein repulsion out of reach.

$\text{Si}_x\text{N}_4$  is often used as an insulator and chemical barrier in manufacturing integrated circuits.<sup>43</sup> As a passivation layer for microchips, it is superior to silicon dioxide, as it provides a significantly better diffusion barrier.<sup>44</sup> Nowadays it is widely used in micro- and nanoelectromechanical systems (MEMS and NEMS).<sup>45</sup> Silicon nitride has excellent fracture toughness and is chemically inert, which presents opportunities for micro/nano devices with high corrosion resistance and high mechanical strength, as alternatives to silicon-based devices.<sup>46</sup> Among other possibilities, this enables the fabrication of microsieves with high porosity and highly homogeneous pore-size distributions.<sup>47</sup> Microsieves therefore have a high flux and excellent selectivity in microfractionation processes. They have been applied in many fields, for instance, in biological sample preparation, food processing, emulsification, filtration, atomization, and diagnostics.<sup>48, 49</sup>

However, as for any conventional membrane, microsieves also face fouling issues, that is, nonspecific adsorption of biomolecules on surfaces during filtration. Proteins especially initiate surface contamination<sup>50</sup> and thereby facilitate the growth of thicker biofouling layers, which considerably affects device performance.<sup>51</sup> Therefore, the development of stable protein-resistant coatings on membrane surfaces is needed to minimize fouling and to maintain process capacity.<sup>52</sup>

In this study, we introduce a method to obtain dense monolayers of ATRP initiators coated onto  $\text{Si}_x\text{N}_4$  surfaces via stable Si-C linkages, which serve as an excellent template for growing polymers. ATRP is employed to graft zwitterionic polymer brushes from the  $\text{Si}_x\text{N}_4$  surfaces. The polymer-coated surfaces are characterized in detail, and their stability is assessed. Finally, the protein repelling properties are evaluated by long-term (1 week) exposure of the surfaces to fibrinogen (FIB) solution and following the adsorption by in situ reflectometry, to reveal the long-term potential of zwitterionic polymer coatings as protein-repelling layers.

## 2. Experimental Section

### 2.1. Materials and Methods

Fibrinogen (fraction I from porcine plasma, 78% in protein) was purchased from Sigma Adrich. Sodium phosphate dibasic (analytical grade, Acros), potassium dihydrogenophosphate (ACS grade, Merck), potassium chloride (pro analysis, Merck), and sodium chloride (puriss, Riedel-de-Haën) were used to prepare the PBS buffer.

1,2-Epoxy-9-decene (96%), 1,2-ethylenediamine (p.a., absolute,  $\geq 99.5\%$ ), *n*-propylamine ( $\geq 99\%$ ), dichloromethane (DCM, 99.8%, extra dry over molecular sieve, stabilized with amylene), acetone (semiconductor grade), copper(I) bromide (99.999%), [3-(methacryloylamino)propyl]dimethyl(3-sulfopropyl)ammonium hydroxide inner salt (96%), 2,2'-bipyridine (99%), 2-bromoisobutyl bromide (98%), isopropanol (*i*-PrOH, 99.9%), and triethylamine ( $\text{Et}_3\text{N}$ ) were purchased from Sigma-Aldrich. Petroleum ether 40-60 was distilled before use. Water used in all experiments was purified by a Barnsted water purification system, with a resistivity of 18.3 M $\Omega$ .cm. For the formation of epoxide monolayers, 1,2-epoxy-9-decene was purified by column chromatography. The obtained purity was  $>99\%$  as determined by gas chromatography/mass spectroscopy (GC-MS).

### 2.2. Monolayer Formation

$\text{Si}_x\text{N}_4$  ( $x > 3$ ) was deposited on Si <100> substrates (p-type, slightly boron doped, resistivity 8-22  $\Omega$ .cm) by low-pressure chemical vapor deposition (LPCVD) with a thickness of 150 nm (Nanosens B.V., The Netherlands). The  $\text{Si}_x\text{N}_4$  wafers were cut into appropriate sizes for each experiment.  $\text{Si}_x\text{N}_4$  samples were cleaned by dust-free wipers with acetone, followed by oxidation in air-based plasma for 10 min. The oxidized samples were then etched with a 2.5% aqueous solution of HF for 2 min and dried under an argon flow. Immediately the samples were transferred into degassed neat 1,2-epoxy-9-decene in a quartz flask, followed by three vacuum-argon cycles to remove trace amounts of oxygen that might enter the flask during sample transfer. Finally, the flask was backfilled with argon. A UV pen-lamp (254 nm, low pressure mercury vapor, double bore lamp from Jelight Company Inc., California) with the output intensity of 9 mW.cm<sup>-2</sup> was aligned 4 mm away from the quartz flask. The samples were irradiated under argon for 24 h. The samples were removed from the flask and sonicated in acetone for 5 min, rinsed several times with acetone and distilled petroleum ether, and finally dried in a stream of argon. Subsequently, the samples were transferred to degassed neat 1,2-ethylenediamine. The reaction was carried out for 24 h at 40 °C. The samples were removed from the flask, and the same cleaning procedure was employed as described for the previous experiment. The ATRP initiator was attached onto the amine-terminated surfaces via reaction with

2-bromoisobutyryl bromide (0.54 g, 2.0 mmol) in dry dichloromethane (1 mL) containing Et<sub>3</sub>N (0.2 mL) at room temperature for 30 min. The surfaces were removed and subsequently cleaned by sonication in DCM for 5 min and rinsed thoroughly with acetone and distilled petroleum ether.

The hexadecyl-coated Si<sub>x</sub>N<sub>4</sub> surfaces (C<sub>16</sub>-Si<sub>x</sub>N<sub>4</sub>) and hexa(ethylene oxide)-coated Si<sub>x</sub>N<sub>4</sub> surfaces (EO<sub>6</sub>-Si<sub>x</sub>N<sub>4</sub>) were prepared with the same procedure as used for immobilization of 1,2-epoxy-9-decene on Si<sub>x</sub>N<sub>4</sub> surfaces as described above. The hexadec-1-ene and methoxy-hexa(ethylene oxide) undec-1-ene were employed to react with hydrogen-terminated surfaces obtained by HF etching. The synthesis of EO<sub>6</sub> compound and the characterization of C<sub>16</sub>-Si<sub>x</sub>N<sub>4</sub> and EO<sub>6</sub>-Si<sub>x</sub>N<sub>4</sub> surfaces are described in Appendix 1 and Chapter 2, respectively.

### 2.3. Surface-Initiated Polymerization

Sulfobetaine methacrylamide (SBMAA) (1.2 g, 4.0 mmol) and 2,2'-bipyridine (0.32 g, 2.0 mmol) were dissolved in a mixture of isopropanol (7.5 mL) and water (2.5 mL) in a round-bottomed flask by stirring. The solution was degassed for 30 min by purging with argon. CuBr (0.14 g, 1.0 mmol) was added to a separate round-bottomed flask under argon (in a glovebox) which was closed by a septum. Subsequently, the degassed solution was transferred into the flask containing CuBr by means of a syringe (flushed with argon in advance). The mixture was stirred further for an additional 30 min under argon to dissolve all CuBr. Afterward, the mixture was transferred to the reaction flask containing the initiator-coated Si<sub>x</sub>N<sub>4</sub> surface by means of a syringe. The polymerization was carried out under argon pressure (0.14 bar overpressure) while stirring at room temperature for 3 h (Scheme 1). The samples were removed and rinsed with warm water (60-65 °C) for 5 min and cleaned by sonication in water and further with acetone. Finally, the samples were dried under a stream of argon.

The thickness of the polySBMAA layer was determined as a function of reaction time. To this purpose the substrate was placed in a special holder equipped with a magnet, which made it possible to move the holder by an external magnet. The degassed polymerization solution prepared as described above was injected into the reaction flask containing the initiator-coated Si<sub>x</sub>N<sub>4</sub> surface. Subsequently, the sample holder was submerged partly into the polymerization solution and moved in further in a stepwise manner with several intervals. The polymerization was carried out under argon pressure with agitation for 8 h. Finally, the sample was removed, and the same cleaning procedure was employed as described earlier. Thicknesses of the different areas were determined by atomic force microscopy (AFM).



## 2.4. Protein Adsorption

Fibrinogen (FIB) solutions ( $0.1 \text{ g.L}^{-1}$ ) were freshly prepared in PBS solution (pH 6.7, ionic strength 0.08 M) and settled for 1 h at room temperature before use. Because of the low solubility of FIB in water, FIB solutions were prepared as follows. First, a PBS solution was prepared at pH 6.7 with high ionic strength (0.16 M). Next, the desired amount of FIB was added, and the solution was gently shaken at 80 rpm at room temperature. After 15 min, FIB had completely dissolved, and a clear protein solution was obtained. Finally, the solution was diluted 2 times to obtain  $0.1 \text{ g.L}^{-1}$  of FIB in PBS solution at pH 6.7 with an ionic strength of 0.08 M.

All reflectometry experiments were performed at room temperature (see Chapter 2, section 2.7 for the details of reflectometer). Before measurements, surfaces were incubated for 1 h in warm water (60–65 °C) to sufficiently wet the coatings and subsequently in PBS solution for 1 h to avoid artifacts. Consecutively, after placing the samples in the reflectometer, buffer solution was injected until the output signal remained constant: fluctuations of less than 0.01 V over 5 min were considered satisfactory. Each experiment involved at least one adsorption phase, in which protein solutions was added to the surface, and one desorption phase, in which only buffer was injected. Details on the calculation of adsorbed protein amount are described in Appendix 2.<sup>53</sup>

## 2.5. Stability of Zwitterionic SBMAA-Coated $\text{Si}_x\text{N}_4$ Surfaces in PBS Solution

Three samples of zwitterionic SBMAA-coated  $\text{Si}_x\text{N}_4$  surfaces were prepared in a single batch as described above. A study on the stability of zwitterionic SBMAA-coated on  $\text{Si}_x\text{N}_4$  surfaces in PBS solution was performed at room temperature for 1 week. Before and after exposure to PBS solution, the samples were characterized by XPS, their thicknesses were determined by AFM and reflectometry measurements were carried out to evaluate their protein repellency. Static water contact angle measurements were performed daily, after rinsing the samples thoroughly with pure water followed by acetone. The samples were immersed every day in fresh PBS solution. After 1 week of immersion in PBS solution, the samples were rinsed thoroughly with pure water prior to protein adsorption experiments. Afterward, the samples were rinsed thoroughly with 1% sodium dodecyl sulfate in water (SDS) to remove any adsorbed FIB, subsequently with pure water and sonication in water, followed by acetone, before XPS and AFM measurements.



## 2.6. X-ray Photoelectron Spectroscopy (XPS)

Modified surfaces were characterized by XPS using a JPS-9200 photoelectron spectrometer (JEOL, Japan). High-resolution spectra were obtained under UHV conditions using monochromatic Al K $\alpha$  X-ray radiation at 12 kV and 20 mA, using an analyzer pass energy of 10 eV. All high-resolution spectra were corrected with a linear background before fitting.

## 2.7. Static Water Contact Angle Measurements

The wettability of the modified surfaces was determined by automated static water contact angle measurements with the use of Krüss DSA 100 goniometer (volume of the drop of demineralized water is 2.5  $\mu$ L).

## 2.8. Atomic Force Microscopy (AFM) for Thickness and Roughness Measurements

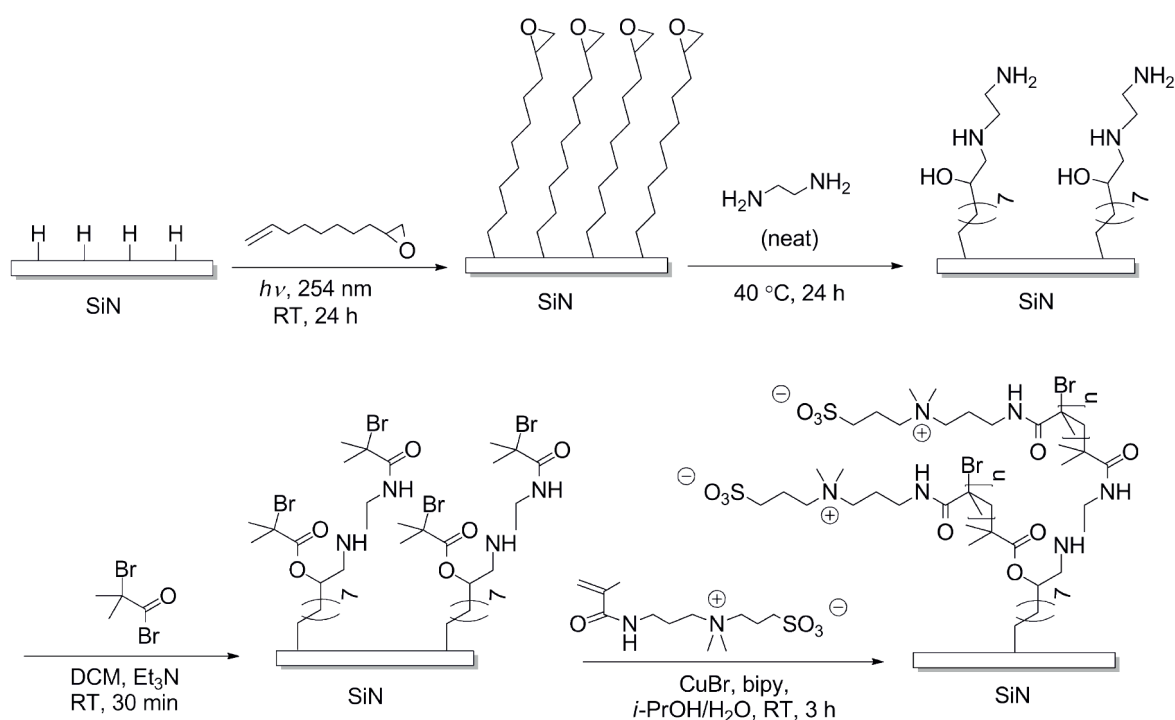
AFM surface images were measured with Tap300Al-G silicon cantilevers (Budgetsensors) in AC mode in air using an Asylum Research MFP-3D SA AFM. Prior to the thickness measurements, surfaces were prepared as follows. The polymer-coated surfaces were immersed in pure water for 4 h at room temperature to fully swell polymer. A knife was used to scratch the surfaces. The scratched surfaces were sonicated to remove any residuals from cutting, and the sample surface was subsequently dried with argon. The scratched surfaces were directly measured by AFM. The thickness of the swollen polymer layer was determined from the height difference in the topography profile. The root-mean-square (rms) roughness was calculated from the topography of the surface.

# 3. Results and Discussion

## 3.1. Formation and Characterization of Monolayers on SiN

### 3.1.1. Epoxide-Terminated Monolayer

Silicon nitride was functionalized in a four-step procedure (Scheme 1). Hydrogen-terminated Si<sub>x</sub>N<sub>4</sub> surfaces were obtained through etching with HF and employed in the photochemical attachment of 1,2-epoxy-9-decene.<sup>35, 54</sup>



**Scheme 1.**  $\text{Si}_x\text{N}_4$  surface modification reactions and surface initiated controlled radical polymerization.

A static water contact angle of  $71 \pm 1^\circ$  was observed for the epoxide-terminated  $\text{Si}_x\text{N}_4$  surface, which is identical to that reported earlier for epoxy-coated silicon surfaces.<sup>54</sup> No signal corresponding to silicon oxide was observed in the narrow-scan XPS spectrum of  $\text{Si}_{2p}$  region (Figure 1, right). The narrow-scan XPS spectrum of  $\text{C}_{1s}$  region displays a peak at 287.0 eV corresponding to carbon atoms bound to oxygen (C-O) derived from the epoxide moiety and a peak at 285.0 eV corresponding to carbon bound to carbon (C-C) which results from the alkyl chain (Figure 1, left). The ratio of (C-C)/(C-O) is 4.0, that is, in excellent agreement with the theoretical composition. These results indicate that high-quality epoxide monolayers on  $\text{Si}_x\text{N}_4$  were obtained.

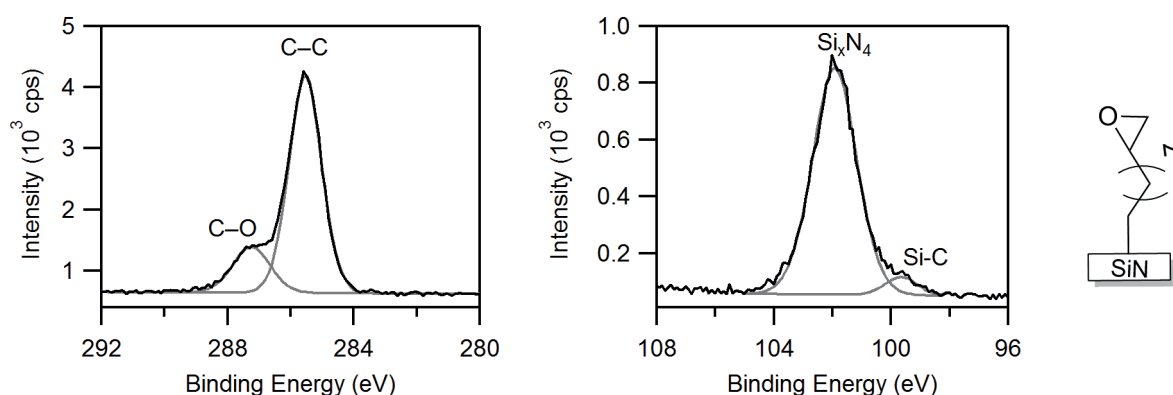


**Figure 1.** Narrow-scan XPS spectra of  $\text{C}_{1s}$  region (left) and  $\text{Si}_{2p}$  (right) region of epoxide-terminated  $\text{Si}_x\text{N}_4$  surface.

### 3.1.2. Amine-Terminated Monolayer

The epoxide-terminated  $\text{Si}_x\text{N}_4$  surface was subsequently converted into an amine-terminated surface via a reaction with neat 1,2-ethylenediamine under argon (Scheme 1). The static water contact angle decreased from  $71 \pm 1^\circ$  to  $63 \pm 1^\circ$ , which is in good agreement with earlier reported amine-terminated monolayers on silicon.<sup>55</sup> A 1 eV shift of the C-O peak was observed in the narrow-scan XPS spectrum of the  $\text{C}_{1s}$  region corresponding to epoxide ring-opening and attachment of the amine moiety. A broad  $\text{C}_{1s}$  peak at 286 eV is attributed to the overlapping signals of C-O (from secondary alcohol) and C-N in the resultant monolayer (Figure 2, left). The experimental ratio of C-C/(C-O&C-N) is 2.1, which corresponds to the attachment of 1,2-ethylenediamine onto the epoxide-terminated surface via a single amine moiety (theoretically expected ratio: 2.0). Bridged conformations, in which a single 1,2-ethylenediamine molecule is coupled to two epoxide moieties, would have resulted in a significantly higher ratio (2.6), while unreacted epoxide moieties would give a ratio of 4.0. In addition, a signal of organic nitrogen at 399 eV from the resultant monolayer appears next to a signal of inorganic nitrogen at 397 eV (Figure 2, right), which further demonstrates the successful attachment of 1,2-ethylenediamine onto the epoxide-terminated  $\text{Si}_x\text{N}_4$  surface. The narrow-scan XPS spectrum of  $\text{C}_{1s}$  region reveals a high conversion of the epoxides, 95% (Appendix 4). The strategy shown here provides a new route to obtain amine-terminated  $\text{Si}_x\text{N}_4$  surfaces via stable Si-C linkages without the need for protective group chemistry,<sup>56, 57</sup> or the use of silane chemistry involving the hydrolytically labile Si-O linkages.

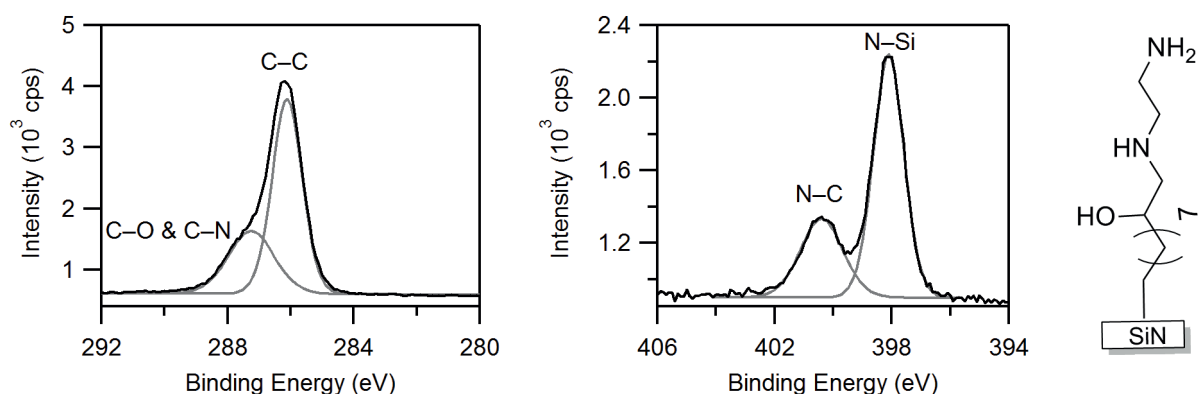


**Figure 2.** Narrow-scan XPS spectra of  $\text{C}_{1s}$  region (left) and  $\text{N}_{1s}$  (right) region of amine-terminated  $\text{Si}_x\text{N}_4$  surface.

### 3.1.3. ATRP-Initiator-Functional Monolayer

ATRP initiators were attached to the amine-terminated surfaces via a reaction with 2-bromoisobutyryl bromide (Scheme 1). The water contact angle of the modified surfaces was  $72 \pm 1^\circ$ , which is very close to those observed for similar monolayers on gold ( $73^\circ$ ).<sup>58</sup> The appearance of characteristic bromine-signals ( $\text{Br}_{3d}$  at 70 eV,  $\text{Br}_{3s}$  at 255 eV and  $\text{Br}_{3p}$  at 188 eV) was observed in the wide-scan XPS spectrum (data not shown). The  $\text{C}_{1s}$  peak at 288.3 eV corresponds to an amide-carbonyl C atom in the resultant monolayer, whereas the peak at 289.5 eV corresponds to the ester-carbonyl moiety. This indicates that not only the amines participate in the coupling reaction, but the secondary alcohol that resulted from the original epoxide-ring-opening as well (Figure 3). The broad peak at 286.5 eV is attributed to overlapping C-N, C-Br and C-O(C=O) peaks.

In order to determine to what extent the secondary alcohol and secondary amine participate in the reaction with 2-bromoisobutyryl bromide, an epoxide-terminated surface was reacted with *n*-propylamine instead of 1,2-ethylenediamine. This results in an *n*-propyl-terminated surface that presents a secondary alcohol and a secondary amine. The resultant surface was reacted with 2-bromoisobutyryl bromide. In this case, the narrow-scan XPS spectrum of  $\text{C}_{1s}$  of the Br-initiator-coated surface shows approximately 40% conversion of secondary alcohols into ester moieties and 30% secondary amide formation. This low conversion is attributed to the sterically hindered positions of the secondary alcohol and the secondary amine in the monolayer (see Appendix 4). In the case of amine-terminated surfaces stemming from the 1,2-ethylenediamine reaction, carried out under water-free conditions, roughly 30% conversion was observed for the secondary alcohol and approximately 70% conversion of primary or secondary amine into amide moieties (see Appendix 4). These results show a high overall conversion ( $\sim 100\%$ ) for the attachment of Br-initiators, with respect to each alkyl chain, hence providing an excellent template for growing dense polymeric coatings.

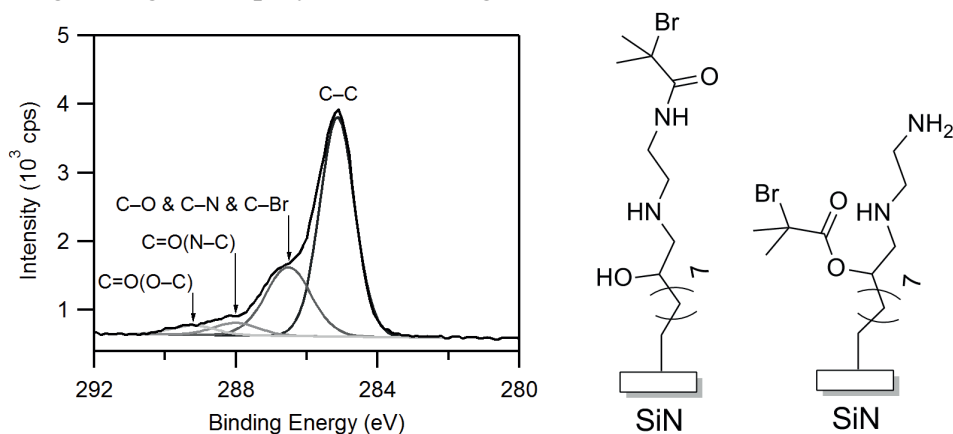


**Figure 3.** Narrow-scan XPS spectrum of  $\text{C}_{1s}$  region of Br-initiators terminated  $\text{Si}_x\text{N}_4$  surface.

### 3.2. Surface Initiated Polymerization

PolySBMAA was grafted from the Br-initiator coated  $\text{Si}_x\text{N}_4$  surfaces via ATRP (Scheme 1). After polymerization, the water contact angle values of the modified surfaces were below the detection limit of the equipment ( $<15^\circ$ ), which is in agreement with earlier observations for similar polymer-coated gold surfaces.<sup>22, 28-30</sup> The wide-scan XPS spectrum of the SBMAA-grafted  $\text{Si}_x\text{N}_4$  surface no longer displays a signal of silicon at 102 eV, demonstrating the presence of a thick polymer layer coated on the substrate (Figure 4). Furthermore, the wide-scan XPS spectrum showed the presence of oxygen (20%), carbon (65%), nitrogen (10%), and sulfur (5%), with an elemental composition in agreement with the composition of the SBMAA monomeric unit. The narrow-scan XPS spectrum of the  $\text{N}_{1s}$  region revealed two distinct peaks for nitrogen, one for nitrogen atoms corresponding to amide, and the other signal stemming from the quaternary amine in the monomer. The roughness of the polySBMAA-grafted surfaces measured by AFM was  $1.5 \pm 0.1$  nm, demonstrating the presence of a smooth polySBMAA layer. The thickness of the polySBMAA layer was measured by AFM, by comparing it with an area where the polymer layer was removed (Figure 5). A kinetics study was performed, and the polymer film thicknesses were determined as a function of reaction time as shown in Figure 6. A high initial polymerization rate was observed, after which the thickness increased approximately linear with time at a rate of  $\sim 6 \text{ nm}\cdot\text{h}^{-1}$ . These data demonstrate that polySBMAA was grafted successfully from the initiator-coated  $\text{Si}_x\text{N}_4$  surface in a controlled way.

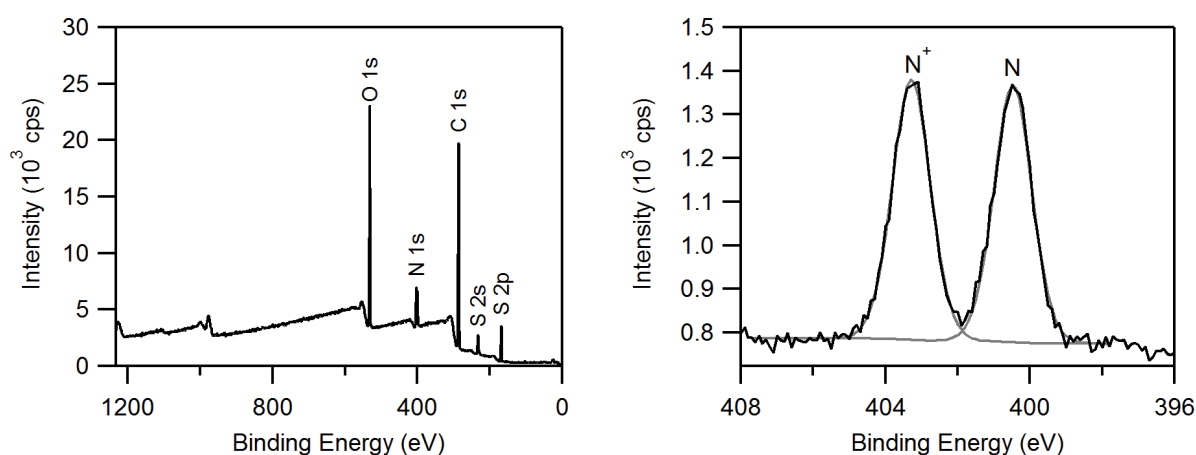


**Figure 4.** Wide-scan XPS spectrum (left) and narrow-scan XPS spectrum of  $\text{N}_{1s}$  (right) region of polySBMAA-grafted  $\text{Si}_x\text{N}_4$  surface.

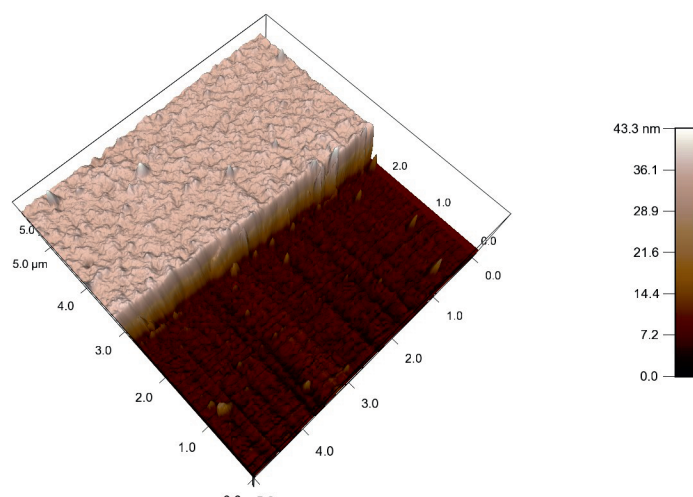


**Figure 5.** AFM image of polySBMAA-grafted  $\text{Si}_x\text{N}_4$  surface scratched by a knife.

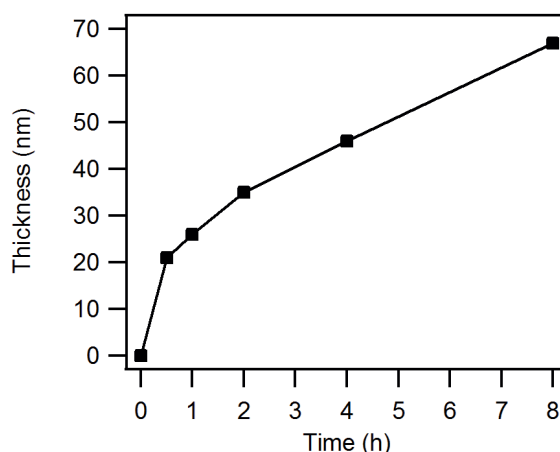


**Figure 6.** Thickness of polySBMAA grafted from  $\text{Si}_x\text{N}_4$  as a function of reaction time.

### 3.3. Protein Adsorption Experiments

The protein-repelling properties of the obtained polySBMAA-grafted  $\text{Si}_x\text{N}_4$  surfaces (polymer thickness of  $34 \pm 2$  nm) were evaluated by reflectometry measurements and compared with several commonly employed substrates. The use of reflectometry in studying protein adsorption enables us to examine real-time changes in the refractive index of the surfaces and thereby reveals both reversible and irreversible adsorption stages.<sup>42</sup> Upon employing the surfaces coated with zwitterionic polymers in a protein adsorption experiment, minimal adsorption of FIB was observed ( $0.06 \text{ mg.m}^{-2}$ ). This result is in good agreement with the resultant protein repellence of zwitterionic polymer coated on gold<sup>19, 22, 26-30</sup> and silicon<sup>24</sup> surfaces. When exposed to FIB solution, the  $\text{C}_{16}\text{-Si}_x\text{N}_4$  surface (hydrophobic surface) rapidly adsorbed protein; a maximum adsorbed amount of  $5.5 \text{ mg.m}^{-2}$  was found (Figure 7). Such behavior was reported earlier for similar

hydrophobic coatings, that is, alkyl coatings on gold<sup>59</sup> and silicon.<sup>60</sup> Hydrophobic surfaces generally have very low surface energy, and as a result proteins readily adsorb to minimize the interfacial tension between the surface coating and the water.<sup>61</sup> In comparison, the plasma-oxidized  $\text{Si}_y\text{O}-\text{Si}_x\text{N}_4$  surface (hydrophilic surface) adsorbed only  $3.1 \text{ mg}\cdot\text{m}^{-2}$ , that is, 44% protein repulsion as compared to the  $\text{C}_{16}-\text{Si}_x\text{N}_4$  surface. Hydrophilic surfaces, such as  $\text{Si}_y\text{O}-\text{Si}_x\text{N}_4$ , generally have much higher surface energy and only low interfacial energy when in contact with water. Thermodynamically, it is not favorable for proteins to adsorb onto the surface. Therefore, many hydrophilic surfaces are known to repel proteins. However, surface hydrophilicity plays only a minor role in protein repulsion. Indeed, Figure 7 shows that the  $\text{EO}_6-\text{Si}_x\text{N}_4$  surface (a typical well-performing antifouling surface) has a water contact angle of  $62^\circ$ , which is thus significantly less hydrophilic than the  $\text{Si}_y\text{O}-\text{Si}_x\text{N}_4$  surface ( $\text{CA} < 5^\circ$ ). Nevertheless,  $\text{EO}_6-\text{Si}_x\text{N}_4$  adsorbed only  $0.96 \text{ mg}\cdot\text{m}^{-2}$ , in other words 83% of FIB was repelled from the modified surface as compared to a  $\text{C}_{16}-\text{Si}_x\text{N}_4$  surface. The ethylene oxide moieties inside the  $\text{EO}_6$  monolayer are able to form hydrogen bonds with water molecules and consequently maintain a persistent hydration layer. This generates a repulsive force which makes it difficult for proteins to reach the surface.<sup>14-16</sup> The  $\text{SiO}_y-\text{Si}_x\text{N}_4$  surface has a hydration layer of only a few water molecules. Thus, the water molecules are easily pushed away by approaching proteins. Hence, an effective antifouling coating must be able to maintain a persistent hydration layer, that is, a good hydration layer should have a strong inherent interaction between water and the coatings and a thick layer of hydration. These factors play a crucial role in the protein repulsion effectiveness of the surfaces.<sup>20</sup> Zwitterionic polymer brushes are significantly more effective (99%) in repelling FIB as compared to  $\text{EO}_6$  monolayers (87%) and  $\text{SiO}_y$  (44%) due to an increased hydration layer (all compared to  $\text{C}_{16}$ -alkyl monolayers as reference).

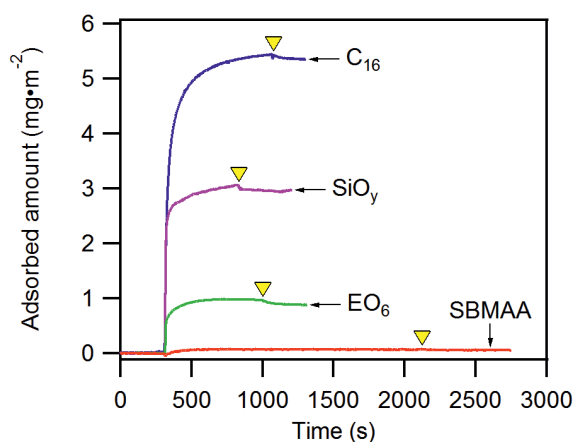


**Figure 7.** FIB adsorption onto the modified  $\text{Si}_x\text{N}_4$  surface (yellow arrows indicate the desorption transition).



### 3.4. Stability of Zwitterionic SBMAA Coated on $\text{Si}_x\text{N}_4$ Surfaces in PBS Solution

To study the stability of the polySBMAA coated on  $\text{Si}_x\text{N}_4$  surfaces in an aqueous medium, the samples were immersed in PBS solution and characterized before and after a 1-week exposure. The water contact angle values remained lower than  $15^\circ$  throughout the experiment. The wide-scan XPS spectrum shows minor signals of silicon ( $<1.5\%$  on average for three samples) after immersion in PBS solution for 1 week, indicating that the zwitterionic polymeric coating was still intact. In addition, the narrow-scan XPS spectrum of  $\text{C}_{1s}$  region showed the same elemental composition for the exposed surfaces as observed for the fresh samples, showing no hydrolysis or degradation of the zwitterionic polymer (Figure 8). The thickness measured by AFM remained unchanged within the error of measurement and further confirms that no significant polymer detachment occurred. The integrity of the polymeric coating was further verified by again measuring its protein-repellent behavior. The adsorbed amount of FIB on the exposed surfaces was still only  $0.12 \pm 0.02 \text{ mg.m}^{-2}$ , that is, the surfaces still repel 98% of FIB as compared to the  $\text{C}_{16}\text{-Si}_x\text{N}_4$  surface.

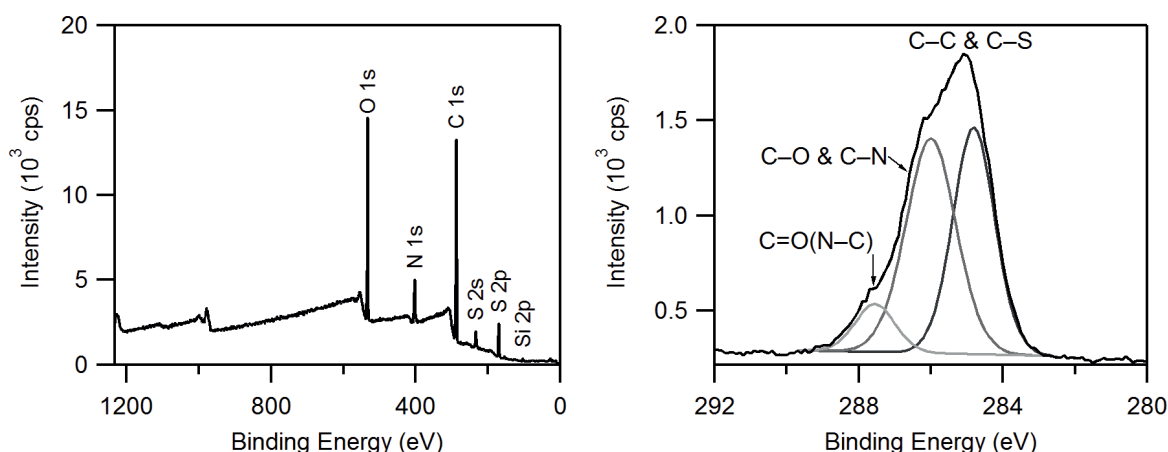


**Figure 8.** Wide-scan XPS spectrum (left) and narrow-scan XPS spectrum of  $\text{C}_{1s}$  region of zwitterionic polymer coated on  $\text{Si}_x\text{N}_4$  surface after immersion in PBS solution for 1 week.

## 4. Conclusions

SBMAA zwitterionic polymer brushes were successfully grafted from  $\text{Si}_x\text{N}_4$  surfaces. The use of functional monolayers on  $\text{Si}_x\text{N}_4$  served as an excellent template for polymer grafting as well as providing stability to the polymer coating. The SBMAA zwitterionic polymer brushes grafted on  $\text{Si}_x\text{N}_4$  surfaces show excellent antifouling behavior in FIB solution as compared to hydrophobic  $\text{C}_{16}\text{-Si}_x\text{N}_4$  surfaces ( $>99\%$  repulsion) and other commonly applied protein-repelling surfaces. After exposure to PBS solution for 1 week,



the surfaces still repelled 98% FIB as compared to the  $C_{16}-Si_xN_4$  surface, while the polymeric coating remained intact. The inertness of the silicon nitride substrate and the robust Si-C linkage through which the zwitterionic polymers are coupled provide for highly stable and effective antifouling surfaces, greatly contributing to the development of long-term use biological devices such as in membrane filters, microreactors, biosensors, and medical instruments in general.

## 5. Acknowledgment

The authors thank MicroNed (project 6163510587) for financial support and Hien Duy Tong (Nanosens B.V., Zutphen, The Netherlands) for his kind donation of  $Si_xN_4$  wafers.

## 6. References

- (1) Desai, T. A.; Hansford, D. J.; Leoni, L.; Essenpreis, M.; Ferrari, M., Nanoporous anti-fouling silicon membranes for biosensor applications. *Biosens. Bioelectron.* **2000**, *15*, 453-462.
- (2) Mandrusov, E.; Puszkin, E.; Vroman, L.; Leonard, E. F., Separated Flows in Artificial Organs: A Cause of Early Thrombogenesis? *ASAIO Journal* **1996**, *42*, M506-513.
- (3) Sampedro, M. F.; Patel, R., Infections Associated with Long-Term Prosthetic Devices. *Infect. Dis. Clin. North. Am.* **2007**, *21*, 785-819.
- (4) Turner, R. F. B.; Harrison, D. J.; Rojotte, R. V., Preliminary in vivo biocompatibility studies on perfluorosulphonic acid polymer membranes for biosensor applications. *Biomaterials* **1991**, *12*, 361-368.
- (5) Roosjen, A.; van der Mei, H. C.; Busscher, H. J.; Norde, W., Microbial adhesion to poly(ethylene oxide) brushes: Influence of polymer chain length and temperature. *Langmuir* **2004**, *20*, 10949-10955.
- (6) Roosjen, A.; Kaper, H. J.; van der Mei, H. C.; Norde, W.; Busscher, H. J., Inhibition of adhesion of yeasts and bacteria by poly(ethylene oxide)-brushes on glass in a parallel plate flow chamber. *Microbiology* **2003**, *149*, 3239-3246.
- (7) Roosjen, A.; de Vries, J.; van der Mei, H. C.; Norde, W.; Busscher, H. J., Stability and effectiveness against bacterial adhesion of poly(ethylene oxide) coatings in biological fluids. *J. Biomed. Mater. Res. Part B Appl. Biomater.* **2005**, *73B*, 347-354.
- (8) Norde, W., Surface modifications to influence adhesion of biological cells and adsorption of globular proteins. In *Surface Chemistry in Biomedical and Environmental Science*, Blitz, J.; Gun'ko, V.; Norde, W., Eds. Springer Netherlands: 2006; pp 159-176.

- (9) Harder, P.; Grunze, M.; Dahint, R.; Whitesides, G. M.; Laibinis, P. E., Molecular conformation in oligo(ethylene glycol)-terminated self-assembled monolayers on gold and silver surfaces determines their ability to resist protein adsorption. *J. Phys. Chem. B* **1998**, *102*, 426-436.
- (10) Palegrosdemange, C.; Simon, E. S.; Prime, K. L.; Whitesides, G. M., Formation of Self-Assembled Monolayers by Chemisorption of Derivatives of Oligo(Ethylene Glycol) of Structure  $\text{HS}(\text{CH}_2)_{11}(\text{OCH}_2\text{CH}_2)_m\text{OH}$  on Gold. *J. Am. Chem. Soc.* **1991**, *113*, 12-20.
- (11) Schlapak, R.; Pammer, P.; Armitage, D.; Zhu, R.; Hinterdorfer, P.; Vaupel, M.; Fruhwirth, T.; Howorka, S., Glass surfaces grafted with high-density poly(ethylene glycol) as substrates for DNA oligonucleotide microarrays. *Langmuir* **2006**, *22*, 277-285.
- (12) Sharma, S.; Johnson, R. W.; Desai, T. A., Evaluation of the stability of nonfouling ultrathin poly(ethylene glycol) films for silicon-based microdevices. *Langmuir* **2004**, *20*, 348-356.
- (13) Sofia, S. J.; Premnath, V.; Merrill, E. W., Poly(ethylene oxide) grafted to silicon surfaces: Grafting density and protein adsorption. *Macromolecules* **1998**, *31*, 5059-5070.
- (14) Zheng, J.; Li, L. Y.; Chen, S. F.; Jiang, S. Y., Molecular simulation study of water interactions with oligo (ethylene glycol)-terminated alkanethiol self-assembled monolayers. *Langmuir* **2004**, *20*, 8931-8938.
- (15) Zheng, J.; Li, L. Y.; Tsao, H. K.; Sheng, Y. J.; Chen, S. F.; Jiang, S. Y., Strong repulsive forces between protein and oligo (ethylene glycol) self-assembled monolayers: A molecular simulation study. *Biophys. J.* **2005**, *89*, 158-166.
- (16) Zolk, M.; Eisert, F.; Pipper, J.; Herrwerth, S.; Eck, W.; Buck, M.; Grunze, M., Solvation of oligo(ethylene glycol)-terminated self-assembled monolayers studied by vibrational sum frequency spectroscopy. *Langmuir* **2000**, *16*, 5849-5852.
- (17) Qin, G.; Cai, C., Oxidative degradation of oligo(ethylene glycol)-terminated monolayers. *Chem. Commun.* **2009**, 5112-4.
- (18) Leckband, D.; Sheth, S.; Halperin, A., Grafted poly(ethylene oxide) brushes as nonfouling surface coatings. *J. Biomater. Sci., Polym. Ed.* **1999**, *10*, 1125-1147.
- (19) Jiang, S.; Cao, Z., Ultralow-Fouling, Functionalizable, and Hydrolyzable Zwitterionic Materials and Their Derivatives for Biological Applications. *Adv. Mater.* **2010**, *22*, 920-932.
- (20) He, Y.; Hower, J.; Chen, S.; Bernards, M. T.; Chang, Y.; Jiang, S., Molecular Simulation Studies of Protein Interactions with Zwitterionic Phosphorylcholine Self-Assembled Monolayers in the Presence of Water. *Langmuir* **2008**, *24*, 10358-10364.

- (21) Holmlin, R. E.; Chen, X.; Chapman, R. G.; Takayama, S.; Whitesides, G. M., Zwitterionic SAMs that Resist Nonspecific Adsorption of Protein from Aqueous Buffer. *Langmuir* **2001**, *17*, 2841-2850.
- (22) Ladd, J.; Zhang, Z.; Chen, S.; Hower, J. C.; Jiang, S., Zwitterionic Polymers Exhibiting High Resistance to Nonspecific Protein Adsorption from Human Serum and Plasma. *Biomacromolecules* **2008**, *9*, 1357-1361.
- (23) Yang, W.; Xue, H.; Li, W.; Zhang, J.; Jiang, S., Pursuing "Zero" Protein Adsorption of Poly(carboxybetaine) from Undiluted Blood Serum and Plasma. *Langmuir* **2009**, *25*, 11911-11916.
- (24) Zhang, Z.; Chao, T.; Chen, S.; Jiang, S., Superlow Fouling Sulfobetaine and Carboxybetaine Polymers on Glass Slides. *Langmuir* **2006**, *22*, 10072-10077.
- (25) Zhao, C.; Li, L.; Zheng, J., Achieving Highly Effective Nonfouling Performance for Surface-Grafted Poly(HPMA) via Atom-Transfer Radical Polymerization. *Langmuir* **2010**, *26*, 17375-17382.
- (26) Chang, Y.; Chen, W.-Y.; Yandi, W.; Shih, Y.-J.; Chu, W.-L.; Liu, Y.-L.; Chu, C.-W.; Ruaan, R.-C.; Higuchi, A., Dual-Thermoresponsive Phase Behavior of Blood Compatible Zwitterionic Copolymers Containing Nonionic Poly(*N*-isopropyl acrylamide). *Biomacromolecules* **2009**, *10*, 2092-2100.
- (27) Chang, Y.; Shu, S.-H.; Shih, Y.-J.; Chu, C.-W.; Ruaan, R.-C.; Chen, W.-Y., Hemocompatible Mixed-Charge Copolymer Brushes of Pseudozwitterionic Surfaces Resistant to Nonspecific Plasma Protein Fouling. *Langmuir* **2009**, *26*, 3522-3530.
- (28) Cheng, N.; Brown, A. A.; Azzaroni, O.; Huck, W. T. S., Thickness-Dependent Properties of Polyzwitterionic Brushes. *Macromolecules* **2008**, *41*, 6317-6321.
- (29) Omar, A.; Andrew, A. B.; Huck, W. T. S., UCST Wetting Transitions of Polyzwitterionic Brushes Driven by Self-Association. *Angew. Chem. Int. Ed.* **2006**, *45*, 1770-1774.
- (30) Rodriguez Emmenegger, C.; Brynda, E.; Riedel, T.; Sedlakova, Z.; Houska, M.; Alles, A. B., Interaction of Blood Plasma with Antifouling Surfaces. *Langmuir* **2009**, *25*, 6328-6333.
- (31) Zhou, M.; Liu, H.; Kilduff, J. E.; Langer, R.; Anderson, D. G.; Belfort, G., High-Throughput Membrane Surface Modification to Control NOM Fouling. *Environ. Sci. Technol.* **2009**, *43*, 3865-3871.
- (32) Ohno, K.; Kayama, Y.; Ladmiral, V.; Fukuda, T.; Tsujii, Y., A Versatile Method of Initiator Fixation for Surface-Initiated Living Radical Polymerization on Polymeric Substrates. *Macromolecules* **2010**, *43*, 5569-5574.

- (33) Matyjaszewski, K.; Xia, J., Atom Transfer Radical Polymerization. *Chem. Rev.* **2001**, *101*, 2921-2990.
- (34) Sano, H.; Maeda, H.; Ichii, T.; Murase, K.; Noda, K.; Matsushige, K.; Sugimura, H., Alkyl and Alkoxyl Monolayers Directly Attached to Silicon: Chemical Durability in Aqueous Solutions. *Langmuir* **2009**, *25*, 5516-5525.
- (35) de Smet, L. C. P. M.; Pukin, A. V.; Sun, Q.-Y.; Eves, B. J.; Lopinski, G. P.; Visser, G. M.; Zuilhof, H.; Sudhölter, E. J. R., Visible-light attachment of SiC linked functionalized organic monolayers on silicon surfaces. *Appl. Surf. Sci.* **2005**, *252*, 24-30.
- (36) Effenberger, F.; Gotz, G.; Bidlingmaier, B.; Wezstein, M., Photoactivated preparation and patterning of self-assembled monolayers with 1-alkenes and aldehydes on silicon hydride surfaces. *Angew. Chem. Int. Ed.* **1998**, *37*, 2462-2464.
- (37) Stewart, M. P.; Buriak, J. M., Photopatterned hydrosilylation on porous silicon. *Angew. Chem. Int. Ed.* **1998**, *37*, 3257-3260.
- (38) Rosso, M.; Giesbers, M.; Arafat, A.; Schroën, K.; Zuilhof, H., Covalently Attached Organic Monolayers on SiC and Si<sub>3</sub>N<sub>4</sub> Surfaces: Formation Using UV Light at Room Temperature. *Langmuir* **2009**, *25*, 2172-2180.
- (39) Coffinier, Y.; Boukherroub, R.; Wallart, X.; Nys, J. P.; Durand, J. O.; Stievenard, D.; Grandidier, B., Covalent functionalization of silicon nitride surfaces by semicarbazide group. *Surf. Sci.* **2007**, *601*, 5492-5498.
- (40) Arafat, A.; Schroën, K.; de Smet, L. C. P. M.; Sudhölter, E. J. R.; Zuilhof, H., Tailor-made functionalization of silicon nitride surfaces. *J. Am. Chem. Soc.* **2004**, *126*, 8600-8601.
- (41) Scheres, L.; Arafat, A.; Zuilhof, H., Self-assembly of high-quality covalently bound organic monolayers onto silicon. *Langmuir* **2007**, *23*, 8343-8346.
- (42) Rosso, M.; Nguyen, A. T.; de Jong, E.; Baggerman, J.; Paulusse, J. M. J.; Giesbers, M.; Fokkink, R. G.; Norde, W.; Schroën, K.; van Rijn, C. J. M.; Zuilhof, H., Protein-Repellent Silicon Nitride Surfaces: UV-Induced Formation of Oligoethylene Oxide Monolayers. *ACS Appl. Mater. Interfaces* **2011**, *3*, 697-704.
- (43) Bermudez, V. M.; Perkins, F. K., Preparation and properties of clean Si<sub>3</sub>N<sub>4</sub> surfaces. *Appl. Surf. Sci.* **2004**, *235*, 406-419.
- (44) Rathi, V. K.; Gupta, M.; Agnihotri, O. P., The Dependence of Etch Rate of Photo-CVD Silicon-Nitride Films on NH<sub>4</sub>F Content in Buffered HF. *Microelectron. J.* **1995**, *26*, 563.

- (45) Patil, L. S.; Pandey, R. K.; Bange, J. P.; Gaikwad, S. A.; Gautam, D. K., Effect of deposition temperature on the chemical properties of thermally deposited silicon nitride films. *Opt. Mater.* **2005**, *27*, 663-670.
- (46) Antsiferov, V. N.; Gilev, V. G.; Karmanov, V. I., Infrared spectra and structure of  $\text{Si}_3\text{N}_4$ ,  $\text{Si}_2\text{ON}_2$ , and sialons. *Refract. Ind. Ceram.* **2003**, *44*, 108-114.
- (47) van Rijn, C. J. M., *Nano and Micro Engineered Membrane Technology*. Elsevier: Amsterdam, The Netherlands, 2004.
- (48) Girones, M.; Bolhuis-Versteeg, L.; Lammertink, R.; Wessling, M., Flux stabilization of silicon nitride microsieves by backpulsing and surface modification with PEG moieties. *J. Colloid Interface Sci.* **2006**, *299*, 831-840.
- (49) Wagdare, N. A.; Marcelis, A. T. M.; Ho, O. B.; Boom, R. M.; van Rijn, C. J. M., High throughput vegetable oil-in-water emulsification with a high porosity micro-engineered membrane. *J. Membr. Sci.* **2010**, *347*, 1-7.
- (50) Norde, W., Adsorption of proteins from solution at the solid-liquid interface. *Adv. Colloid Interface Sci.* **1986**, *25*, 267-340.
- (51) Marshall, A. D.; Munro, P. A.; Tragardh, G., The Effect of Protein Fouling in Microfiltration and Ultrafiltration on Permeate Flux, Protein Retention and Selectivity - a Literature-Review. *Desalination* **1993**, *91*, 65-108.
- (52) Rosso, M.; Schroën, K.; Zuilhof, H., Biorepellent Organic Coatings for Improved Microsieve Filtration. In *New Membranes and Advanced Materials for Wastewater Treatment*, American Chemical Society: 2009; Vol. 1022, pp 151-163.
- (53) Dijt, J. C.; Cohen Stuart, M. A.; Fleer, G. J., Reflectometry as a Tool for Adsorption Studies. *Adv. Colloid Interface Sci.* **1994**, *50*, 79-101.
- (54) Böcking, T.; Kilian, K. A.; Gaus, K.; Gooding, J. J., Single-Step DNA Immobilization on Antifouling Self-Assembled Monolayers Covalently Bound to Silicon (111). *Langmuir* **2006**, *22*, 3494-3496.
- (55) Balachander, N.; Sukenik, C. N., Monolayer transformation by nucleophilic substitution: Applications to the creation of new monolayer assemblies. *Langmuir* **1990**, *6*, 1621-1627.
- (56) Arafat, A.; Giesbers, M.; Rosso, M.; Sudhölter, E. J. R.; Schroën, K.; White, R. G.; Yang, L.; Linford, M. R.; Zuilhof, H., Covalent biofunctionalization of silicon nitride surfaces. *Langmuir* **2007**, *23*, 6233-6244.
- (57) Sieval, A. B.; Linke, R.; Heij, G.; Meijer, G.; Zuilhof, H.; Sudhölter, E. J. R., Amino-Terminated Organic Monolayers on Hydrogen-Terminated Silicon Surfaces. *Langmuir* **2001**, *17*, 7554-7559.

- (58) Jones, D. M.; Brown, A. A.; Huck, W. T. S., Surface-Initiated Polymerizations in Aqueous Media: Effect of Initiator Density. *Langmuir* **2002**, *18*, 1265-1269.
- (59) Herrwerth, S.; Eck, W.; Reinhardt, S.; Grunze, M., Factors that determine the protein resistance of oligoether self-assembled monolayers - Internal hydrophilicity, terminal hydrophilicity, and lateral packing density. *J. Am. Chem. Soc.* **2003**, *125*, 9359-9366.
- (60) Yam, C. M.; Lopez-Romero, J. M.; Gu, J. H.; Cai, C. Z., Protein-resistant monolayers prepared by hydrosilylation of  $\alpha$ -oligo(ethylene glycol)- $\omega$ -alkenes on hydrogen-terminated silicon (111) surfaces. *Chem. Commun.* **2004**, 2510-2511.
- (61) Krishnan, S.; Weinman, C. J.; Ober, C. K., Advances in polymers for anti-biofouling surfaces. *J. Mater. Chem.* **2008**, *18*, 3405-3413.





## Rapid Microsieve-Based Microbial Diagnostics

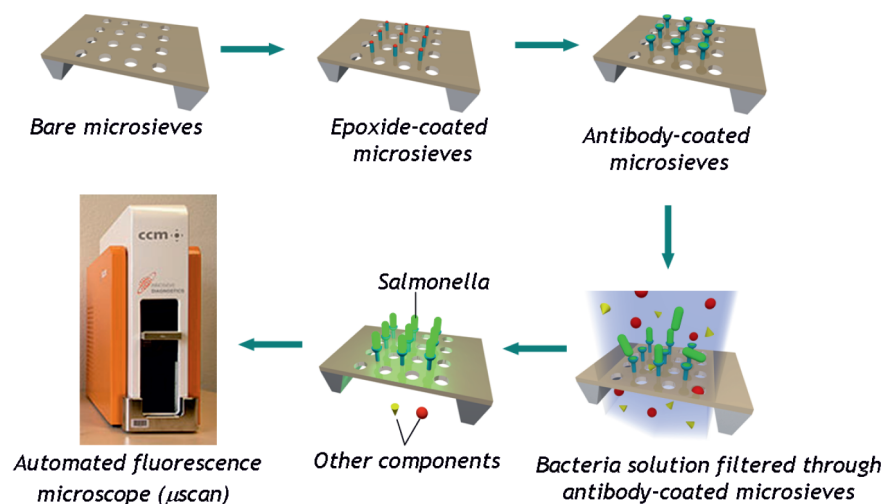
A new method combining selective capture, microfiltration and automated fluorescence imaging for the rapid detection of microorganisms has been developed. Selective capture of *Salmonella* was demonstrated with highly porous micro-engineered silicon nitride membranes (microsieves) with uniform pore sizes in the range of 0.45 to 5.0  $\mu\text{m}$ . 1,2-Epoxy-9-decene was photochemically attached to the silicon nitride microsieve surface via stable Si-C and N-C linkages. The resultant epoxide-terminated microsieves were subsequently bio-functionalized with anti-*Salmonella* antibodies. Capture efficiency and sensitivity of antibody-coated microsieves were evaluated with *Salmonella enterica enterica* serotype Typhimurium solutions (80 - 80,000 cfu.mL<sup>-1</sup>). The antibody-coated microsieves captured 52% (2- $\mu\text{m}$  microsieves), 30% (3.5- $\mu\text{m}$  microsieves) and 12% (5- $\mu\text{m}$  microsieves) of *Salmonella* solution. In semi-skimmed milk samples, the platform enabled to capture *Salmonella*, although with a somewhat lower efficiency than in buffered clear solutions. The use of antibody-coated microsieves as microbial selective capture devices was shown to be promising for the direct detection of microorganisms, giving a strong impulse to the further development of rapid diagnostics.

Nguyen, A. T.; Van Doorn, R.; Baggerman, J.; Paulusse, J. M. J.; Zuilhof, H.; Klerks, M.; Van Rijn, C. J. M Rapid Microsieve-Based Microbial Diagnostics. in preparation, 2011

## 1. Introduction

The detection of food-borne pathogenic microorganisms received a lot of attention over the past decades, because of its paramount importance to human and animal health.<sup>1, 2</sup> Nowadays, the majority of the performed detection assays still includes numerous culture-based enrichment steps and gives only conclusive results after 2-4 days.<sup>3</sup> Modern microbial diagnostics, e.g., antibody-based biosensors including planar microarray,<sup>4</sup> bead-based microarray<sup>5</sup> and protein biochips,<sup>6</sup> are promising tools for a new generation of microbial detection devices. However, direct selective capture of microorganisms by these techniques is still facing limitations with respect to detection sensitivity, applicability and total analysis time. For instance, detection of antibody-based planar microarrays is limited by mass transfer, in particular diffusion of cells towards surfaces, as well as adequate affinity of the sensor surface to overcome fluid forces.<sup>7</sup> Bead-based microarrays have proven particularly versatile and sensitive in multiplex detection, however, the sensitivity of this technique depends on the reliability of filtration-based washing steps, which may suffer from clogging, leakage and nonspecific adsorption.<sup>5, 8</sup> Recently, bead-based technology has been introduced with magnetic microspheres in microarrays, which significantly improves its applicability.<sup>9</sup>

Despite these achievements, the need for a fast and sensitive technique that allows for on-site and rapid selective capture of microorganisms remains. Recently, micro-engineered membranes (microsieves) with uniform pore size and high porosity were described as an innovative microfractionation device for biological samples.<sup>10</sup> This method uses a combination of microfiltration with microsieves followed by fully automated fluorescence imaging of the microsieve surface. The pore sizes of the microsieves were selected to be smaller than the size of the bacterium to be captured. However, microfiltration of larger volumes of crude biological samples over microsieves with small pores is often cumbersome due to fouling issues, resulting in low sample throughput. In order to minimize fouling issues, microsieves with sufficiently large pore sizes were employed, allowing for easier passage of larger contaminants, such as protein granules and larger microorganisms. The use of larger pore sizes, however, also leads to a dramatic reduction of bacterial retention of the microsieve membranes. To circumvent the resulting loss of capture efficiency, an innovative biofunctionalization approach of the microsieves with antibodies for selective capture of the bacteria of interest is presented here. This approach not only overcomes the limitation of cell diffusion towards the surface, as typically encountered in biochip detection, but also prevents the complex washing and collection steps required in bead-based microarrays (Scheme 1).



**Scheme 1.** Stepwise procedure of microbial detection based on antibody-coated microsieves.

A multitude of techniques has been developed for the attachment onto solid supports of biomolecules such as antibodies, proteins and DNA. Covalent coupling of antibodies may be achieved via reaction of primary amines present in lysine residues or thiols in cysteine residues with suitable active supports, such as *N*-hydroxysuccinimide (NHS) ester,<sup>11</sup> aldehyde,<sup>12</sup> carboxylic acid<sup>13</sup> or epoxide<sup>14</sup> functionalized surfaces. Amongst these techniques, active supports bearing NHS ester moieties to form amide bonds are most commonly employed. The NHS ester is, however, also reactive towards water, so that under aqueous conditions partial hydrolysis may occur, resulting in only modest immobilization yields.<sup>15</sup> Another common method to immobilize antibodies is the use of aldehyde-modified supports involving the formation of labile imine bonds. However, these imine linkages need to be subsequently stabilized by a reduction reaction with sodium (cyano-)borohydride, resulting in a secondary amine.<sup>12, 15, 16</sup> Recently, epoxide-modified supports have been receiving a great attention due to their stability in aqueous media with neutral pH, which facilitates handling of materials. Epoxide moieties exhibit an excellent reactivity towards primary amines<sup>15, 17, 18</sup> although the coupling reaction is reported to be relatively slow.<sup>18-20</sup> In addition, epoxides may also be reacted with thiol groups, which gives more possibilities for antibody coupling onto surfaces.<sup>18, 21</sup>

Epoxy-coated microarray glass slides are nowadays commercially available, offering an easy attachment of a variety of proteins, antibodies and DNA, with high coupling efficiency and low background, i.e., low signal-to-noise ratios.<sup>22, 23</sup> However, attachment of epoxy on glass slide is typically achieved via silanization, resulting in Si-O-Si-C linkages, which have been reported to hydrolyze easily in aqueous media.<sup>24, 25</sup> This may

result in a reduced sensitivity due to partial monolayer detachment during the attachment of antibodies and/or under detection conditions. Recently, several alternative approaches were introduced to immobilize various alkene-based or alkyne-based coupling agents onto silicon-based materials, such as silicon<sup>26, 27</sup> and silicon nitride ( $\text{Si}_x\text{N}_4$ )<sup>28-31</sup> substrates. These approaches result in well-defined monolayers, where the coupling agents are attached via robust Si-C and N-C linkages. A high surface coverage is typically achieved, leading to densely packed layers of attached biomolecules. Moreover, the superior stability of these monolayers was demonstrated in both acidic and mild basic media.<sup>31-33</sup> The combination of a versatile coupling of epoxide moieties, and the robust nature of the Si-C and N-C linkages greatly improves the reliability of epoxide functionalization for biochips and biosensors.

In this study, we describe the development of a novel, easy-to-use *Salmonella* diagnostic method based on selective-capture microsieve filtration and automated fluorescence imaging. Well-defined epoxide-functional monolayers on oxide-free  $\text{Si}_x\text{N}_4$  substrates were obtained via a photochemical reaction and used as an active precursor platform for the attachment of antibodies. The antibody-coated microsieves were employed to capture *Salmonella* bacteria (*Salmonella enterica enterica* serotype Typhimurium) from the biological solution. The capture efficiencies of antibody-coated microsieves with different pore sizes and various concentrations of *Salmonella* solution in different matrices were surveyed. The combined results were used to determine the optimal conditions for a *Salmonella* assay in terms of sample throughput and sufficient capture efficiency.

## 2. Experimental Section

### 2.1. Materials

1,2-Epoxy-9-decene (96%) and acetone (semiconductor grade) were purchased from Sigma-Aldrich. 1,2-Epoxy-9-decene was purified by column chromatography; the obtained purity was >99% as determined by GC-MS. Hydrofluoric acid (50%) was purchased from Fluka. Petroleum ether was distilled before use. Ultrapure water from a Barnstead water purification system with a resistivity of 18.3 M $\Omega$ .cm was used.

Anti-*Salmonella* antibody and fluorescein isothiocyanate (FITC)-labeled anti-*Salmonella* antibody were purchased from KPL Inc., USA. Green-fluorescent nucleic acid stain SYTO®9 was purchased from Invitrogen Company, UK. Bovine Serum Albumin (BSA), Fraction V, minimum 96%, lyophilized powder was purchased from Sigma Aldrich. Protein printing buffer solution (PPB) 2 $\times$  and epoxide-coated glass slides were

purchased from Arrayit corporation, USA. Phosphate-buffered saline (PBS) solutions:  $1\times$  PBS (buffer B), blocking solution (buffer C),  $0.1\times$  PBS (buffer D) used in biological experiments for dilution and washing were provided by Innosieve Diagnostics B.V., The Netherlands. *Salmonella enterica enterica* serotype Typhimurium bacteria, ATCC 13311 (abbreviated as *Salmonella* throughout the text) were incubated and subsequently diluted to desired concentrations in buffer B. Semi-skimmed milk was purchased from Friesland Campina company, The Netherlands.  $\text{Si}_x\text{N}_4$  ( $x>3$ ) thin films deposited on Si(100) substrates (p-type, slightly boron doped, resistivity 8-22  $\Omega\cdot\text{cm}$ ) by LPCVD with a thickness of 150 nm was provided by Nanosens B.V., The Netherlands. Micro-engineered membranes (microsieves) made of  $\text{Si}_x\text{N}_4$  thin films standing on silicon supports with circular pores of various well-defined sizes were provided by Aquamarijn Micro Filtration B.V, The Netherlands.

## 2.2. X-ray Photoelectron Spectroscopy (XPS)

Modified surfaces were characterized by XPS using a JPS-9200 Photoelectron Spectrometer (JEOL, Japan). High-resolution spectra were obtained under UHV conditions using monochromatic Al  $K\alpha$  X-ray radiation at 12 kV and 20 mA with an analyzer energy pass of 10 eV. All high-resolution spectra were corrected with a linear background before fitting. The data was fitted using Gaussian-Lorentzian line shapes (GL30, as implemented in CasaXPS).

## 2.3. Static Water Contact Angle Measurements

The wettability of the modified surfaces was determined by automated static water contact angle measurements with the use of a Krüss DSA 100 goniometer (volume of the drop of demineralized water is 2.5  $\mu\text{l}$ ).

## 2.4. Automated Fluorescence Microscope ( $\mu\text{scan}$ )

*Salmonella* enumeration assays on microsieves were scanned by an automated fluorescence microscope ( $\mu\text{scan}$ ) from CCM, The Netherlands. The fluorescein isothiocyanate (FITC) and SYTO®9 dyes were excited with blue LEDs at  $470 \pm 12.5$  nm and the emission was measured with a band-pass filter at  $528 \pm 17$  nm. The obtained images were analyzed by custom  $\mu\text{scan}$  software, version 2.0.6.

## 2.5. Attachment of Epoxide on $\text{Si}_x\text{N}_4$ Surface and Microsieves

$\text{Si}_x\text{N}_4$  ( $x > 3$ ) thin films on silicon wafers were similar with that used for microsieves fabrication.  $\text{Si}_x\text{N}_4$  surfaces were cut into appropriate sizes for each experiment. The  $\text{Si}_x\text{N}_4$

surfaces were cleaned by dust-free wipers with acetone, followed by oxidation in air-based plasma for 10 min. The oxidized samples were then etched with a 2.5% aqueous solution of HF for 2 min and dried under an argon flow. Immediately samples were transferred into degassed neat 1,2-epoxy-9-decene in a quartz flask, followed by three vacuum-argon cycles to remove trace amounts of oxygen that might have entered the flask during sample transfer. Finally, the flask was back-filled with argon. A UV pen-lamp (254 nm, double bore lamp from Jelight Company Inc., California, USA) was aligned 4 mm away from the quartz flask and operated at maximum intensity ( $9 \text{ mW.cm}^{-2}$ ). The samples were irradiated under argon for 24 h. Samples were removed from the flask, rinsed several times with acetone and distilled petroleum ether and finally dried in a stream of argon. The epoxide surface modification for microsieves was obtained by the identical condition employed for  $\text{Si}_x\text{N}_4$  surfaces.

## 2.6. Biofunctionalization of $\text{Si}_x\text{N}_4$ Surfaces and Microsieves

All biological experiments with microsieves were performed in triplicate.

Epoxide-coated  $\text{Si}_x\text{N}_4$  surfaces, epoxide-coated glass slides as positive control, and bare  $\text{Si}_x\text{N}_4$  surfaces as negative control, were incubated with  $1.0 \text{ mg.mL}^{-1}$  anti-*Salmonella* antibody and  $1.0 \text{ mg.mL}^{-1}$  BSA in  $0.5\times$  PPB solution for 10 min at room temperature and further stored at  $4^\circ\text{C}$  overnight to obtain antibody-coated and BSA-coated surfaces, respectively. Finally, the surfaces were rinsed with an excess of buffer B and buffer C solution prior to next experiments.

In the case of microsieves, epoxide-coated microsieves were mounted carefully onto spin tubes with epoxy glue after surface modification, subsequently cured overnight under ambient conditions. Anti-*Salmonella* antibody-coated and BSA-coated microsieves were obtained under identical condition employed for  $\text{Si}_x\text{N}_4$  surfaces as described above (Figure 1).

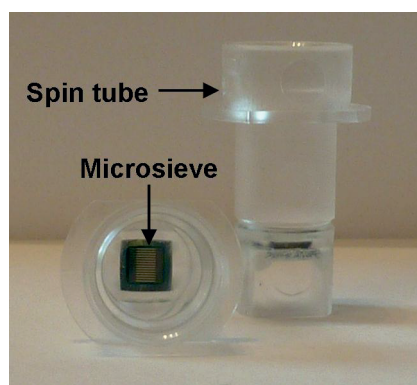


**Figure 1.** Microsieve mounted to spin tube.



## 2.7. Capture of *Salmonella* by Anti-*Salmonella* Antibody-Coated Si<sub>x</sub>N<sub>4</sub> Surfaces

A *Salmonella* solution was diluted to a concentration of  $10^7$  colony forming units per milliliter (cfu.mL<sup>-1</sup>) in buffer B, and subsequently fluorescently stained by using an excess of SYTO®9 at a final SYTO®9 concentration of 5 µM. The antibody-coated Si<sub>x</sub>N<sub>4</sub> and glass surfaces were incubated with blocking solution (buffer C) for 15 min, after which the excess of buffer C was removed. The surfaces were incubated with stained *Salmonella* solution at room temperature for 1 h. After incubation, the surfaces were rinsed with an excess of buffer B and briefly dried with a stream of nitrogen prior to fluorescence microscopy analysis.

## 2.8. Capture of *Salmonella* by Anti-*Salmonella* Antibody-Coated Microsieves

The epoxide-coated and uncoated (bare Si<sub>x</sub>N<sub>4</sub>) microsieves mounted into spin tubes were incubated with 100 µl of 1.0 mg.mL<sup>-1</sup> anti-*Salmonella* antibody in 0.5× PPB, 1.0 mg.mL<sup>-1</sup> BSA and PPB solution for 10 min at room temperature and further stored at 4 °C overnight to obtain antibody-coated, BSA-coated, and protein-free surfaces, respectively. The microsieves were washed with 500 µl buffer B and 500 µl buffer C by centrifugation at 6000 relative centrifuge force (rcf) for 30 s. After washing, 500 µl buffer B containing  $10^7$  cfu.mL<sup>-1</sup> of *Salmonella* was immediately filtered over the microsieve by centrifugation at 1000 rcf for 30 s, or incubated for 1 h at room temperature before filtration. Next, the microsieves were washed with 500 µl buffer B and 500 µl buffer C by centrifugation at 6000 rcf for 30 s. The microsieves were incubated with 100 µl buffer B containing 5 µg FITC-labeled anti-*Salmonella* antibodies in the dark at room temperature for 15 min. Immediately after antibody incubation, the microsieves were washed with 400 µl buffer B by centrifugation at 1000 rcf for 30 s. Next, the microsieves were washed twice with 500 µl buffer D by centrifugation at 6000 rcf for 30 s. Finally, the microsieve surfaces were imaged with an automated fluorescence microscope (µscan).

## 2.9. Optimization of Anti-*Salmonella* Antibody Attachment on Microsieves

Epoxide-coated 5-µm microsieves were prepared and mounted into spin tubes as described previously. The procedure of anti-*Salmonella* antibody attachment was optimized in respect of concentration of the antibody. The epoxide-coated microsieves were incubated with 100 µl 0.5× PPB containing 1.0, 0.50, 0.25, 0.10, 0.050, 0.025 and 0.010 mg.mL<sup>-1</sup> anti-*Salmonella* antibody for 10 min at room temperature and further stored at 4 °C overnight. Next, the same capture procedure as described in Section 2.8 was



employed prior to image analysis. The lowest possible concentration that yields a high number of captured *Salmonella* was selected for further experiments. It is noticed that an excess of *Salmonella* solution ( $10^7$  cfu.mL<sup>-1</sup>) was used in these experiments to assure that each of the antibody-coated microsieves can reach the maximum capture capacity thereof.

## 2.10. Capture Efficiency

Epoxide-coated and uncoated microsieves with different pore sizes (0.45  $\mu$ m, 2.0  $\mu$ m, 3.5  $\mu$ m and 5.0  $\mu$ m) were prepared and mounted into spin tubes as described in Section 2.6. Next, the epoxide-coated microsieves were incubated with 100  $\mu$ l 0.5 $\times$  PPB containing 0.1 mg.mL<sup>-1</sup> anti-*Salmonella* antibody for 10 min at room temperature and further stored at 4 °C overnight. Subsequently, the antibody-coated and uncoated microsieves were subjected to the same capture procedure as described in Section 2.8 prior to image analysis.

## 2.11. Assay sensitivity and validation

Epoxide-coated microsieves with pore sizes of 3.5  $\mu$ m were prepared and mounted into spin tubes as described in Section 2.6. Next, the epoxide-coated microsieves were incubated with 100  $\mu$ l 0.5 $\times$  PPB containing 0.1 mg.mL<sup>-1</sup> anti-*Salmonella* antibodies for 10 min at room temperature and stored at 4° C overnight. A serial dilution series of *Salmonella* solution were spiked in buffer B and in milk in concentrations of 80 - 80,000 cfu.mL<sup>-1</sup>. The *Salmonella* solution at each concentration was filtered through the antibody-coated microsieves. Subsequently, the microsieves were subjected to the same enumeration procedure as described in Section 2.8.

*Salmonella* enumeration using a conventional plating method was performed in parallel with the microsieve experiments. Dilution series of all samples were prepared in buffer B and 100  $\mu$ l of each dilution series was analyzed on ASAP agar plates in triplicate.

# 3. Results and Discussion

## 3.1. Formation and Characterization of Epoxide-Terminated Monolayers on Si<sub>x</sub>N<sub>4</sub> Surfaces

Silicon nitride (Si<sub>x</sub>N<sub>4</sub>) surfaces were functionalized with an epoxide-terminated monolayer by a UV-induced reaction. Hydrogen-terminated Si<sub>x</sub>N<sub>4</sub> substrates were obtained through etching with HF solution, and employed in the photochemical ( $\lambda$  = 254 nm) attachment of 1,2-epoxy-9-decene. Detailed characterization of epoxide-coated Si<sub>x</sub>N<sub>4</sub> surfaces was described in Chapter 3.

The stability of the epoxide-terminated monolayers on  $\text{Si}_x\text{N}_4$  surfaces as well as on microsieves was studied in argon atmosphere for 1 month. No significant changes in both water contact angle and XPS spectra of the surfaces were found after 1-month storage, indicating long-term stability.

### 3.2. Covalent Attachment of Anti-*Salmonella* Antibodies on $\text{Si}_x\text{N}_4$ Surfaces

Anti-*Salmonella* antibodies-coated  $\text{Si}_x\text{N}_4$  surfaces were obtained via coupling of lysine residues at the outside of the antibodies to the epoxide-coated surface (Figure 2). The static water contact angle changed from  $71 \pm 1^\circ$  for epoxide-coated surfaces to  $64 \pm 1^\circ$  for the antibody-coated surfaces. XPS analysis revealed a reduction of 87% in the  $\text{Si}_{2p}$  signal as compared to epoxide-coated surfaces, indicating the successful attachment of antibodies onto the monolayer. No signal corresponding to silicon oxide was detected after the attachment of antibody, confirming that the surface remained largely oxide-free. The narrow-scan XPS spectrum of the  $\text{C}_{1s}$  region (Figure 3, left) displays a peak at 285.0 eV corresponding to carbon bound to carbon (C-C), which results from the alkyl chain. The broad peak at 286.5 eV corresponds to carbon atoms bound to oxygen (C-O) and/or nitrogen (C-N) from the ester and amide moieties present in the antibodies, as well as from alcohols that form following epoxide ring opening. A signal at 288.5 eV stems from carbon atoms bound to oxygen (C-O) from carbonyl groups. In addition, the narrow-scan XPS spectrum of  $\text{N}_{1s}$  region shows the appearance of an organic nitrogen peak at 401 eV, next to the signal of inorganic nitrogen corresponding to the nitrogen of the  $\text{Si}_x\text{N}_4$  substrate (Figure 3, right). The thickness of the antibody layer coated on  $\text{Si}_x\text{N}_4$  surfaces was found to be approximately  $6 \pm 2$  nm, calculated from the differences in  $\text{Si}_{2p}$  signal before and after attachment of antibodies. These results indicate that a dense layer of antibodies attached onto epoxide-coated  $\text{Si}_x\text{N}_4$  was obtained.

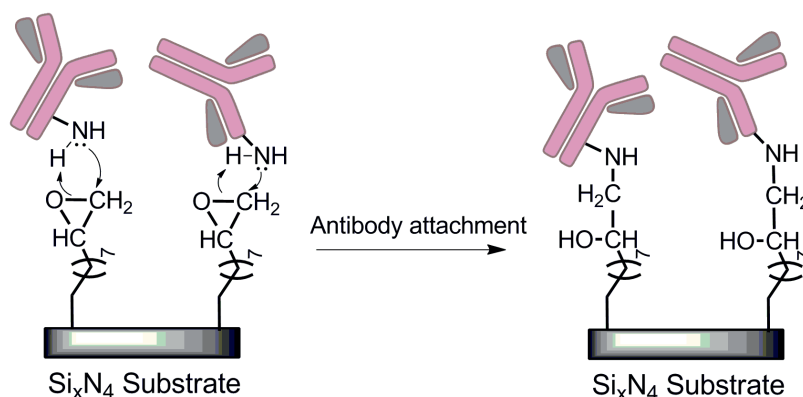


**Figure 2.** Schematic nucleophilic substitution mechanism of antibody attachment onto epoxide-coated  $\text{Si}_x\text{N}_4$  substrate.

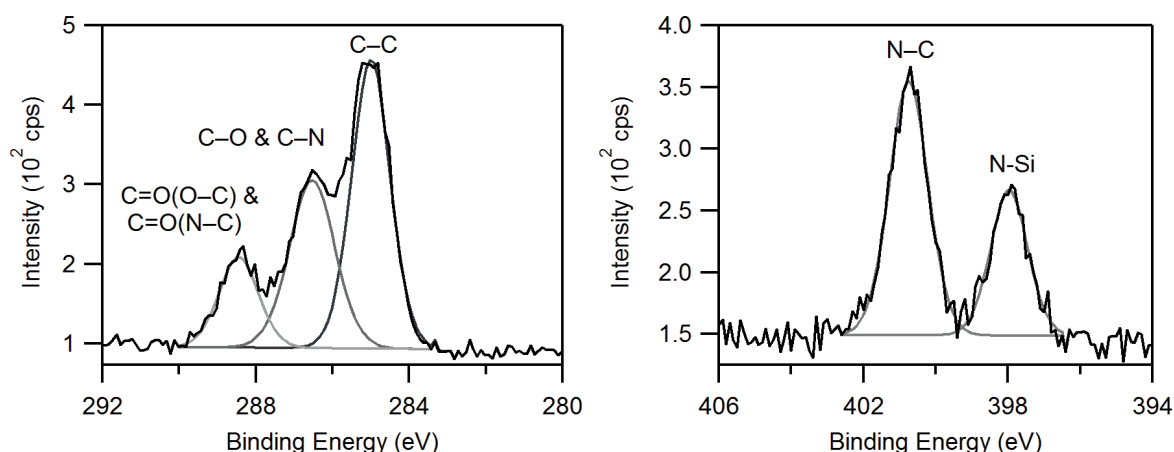


**Figure 3.** Narrow-scan XPS spectra of C<sub>1s</sub> region (left) and N<sub>1s</sub> region (right) of an antibody-coated Si<sub>3</sub>N<sub>4</sub> surface.

### 3.3. Capture of *Salmonella* on Anti-*Salmonella* Antibody-Coated Si<sub>3</sub>N<sub>4</sub> Nonporous Surfaces

The biological activity of anti-*Salmonella* antibodies on Si<sub>3</sub>N<sub>4</sub> surfaces was evaluated by capture of *Salmonella* from solutions and comparison with antibody-coated epoxide glass slides (commercially available) as positive control and bare Si<sub>3</sub>N<sub>4</sub> surfaces as negative control. After incubation (1 h, room temperature) with a solution of SYTO®9-stained *Salmonella* (10<sup>7</sup> cfu.mL<sup>-1</sup>), the samples were subsequently washed with an excess of buffer D prior to observation with a fluorescence microscope. The epoxide-coated Si<sub>3</sub>N<sub>4</sub> surfaces with the covalently attached antibody layers displayed a high number of captured *Salmonella* bacteria, demonstrating the biological accessibility of these antibody layers. Only a few *Salmonella* were observed on the bare Si<sub>3</sub>N<sub>4</sub> surface (Figure 3, right), as a negative control, due to non-specific adsorption. This observation clearly shows that the *Salmonella* captured on the surfaces are bound near-exclusively due to specific interaction with anti-*Salmonella* antibodies.

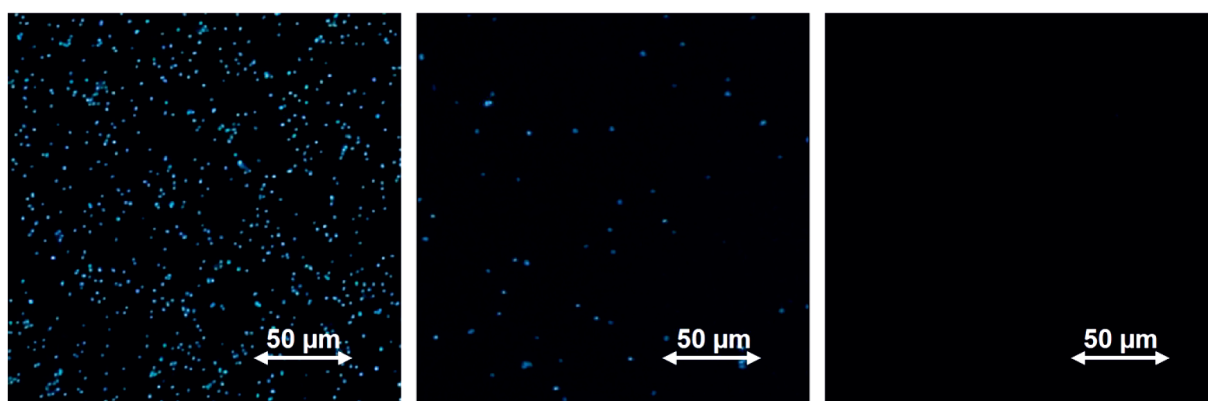


**Figure 4.** Fluorescence images of detected *Salmonella* on antibody-coated  $\text{Si}_3\text{N}_4$  (left); antibody-coated glass slide (middle); and bare  $\text{Si}_3\text{N}_4$  (right) surfaces.

Interestingly, antibody-coated  $\text{Si}_3\text{N}_4$  showed a higher density of captured *Salmonella* bacteria as compared to antibody-coated glass slides obtained under identical conditions (Figure 4, left and middle). This may be attributed to the well-defined monolayer of epoxides attached onto  $\text{Si}_3\text{N}_4$  surfaces via the alkene approach, leading to a dense layer of antibodies attached to the surfaces. The epoxide layers coated on glass slides via silanization techniques often yield less defined layers and lower surface coverage due to a self-aggregation of organosilane molecules, thus resulting in only moderate attachment of antibodies. Consequently, the resultant antibody layer coated on  $\text{Si}_3\text{N}_4$  surfaces enables for detection with higher sensitivity as compared to analogous glass slides. The results indicate the importance of obtaining well-defined layers of active groups on the surfaces, resulting in dense layers of antibodies, and consequently giving access to highly sensitive microbial sensors based on antibodies.

### 3.4. *Salmonella* Detection on Anti-*Salmonella* Antibody-Coated $\text{Si}_3\text{N}_4$ Microsieves

The attachments of epoxide monolayers and anti-*Salmonella* antibody coatings on 5- $\mu\text{m}$  microsieve surfaces were performed via the same procedure that was employed for non-porous  $\text{Si}_3\text{N}_4$  surfaces as described in Section 2.8. A large number of SYTO®9-stained *Salmonella* was detected on the antibody-coated microsieves (Figure 5A-B), whereas almost no *Salmonella* was found on epoxide-coated and bare  $\text{Si}_3\text{N}_4$  surfaces (Figure 5E-F and 5G-H, respectively). Especially the BSA-coated  $\text{Si}_3\text{N}_4$  surface does not indicate any capture of *Salmonella* (Figure 5C-D), confirming that no nonspecific interaction between cells and proteins is involved in the capture of *Salmonella*. These observations on the microsieves fit well with the results obtained for the nonporous antibody-coated  $\text{Si}_3\text{N}_4$  surfaces. This demonstrates that *Salmonella* was captured on the microsieve surface owing to a specific interaction with anti-*Salmonella* antibody.

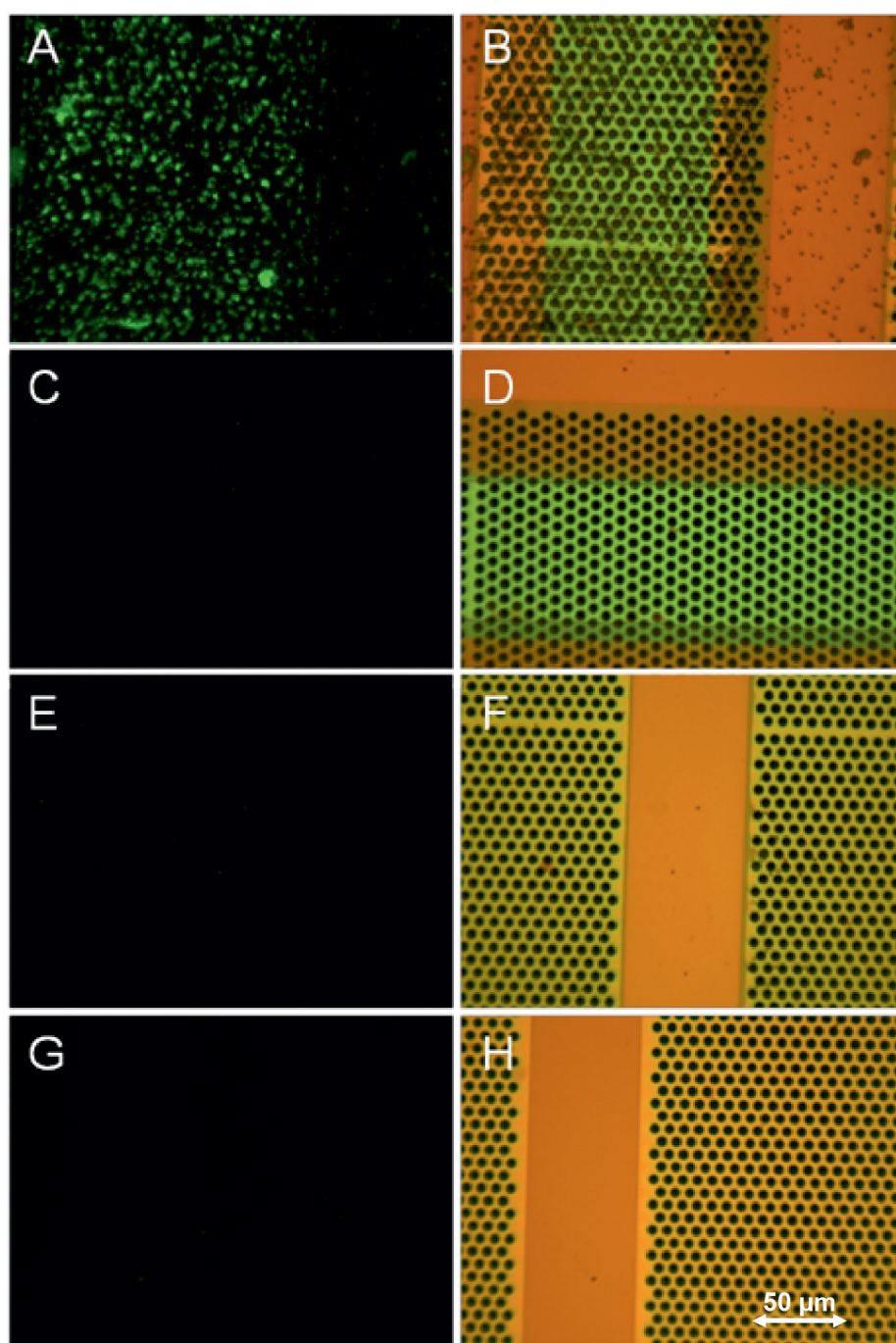


**Figure 5.** Fluorescence images (left column) and corresponding reflected-light images (right column) *Salmonella* detection on modified 5.0- $\mu\text{m}$  microsieves: antibody-coated microsieve (A and B); BSA-coated microsieve (C and D); epoxide-coated microsieve (E and F); and bare microsieve (G and H).

Furthermore, images enlarged at the edge of pores of microsieves showed that *Salmonella* was captured by antibodies not only on the non-porous area, but also at the edge of the pores, which indicates that antibodies could be attached onto the walls of microsieve pores (Figure 6). Interestingly, *Salmonella* detected on the microsieve surface



after 30 s filtration and on the surface after 1 h incubation with an excess of *Salmonella* solution, did not result in significant differences in bacterial counts ( $\sim 1.2 \times 10^5$  counts, both methods). The data demonstrates that capture of *Salmonella* by antibody-coated microsieves is fast enough to be achieved by direct sample filtration over the antibody-coated microsieves, which implies that any incubation steps can be omitted. This significantly shortens the whole detection procedure to an hour, displaying the superiority in terms of time consuming as compared to other known biosensors techniques such as agar-plating,<sup>3</sup> and magnetic microspheres,<sup>9</sup> which are often subjected to the complex process of culturing and washing steps.

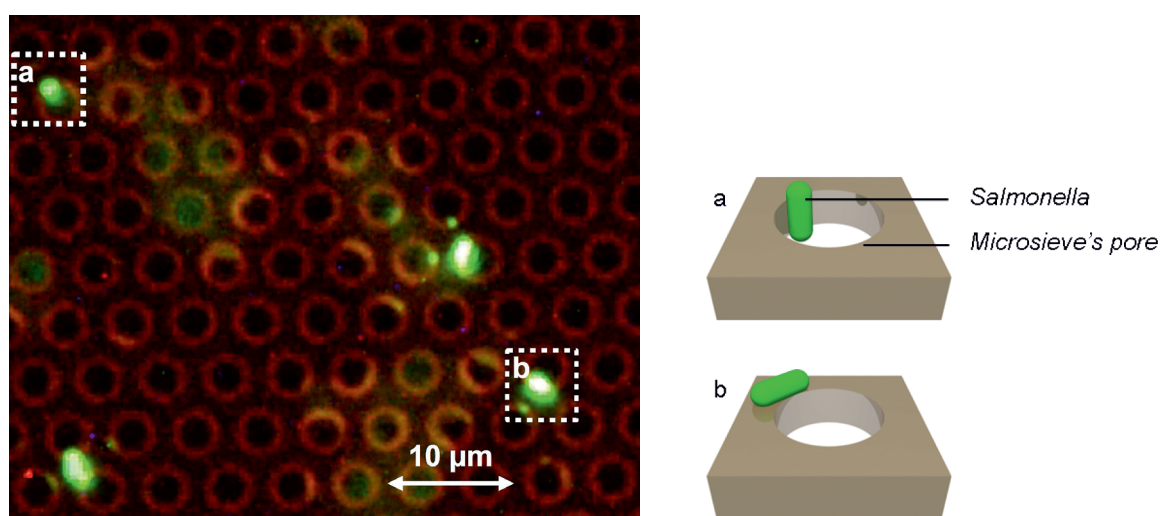


**Figure 6.** Fluorescence image of captured *Salmonella* at the edge of the microsieve pores (3.5 μm), and proposed attachment modes.

### 3.5. Optimization of Anti-*Salmonella* Antibody Attachment onto Microsieves

The antibody coating protocol was optimized with respect to the antibody concentration. Antibody-coated 5-μm microsieves were incubated with antibody concentrations varying from 1.0 to 0.01 mg.mL<sup>-1</sup> at room temperature for 10 min and further stored at 4 °C overnight. As shown in Figure 7 (right), there was no significant change in the number of captured *Salmonella* bacteria when varying antibody concentrations between 1.0 mg.mL<sup>-1</sup> and 0.1 mg.mL<sup>-1</sup> (within error of experiment). However, further diluting antibody concentration down to 0.05 mg.mL<sup>-1</sup> resulted in a significant reduction of the number of captured *Salmonella*. These results demonstrate that an antibody concentration of 0.1 mg.mL<sup>-1</sup> is sufficient to attach antibodies on the microsieves with appreciable performance of *Salmonella* capture.

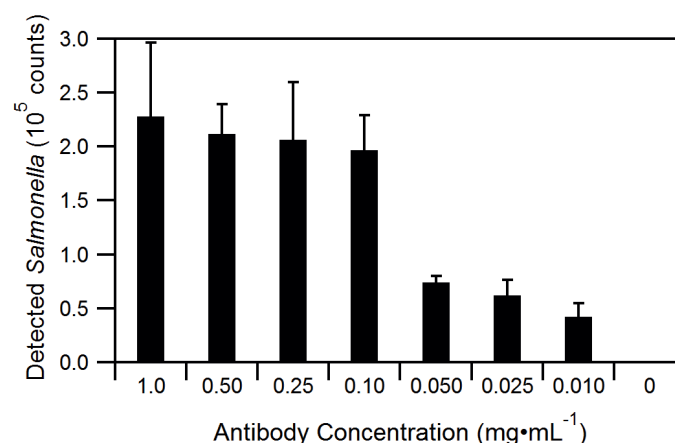


**Figure 7.** *Salmonella* detection on modified 5- $\mu\text{m}$  microsieves as a function of antibody concentration.

### 3.6. Capture Efficiency

Capture efficiency of antibody-coated microsieves with different pore sizes was examined in order to select the appropriate microsieve pore size for sufficient capture efficiency with minimal fouling issues. Antibody-coated and uncoated 0.45- $\mu\text{m}$  microsieves captured a similar number of *Salmonella* as observed for agar plating. This suggests that capturing of *Salmonella* by 0.45- $\mu\text{m}$  microsieve is mainly based on the pore sizes of the microsieve, which were smaller than *Salmonella*. The number of *Salmonella* captured on 0.45- $\mu\text{m}$  microsieves was set for 100% capture efficiency. The capture efficiency of uncoated microsieves with pore sizes ranging from 2 to 5  $\mu\text{m}$  showed nearly no captured *Salmonella* (Figure 8). However, the antibody-coated microsieves did capture 52% (2- $\mu\text{m}$  microsieves), 30% (3.5- $\mu\text{m}$  microsieves) and 12% (5- $\mu\text{m}$  microsieves) of *Salmonella* under similar conditions. Comparison of antibody-coated and uncoated microsieves shows in all cases that capture of *Salmonella* on 3.5- $\mu\text{m}$  and 5- $\mu\text{m}$  microsieves is mainly because of the presence of antibodies. The larger pore sizes of the microsieves result in easier passage of *Salmonella* in the solution and probably decrease the number of capturing events on the microsieves surfaces during filtration. However, the efficiency of capturing events is determined by the combination of the anti-*Salmonella* antibody affinity, the residence time of the *Salmonella* near the membrane surface, the pore size, the porosity of the membrane, and also by the flow rate of the sample through the membrane openings. Currently the relative importance of these (mutually dependent) factors is not fully clear, and further optimizations of these factors are desirable to achieve a maximum capture efficiency.



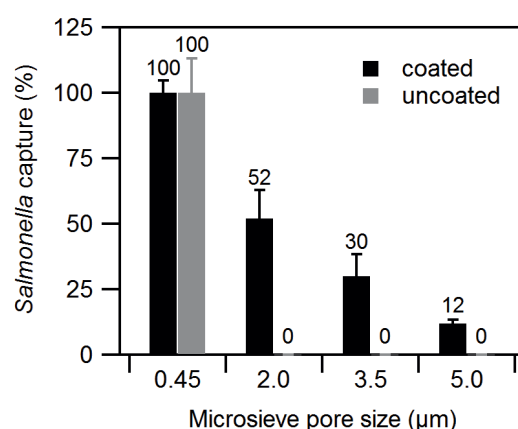


**Figure 8.** Capture efficiency of antibody-coated and uncoated microsieves with different pore sizes. Standard deviations are indicated by the error bars.

Aiming for easy passage of other components in a crude biological solution during the capture of *Salmonella*, filtration of semi-skimmed milk samples (50% diluted) through uncoated microsieves with different pore sizes was examined. The filtration of milk sample through 0.45-μm and 2-μm microsieves was limited to 10-100 μL before the sieve would block, while the filtration capacity of the 3.5-μm and 5-μm microsieves was 10-100 times higher without facing fouling issues. The results suggest that the larger filtration capacity of 3.5-μm and 5-μm microsieves may thus enable for the direct and rapid capture of microorganisms in crude biological samples. Therefore, the 3.5-μm microsieve was chosen to delineate the sensitivity of the platform.

### 3.7. Assay Sensitivity

The sensitivity of antibody-coated 3.5-μm microsieves was examined with a dilution series of *Salmonella* spiked in PBS solution (buffer B) and semi-skimmed milk samples (50% diluted). The number of *Salmonella* captured by antibody-coated 3.5-μm microsieves was lower than the enumeration obtained by the conventional agar plating method. Interestingly, the capture efficiency of *Salmonella* in buffered solution was found to be consistent (~30%) regardless of the concentration of *Salmonella*, which varied from 80 to 80,000 cfu.mL<sup>-1</sup> (Figure 9, left). These results suggest that it is possible to estimate the actual amount of *Salmonella* in the solution by taking into account the capture efficiency (~30%).

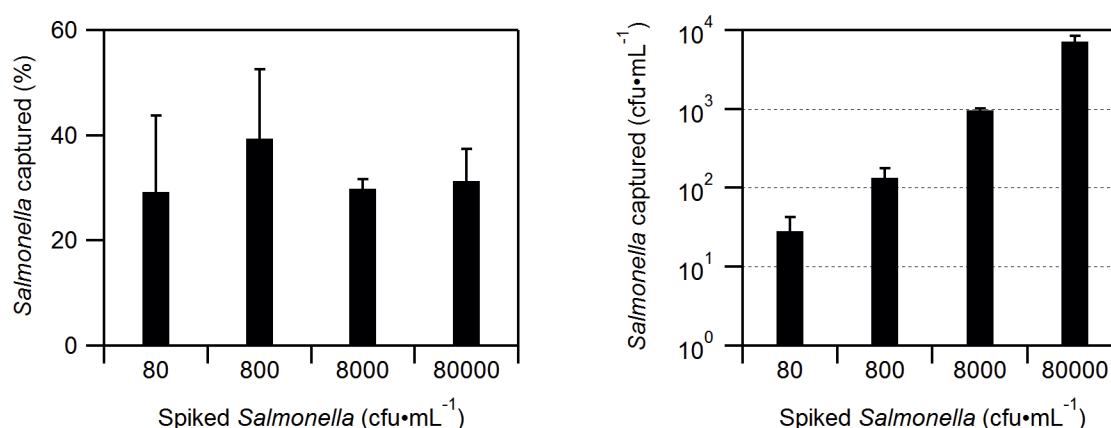


**Figure 9.** *Salmonella* captured by antibody-coated 3.5  $\mu$ m microsieves at different concentrations of *Salmonella* in PBS solution (left) and in semi-skimmed milk solution (right).

The capture efficiency in milk samples is lower than in buffered solution at the high concentrations used in this study ( $>800$  cfu·mL<sup>-1</sup>). Although significantly more *Salmonella* bacteria are captured at higher concentrations, the relative capture efficiency steadily decreased (Figure 9, right). This may be attributed to the nonspecific adsorption of proteins and other components that are present in milk samples. Once these elements stick to the microsieve surfaces, they shield the binding sides of antibodies. Therefore, it lowers the probability for *Salmonella* to find the binding sides of antibodies to be captured on the surface. As a consequence, the capture efficiency of *Salmonella* in milk samples is lower than in buffered solutions. Interestingly, the number of *Salmonella* captured at low concentration (80 cfu·mL<sup>-1</sup>) is comparable with that captured in the corresponding buffered solution. This is possibly because the number of unshielded antibody in milk samples is sufficient to capture *Salmonella* with a similar efficiency to that captured in buffered solution. However, this number of vacant antibodies becomes insufficient to capture the larger amount of *Salmonella* in the higher concentration. Therefore, more *Salmonella* pass through the microsieves at increased concentrations of *Salmonella* in milk samples. The data demonstrates that the developed bioselective capture platform has a high potential for both detection and enumeration assay of microorganisms. In addition, the use of antibody-coated microsieves as selective-capture device in crude biological samples removes the restrictions of the previous method, in which microorganisms are captured by using uncoated microsieves whose pore sizes are smaller than the microorganism itself.

## 4. Conclusions

A highly reproducible and facile method to covalently attach antibodies on the  $\text{Si}_x\text{N}_4$  surface of microsieves was achieved by a two-step procedure: attachment of an epoxide-functionalized monolayer by a photochemical reaction, followed by immobilization of antibodies. Antibody-coated microsieves with pore sizes larger than the size of *Salmonella* displayed a significant increase in the capture efficiency as compared to uncoated microsieves. The high reproducibility of the developed protocol yields a consistent capture efficiency, thus allowing for the actual enumeration assay of *Salmonella*. The detection protocol can be performed within an hour, which is significantly faster than diagnostic techniques such as agar-plating,<sup>3</sup> and magnetic microspheres.<sup>9</sup> The results exhibit the great potential of combining bioselective capture and microfiltration for the direct and rapid detection of microorganisms in crude biological samples.

## 5. Acknowledgment

The authors thank MicroNed (project 6163510587) for financial support and Hien Duy Tong (Nanosens B.V., Zutphen, The Netherlands) for his kind donation of  $\text{Si}_x\text{N}_4$  wafers.

## 6. References

- (1) Byrne, B.; Stack, E.; Gilmartin, N.; O’Kennedy, R., Antibody-Based Sensors: Principles, Problems and Potential for Detection of Pathogens and Associated Toxins. *Sensors* **2009**, *9*, 4407-4445.
- (2) Jasson, V.; Jacxsens, L.; Luning, P.; Rajkovic, A.; Uyttendaele, M., Alternative microbial methods: An overview and selection criteria. *Food Microbiol.* **2010**, *27*, 710-730.
- (3) Hajmeer, M. N.; Fung, D. Y. C.; Marsden, J. L.; Milliken, G. A., Effects of preparation method, age, and plating technique of thin agar layer media on recovery of *Escherichia coli* O157 : H7 injured by sodium chloride. *J. Microbiol. Methods* **2001**, *47*, 249-253.
- (4) Angenendt, P.; Glökler, J.; Sobek, J.; Lehrach, H.; Cahill, D. J., Next generation of protein microarray support materials:: Evaluation for protein and antibody microarray applications. *J. Chromatogr. A* **2003**, *1009*, 97-104.
- (5) Barbee, K. D.; Hsiao, A. P.; Roller, E. E.; Huang, X. H., Multiplexed protein detection using antibody-conjugated microbead arrays in a microfabricated electrophoretic device. *Lab Chip* **2010**, *10*, 3084-3093.
- (6) Rusmini, F.; Zhong, Z.; Feijen, J., Protein Immobilization Strategies for Protein Biochips. *Biomacromolecules* **2007**, *8*, 1775-1789.
- (7) Skottrup, P. D.; Nicolaisen, M.; Justesen, A. F., Towards on-site pathogen detection using antibody-based sensors. *Biosens. Bioelectron.* **2008**, *24*, 339-348.

- (8) Templin, M. F.; Stoll, D.; Bachmann, J.; Joos, T. O., Protein microarrays and multiplexed sandwich immunoassays: What beats the beads? *Comb. Chem. High Throughput Screen* **2004**, *7*, 223-229.
- (9) Opalka, D.; Lachman, C. E.; MacMullen, S. A.; Jansen, K. U.; Smith, J. F.; Chirmule, N.; Esser, M. T., Simultaneous Quantitation of Antibodies to Neutralizing Epitopes on Virus-Like Particles for Human Papillomavirus Types 6, 11, 16, and 18 by a Multiplexed Luminex Assay. *Clin. Diagn. Lab. Immunol.* **2003**, *10*, 108-115.
- (10) van Rijn, C. J. M., *Nano and Micro Engineered Membrane Technology*. Elsevier: Amsterdam, The Netherlands, 2004.
- (11) Wagner, P.; Kernen, P.; Hegner, M.; Ungewickell, E.; Semenza, G., Covalent anchoring of proteins onto gold-directed NHS-terminated self-assembled monolayers in aqueous buffers: SFM images of clathrin cages and triskelia. *FEBS Lett.* **1994**, *356*, 267-271.
- (12) MacBeath, G.; Schreiber, S. L., Printing Proteins as Microarrays for High-Throughput Function Determination. *Science* **2000**, *289*, 1760-1763.
- (13) Arafat, A.; Giesbers, M.; Rosso, M.; Sudhölter, E. J. R.; Schroën, K.; White, R. G.; Yang, L.; Linford, M. R.; Zuilhof, H., Covalent biofunctionalization of silicon nitride surfaces. *Langmuir* **2007**, *23*, 6233-6244.
- (14) Jeanquartier, C.; Schider, G.; Feichtenhofer, S.; Schwab, H.; Schennach, R.; Stettner, J.; Winkler, A.; Gruber-Woelfler, H.; Schitter, G.; Eder, R. J. P.; Khinast, J. G., A Two-Step Method to Covalently Bind Biomolecules to Group-IV Semiconductors: Si(111)/1,2-Epoxy-9-decene/Esterase. *Langmuir* **2008**, *24*, 13957-13961.
- (15) Wong, L. S.; Khan, F.; Micklefield, J., Selective Covalent Protein Immobilization: Strategies and Applications. *Chem. Rev.* **2009**, *109*, 4025-4053.
- (16) Zhu, H.; Bilgin, M.; Bangham, R.; Hall, D.; Casamayor, A.; Bertone, P.; Lan, N.; Jansen, R.; Bidlingmaier, S.; Houfek, T.; Mitchell, T.; Miller, P.; Dean, R. A.; Gerstein, M.; Snyder, M., Global Analysis of Protein Activities Using Proteome Chips. *Science* **2001**, *293*, 2101-2105.
- (17) Grazú, V.; Abian, O.; Mateo, C.; Batista-Viera, F.; Fernández-Lafuente, R.; Guisán, J. M., Novel Bifunctional Epoxy/Thiol-Reactive Support to Immobilize Thiol Containing Proteins by the Epoxy Chemistry. *Biomacromolecules* **2003**, *4*, 1495-1501.
- (18) Mateo, C.; Abian, O.; Fernández-Lorente, G.; Pedroche, J.; Fernández-Lafuente, R.; Guisan, J. M., Epoxy Sepabeads: A Novel Epoxy Support for Stabilization of Industrial Enzymes via Very Intense Multipoint Covalent Attachment. *Biotechnol. Progr.* **2002**, *18*, 629-634.
- (19) Mateo, C.; Torres, R.; Fernández-Lorente, G.; Ortiz, C.; Fuentes, M.; Hidalgo, A.; López-Gallego, F.; Abian, O.; Palomo, J. M.; Betancor, L.; Pessela, B. C. C.; Guisan, J. M.; Fernández-Lafuente, R., Epoxy-Amino Groups: A New Tool for Improved Immobilization of Proteins by the Epoxy Method. *Biomacromolecules* **2003**, *4*, 772-777.
- (20) Jonkheijm, P.; Weinrich, D.; Schröder, H.; Niemeyer, C. M.; Waldmann, H., Chemical Strategies for Generating Protein Biochips. *Angew. Chem. Int. Ed.* **2008**, *47*, 9618-9647.

- (21) Böcking, T.; Kilian, K. A.; Gaus, K.; Gooding, J. J., Single-Step DNA Immobilization on Antifouling Self-Assembled Monolayers Covalently Bound to Silicon (111). *Langmuir* **2006**, *22*, 3494-3496.
- (22) Rivas, L. A.; García-Villadangos, M.; Moreno-Paz, M.; Cruz-Gil, P.; Gómez-Elvira, J.; Parro, V. c., A 200-Antibody Microarray Biochip for Environmental Monitoring: Searching for Universal Microbial Biomarkers through Immunoprofiling. *Anal. Chem.* **2008**, *80*, 7970-7979.
- (23) Seurynck-Servoss, S. L.; White, A. M.; Baird, C. L.; Rodland, K. D.; Zangar, R. C., Evaluation of surface chemistries for antibody microarrays. *Anal. Biochem.* **2007**, *371*, 105-115.
- (24) Menawat, A.; Jr, J. H.; Siriwardane, R., Control of surface energy of glass by surface reactions: Contact angle and stability. *J. Colloid Interface Sci.* **1984**, *101*, 110-119.
- (25) Wei, M.; Bowman, R. S.; Wilson, J. L.; Morrow, N. R., Wetting Properties and Stability of Silane-Treated Glass Exposed to Water, Air, and Oil. *J. Colloid Interface Sci.* **1993**, *157*, 154-159.
- (26) de Smet, L. C. P. M.; Pukin, A. V.; Sun, Q.-Y.; Eves, B. J.; Lopinski, G. P.; Visser, G. M.; Zuilhof, H.; Sudhölter, E. J. R., Visible-light attachment of SiC linked functionalized organic monolayers on silicon surfaces. *Appl. Surf. Sci.* **2005**, *252*, 24-30.
- (27) Stewart, M. P.; Buriak, J. M., Photopatterned hydrosilylation on porous silicon. *Angew. Chem. Int. Ed.* **1998**, *37*, 3257-3260.
- (28) Arafat, A.; Schroën, K.; de Smet, L. C. P. M.; Sudhölter, E. J. R.; Zuilhof, H., Tailor-made functionalization of silicon nitride surfaces. *J. Am. Chem. Soc.* **2004**, *126*, 8600-8601.
- (29) Coffinier, Y.; Boukherroub, R.; Wallart, X.; Nys, J. P.; Durand, J. O.; Stievenard, D.; Grandidier, B., Covalent functionalization of silicon nitride surfaces by semicarbazide group. *Surf. Sci.* **2007**, *601*, 5492-5498.
- (30) Rosso, M.; Giesbers, M.; Arafat, A.; Schroën, K.; Zuilhof, H., Covalently Attached Organic Monolayers on SiC and Si<sub>3</sub>N<sub>4</sub> Surfaces: Formation Using UV Light at Room Temperature. *Langmuir* **2009**, *25*, 2172-2180.
- (31) Nguyen, A. T.; Baggerman, J.; Paulusse, J. M. J.; van Rijn, C. J. M.; Zuilhof, H., Stable Protein-Repellent Zwitterionic Polymer Brushes Grafted from Silicon Nitride. *Langmuir* **2011**, *27*, 2587-2594.
- (32) Sano, H.; Maeda, H.; Ichii, T.; Murase, K.; Noda, K.; Matsushige, K.; Sugimura, H., Alkyl and Alkoxy Monolayers Directly Attached to Silicon: Chemical Durability in Aqueous Solutions. *Langmuir* **2009**, *25*, 5516-5525.
- (33) Scheres, L.; Arafat, A.; Zuilhof, H., Self-assembly of high-quality covalently bound organic monolayers onto silicon. *Langmuir* **2007**, *23*, 8343-8346.



## Bioconjugation of Protein-Repellent Zwitterionic Polymer Brushes Grafted from Silicon Nitride

A new method for attaching antibodies onto protein-repellent zwitterionic polymer brushes is presented, aimed at recognizing microorganisms, while preventing nonspecific adsorption of proteins. The poly(sulfobetaine methacrylate) (SBMA) brushes were grafted from 2-bromoisobutyryl initiator-functionalized silicon nitride ( $\text{Si}_x\text{N}_4$ ,  $x \geq 3$ ) surfaces via controlled atom transfer radical polymerization (ATRP). The Br moieties retained at the end of zwitterionic polymer chains were converted to NHS-terminated surfaces, and subsequently antibodies to *Salmonella* were immobilized onto these polySBMA-grafted  $\text{Si}_x\text{N}_4$  surfaces. Confocal laser scanning microscopy (CLSM) images revealed minimal adsorption of fibrinogen (FIB) onto the antibody-coated polySBMA in comparison with that of antibody-coated epoxide monolayers and also of bare  $\text{Si}_x\text{N}_4$  surfaces. Subsequently, the interaction of antibodies immobilized onto polySBMA with SYTO®9-stained *Salmonella* solution without using blocking solution was examined. The fluorescence images showed that antibody-coated polySBMA efficiently captured *Salmonella* with only low background noise as compared to antibody-coated monolayers lacking the polymer brush. Finally, the antibody-coated polySBMA surfaces were exposed to a mixture of Alexa Fluor 647-labeled FIB and *Salmonella* without prior use of a blocking solution to evaluate the ability of the surfaces to capture bacteria while simultaneously repelling proteins. The fluorescence images showed capture of *Salmonella* with no adsorption of FIB as compared to antibody-coated epoxide surfaces, demonstrating the potential of the zwitterionic layer in preventing nonspecific adsorption of the proteins during the detection of bacteria in complex matrices.

Nguyen, A. T.; Baggerman, J.; Paulusse, J. M. J.; Zuilhof, H.; Van Rijn, C. J. M. Bioconjugation of Protein-Repellent Zwitterionic Polymer Brushes Grafted from Silicon Nitride Surfaces. *Submitted*, 2011.



## 1. Introduction

There is a large need for developing novel biosensing materials that enable attachment of ultra-low fouling and biofunctionalizable surface coatings, which can be used for highly sensitive detection of analytes directly from complex matrices. The pioneering of antibody-based biosensors<sup>1</sup> has had tremendous impact on the development of new biosensing devices, such as planar microarrays,<sup>2</sup> bead-based microarrays<sup>3</sup> and protein biochips.<sup>4</sup> Despite the major advances in the field of diagnostics, several shortcomings still remain, such as interfering background noise as a result of nonspecific adsorption of unwanted species within the biological sample.<sup>5-7</sup> This may lead to misinterpretation of results and limits the precision of diagnostic instruments.<sup>8-11</sup> As a consequence, the use of blocking agents, such as the protein bovine serum albumin, Tween-20 or sodium dodecyl sulfate, is considered a prerequisite step to shield the reactive surface sites so as to minimize nonspecific adsorption of proteins.<sup>5, 7, 12</sup> Achieving sufficiently low degrees of nonspecific binding in sensing devices is therefore of pivotal importance for highly-selective microbial detection directly from crude biological samples.<sup>7</sup>

Several studies have focused on the incorporation of protein-repellent coatings into biorecognition layers to improve selective capture.<sup>13-17</sup> For example, immobilization of horseradish peroxidase and chicken immunoglobulin proteins on poly(ethylene oxide) films grafted from silicon chips via NHS moieties attached onto the polymer chain ends was studied by Feng and coworkers.<sup>15</sup> Although, poly(ethylene oxide) is well known for its protein resistance and biocompatibility, the polymer is also found to auto-oxidize in aqueous solution, resulting in significant cleavage of ethylene oxide units, which deteriorates the protein-repellent performance of poly(ethylene oxide) over time.<sup>18</sup> In addition, poly(ethylene oxide) loses much of its protein resistance at 37 °C (body temperature), which limits its application for *in vivo* biosensors, thereby influencing device-sensitivity.<sup>19, 20</sup>

As an alternative to poly(ethylene oxide), zwitterionic polymer brushes were identified as an outstanding protein-repellent material owing to the hydration layer formed via ionic solvation surrounding adjacent positive and negative charges within zwitterionic brushes.<sup>21-28</sup> Immobilization of antibodies specifically for cancer biomarkers on the zwitterionic poly(carboxy betaine) films was achieved by activation of the carboxylic acid groups with NHS moieties, as reported by Brault et al.<sup>13</sup> and Gao et al.<sup>14</sup> The modified surfaces obtained by this approach show excellent results in recognition of cancer biomarkers from undiluted blood samples. Another approach to biofunctionalize zwitterionic polymers was introduced by Kitano and co-workers, in which a second

polymer containing NHS moieties was grown on top of the zwitterionic polymer brushes.<sup>29</sup> This approach produces a dense layer of NHS moieties, which effects a high surface coverage of a sugar-binding protein, concanavalin A. The protein adsorption of bovine serum albumin on concanavalin-modified surfaces remained low, however, the modified surfaces became less hydrophilic. This reduced hydrophilicity might be caused by the additional dense layer of NHS moieties that may shield the zwitterionic polymer beneath.

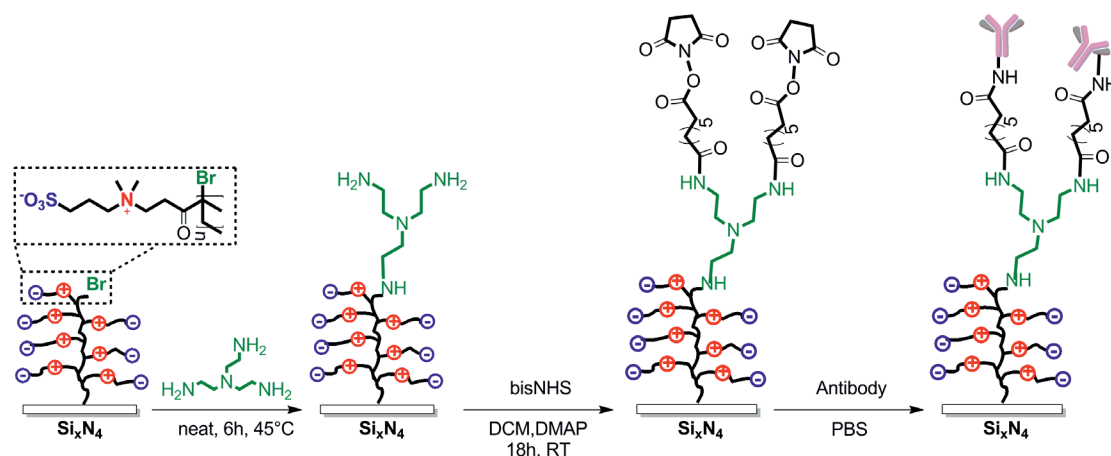
A major disadvantage of these approaches is the limited hydrolytic stability of the Si-O-Si-C<sup>15, 29</sup> and Si-O-C<sup>13, 14</sup> linkages through which the coatings are attached, as reported by Menawat et al.<sup>30, 31</sup> This may result in detachment of the protein-repellent polymer coating, and consequently cleavage of the immobilized biomolecules, keeping long-term application out of reach.

Most antibody-based microarrays are based on planar substrates allowing highly selective multiplex detection.<sup>4, 7, 32</sup> However, planar surfaces are often limited by mass transfer or diffusion of cells towards the surface, as well as adequate affinity of the sensor surface to overcome fluid forces.<sup>33</sup> Recently, silicon nitride micro-engineered membranes, also known as microsieves, have been presented as novel detection devices for microorganisms, which are captured on the microsieve whose pore sizes are smaller than the microorganisms.<sup>34</sup> This method allows for easy passage of other smaller components, while avoiding the limitation of cell diffusion towards the surface as compared to planar microarrays. However, such a microsieve-based approach is hampered by fouling issues and nonspecific adsorption of undesired components from processing crude biological samples. Moreover, the use of a blocking solution before incubation with bacteria solution still is an essential step in order to minimize nonspecific adsorption of proteins, which otherwise leads to interfering background fluorescence. It is advantageous if the use of a blocking solution can be avoided, because of associated material and handling issues. Previously, we presented a method to graft zwitterionic polymer brushes from Si<sub>x</sub>N<sub>4</sub> surfaces, via surface-initiated controlled atom transfer radical polymerization (ATRP).<sup>27</sup> The grafted polymers displayed excellent protein repulsion, and proved to be highly stable during prolonged exposure to phosphate-buffered saline (PBS). In order to reduce nonspecific adsorption on antibody-based biosensor chips, for the current work we decided to covalently immobilize antibodies onto surface-bound protein-repellent zwitterionic polymers. This should provide two advantages: 1) the zwitterionic polymer brushes are grafted from Si<sub>x</sub>N<sub>4</sub> surface via stable Si-C and N-C linkages<sup>27, 31, 35-37</sup> as compared to less stable Si-O-Si-C<sup>15, 29</sup> or Si-O-C<sup>13, 14</sup> linkages; 2) immobilization is facile due to the use of the Br moieties that are retained at the end of zwitterionic polymer chain

after ATRP. As a result the long-term protein repellence properties of the zwitterionic polymer should remain largely unaffected.

In this work, we thus present a method to immobilize antibodies onto zwitterionic polymers grafted from  $\text{Si}_x\text{N}_4$  surfaces and evaluate the sensing properties of the modified surfaces in the specific case of *Salmonella* detection. Sulfobetaine methacrylate (SBMA) zwitterionic polymer brushes were grafted from  $\text{Si}_x\text{N}_4$  surfaces by controlled surface-initiated ATRP. The zwitterionic polymers were biofunctionalized with anti-*Salmonella* antibodies via reaction of the primary amine residues on the antibody with NHS moieties attached onto the polymers (Scheme 1). The modified surfaces were characterized by X-ray photoelectron spectroscopy (XPS), atomic force microscopy (AFM) and water contact angle measurements. The interactivity of the immobilized antibodies was evaluated by fluorescence-based detection of SYTO®9-labeled *Salmonella* from biological solutions, without the aid of a blocking solution.

**Scheme 1.** Procedure for attachment of *Salmonella* antibodies on polySBMA-coated  $\text{Si}_x\text{N}_4$  surfaces.



## 2. Experimental Section

### 2.1. Materials

1,2-Epoxy-9-decene (96%), acetone (semiconductor grade), anhydrous dichloromethane, ethylene diamine (99.5%), tris(2-aminoethyl)amine (96%), 4-dimethylaminopyridine (>99%), suberic acid bis(*N*-hydroxysuccinimide ester) (95%), [2-(methacryloyloxy)ethyl]dimethyl-(3-sulfopropyl)ammonium hydroxide (SBMA) (97%), copper(I) chloride (99.995%) ( $\text{CuCl}$ ), copper(II) chloride (99.995%) ( $\text{CuCl}_2$ ), and 2,2'-bipyridine (99%) (bipy) were purchased from Sigma-Aldrich.  $\text{CuCl}$  was stored under argon. Analytical reagent grade methanol (99.8%) was purchased from VWR. Hydrofluoric acid (50%) was purchased from Fluka. All experiments used ultrapure water, purified by a Barnstead water purification system, with a resistivity of

18.3 M $\Omega$ .cm. FITC-streptavidin, Alexa Fluor 488-labeled fibrinogen and Alexa Fluor 647-labeled fibrinogen were purchased from Invitrogen company, USA. PBS solution at pH 7.4 with ionic strength of 0.2 M was used for subsequent washing steps. Sodium phosphate dibasic (analytical grade, Acros), potassium dihydrogenophosphate (ACS grade, Merck), potassium chloride (pro analysis, Merck) and sodium chloride (puriss., Riedel-de-Haën) were used to prepare the PBS buffer. Protein printing buffer solution (PPB) 2 $\times$  was purchased from Arrayit corporation, USA. Blocking solution was provided by Innosieve Diagnostics B.V., The Netherlands. Fibrinogen (fraction I from porcine plasma, 78% in protein) was purchased from Sigma Aldrich. Anti-*Salmonella* antibody and FITC-labeled anti-*Salmonella* antibodies were purchased from KPL Inc., USA. Green-fluorescent nucleic acid stain SYTO®9 was purchased from Invitrogen Company, United Kingdom. *Salmonella enterica enterica* serotype Typhimurium bacteria, ATCC 13311 (*Salmonella*) were incubated in PBS solution.

## 2.2. X-ray Photoelectron Spectroscopy (XPS)

Modified surfaces were characterized by XPS using a JPS-9200 Photoelectron Spectrometer (JEOL, Japan). High-resolution spectra were obtained under UHV conditions using monochromatic Al K $\alpha$  X-ray radiation at 12 kV and 20 mA with an analyzer energy pass of 10 eV. All high-resolution spectra were corrected with a linear background before fitting. The data were fitted using a deconvolution by Voigt functions (GL30, as implemented in CasaXPS).

## 2.3. Static Water Contact Angle Measurements

The wettability of the modified surfaces was determined by automated static water contact angle measurements with the use of a Krüss DSA 100 goniometer (volume of the drop of demineralized water is 2.5  $\mu$ l).

## 2.4. Atomic Force Microscopy (AFM) for Thickness Measurements

AFM surface images were measured with Tap300Al-G silicon cantilevers (Budgetsensors) in AC mode in air using an Asylum Research MFP-3D SA AFM. Prior to the thickness measurements, the polymer-coated surfaces were immersed in pure water for 4 h at room temperature to fully swell the polymer. A sharp knife was used to scratch the surfaces. The scratched surfaces were sonicated to remove the residuals from cutting, and the sample surface was subsequently dried with argon. The scratched surfaces were directly measured by AFM. The thickness of the swollen polymer layer was determined from the height difference in the topography profile.

## 2.5. Confocal Laser Scanning Microscopy (CLSM)

Fluorescence images were measured with a confocal laser scanning microscope (Zeiss LSM 510 Meta). The dyes fluorescein isothiocyanate (FITC) and Alexa Fluor 488 were excited with an argon ion laser at 488 nm and the emission was measured with a long-pass filter with a cut-off wavelength of 530 nm. Alexa Fluor 647 was excited with a He-Ne laser at 633 nm and the emission was measured with a long-pass filter with a cut-off wavelength of 650 nm.

## 2.6. Attachment of ATRP Initiators on $\text{Si}_x\text{N}_4$ Surface

$\text{Si}_x\text{N}_4$  ( $x > 3$ ) was deposited on Si (100) substrates (p-type, slightly boron doped, resistivity 8-22  $\Omega\cdot\text{cm}$ ) by LPCVD with a thickness of 150 nm (Nanosens B.V., The Netherlands). The  $\text{Si}_x\text{N}_4$  wafers were cut into appropriate sizes for each experiment. ATRP initiators were attached onto  $\text{Si}_x\text{N}_4$  through stable Si-C linkages via 3 consecutive reactions as described previously.<sup>27</sup> In brief: UV-induced reaction of 1,2-epoxy-9-decene with hydrogen-terminated  $\text{Si}_x\text{N}_4$  surfaces was followed by conversion of the epoxide with 1,2-ethylenediamine resulting in primary and secondary amine-terminated surfaces. Reaction with 2-bromoisobutyryl bromide led to ATRP initiator-coated surfaces.

## 2.7. Surface-Initiated Polymerization

[2-(Methacryloyloxy)ethyl]dimethyl-(3-sulfopropyl)ammonium hydroxide (SBMA, 4.90 g, 17.5 mmol) and 2,2'-bipyridine (0.14 g, 0.90 mmol) were dissolved in a mixture of methanol (4.0 mL) and water (16.0 mL) in a round-bottomed flask by stirring. The solution was degassed for 30 min by purging with argon. A mixture of CuCl (36.0 mg, 0.36 mmol) and CuCl<sub>2</sub> (4.8 mg, 0.036 mmol) was added to a separate round-bottomed flask under argon (in a glovebox), which was closed with a rubber septum. Subsequently, the degassed solution was transferred into the flask containing the mixture of CuCl and CuCl<sub>2</sub> by means of a syringe (flushed with argon in advance). The mixture was stirred further for an additional 30 min under argon to dissolve all CuCl and CuCl<sub>2</sub>. Afterwards, the mixture was transferred to the reaction flask containing the initiator-coated  $\text{Si}_x\text{N}_4$  surface by means of a syringe (argon flushed). The polymerization was carried out under argon pressure (0.14 bar over-pressure) while stirring at room temperature for a period of time. The samples were removed and rinsed with warm water (60 – 65 °C) for 5 min, cleaned by sonication in water, and dried under a stream of argon.

PolySBMA-coated surfaces with different thicknesses were prepared with a special holder equipped with a magnet, by which the holder can be moved with an external magnet. The degassed polymerization solution prepared as described above was injected

into the reaction flask containing the initiator-coated  $\text{Si}_x\text{N}_4$  surface. Subsequently, the sample holder was submerged partially into the polymerization solution and moved in further in a stepwise manner at several intervals. The polymerization was carried out under argon pressure with agitation. Finally, the samples were removed and the same cleaning procedure was employed as described earlier.

## 2.8. NHS-Terminated polySBMA Surfaces

The polySBMA-coated  $\text{Si}_x\text{N}_4$  surfaces were further functionalized in two steps. First, polySBMA-coated  $\text{Si}_x\text{N}_4$  surfaces were reacted with neat tris(2-aminoethyl)amine at 45 °C under argon for 6 h to obtain amine-terminated polySBMA ( $\text{NH}_2$ -polySBMA)  $\text{Si}_x\text{N}_4$  surfaces. The surfaces were then washed thoroughly with pure water, followed by acetone, and dried under a stream of argon. Subsequently, the surfaces were immersed into a solution of bifunctional suberic acid bis(*N*-hydroxysuccinimide ester) ( $8.6 \text{ mmol.L}^{-1}$ ) and DMAP ( $0.98 \text{ mol.L}^{-1}$ ) in anhydrous dichloromethane under argon for 18 h.<sup>15</sup> The obtained NHS-terminated polySBMA (NHS-polySBMA)  $\text{Si}_x\text{N}_4$  surfaces were washed with dichloromethane three times and dried under a stream of argon.

## 2.9. Attachment of Streptavidin on polySBMA Surfaces

To evaluate the reactivity of NHS-terminated polySBMA-coated  $\text{Si}_x\text{N}_4$  surfaces, FITC-streptavidin conjugates were attached onto the surfaces. NHS-terminated polySBMA-coated  $\text{Si}_x\text{N}_4$  surfaces were immersed in fluorescein isothiocyanate (FITC)-labeled streptavidin solution ( $0.5 \text{ mg.mL}^{-1}$  in PBS) at room temperature for 30 min. The surfaces were rinsed thoroughly with PBS before confocal laser scanning microscopy (CLSM) measurements.

## 2.10. Attachment of Antibodies on Modified $\text{Si}_x\text{N}_4$ Surfaces

Epoxide-coated  $\text{Si}_x\text{N}_4$  surfaces<sup>27</sup> were completely covered with antibody solution with a concentration of  $1 \text{ mg.mL}^{-1}$  in  $0.5\times$  protein printing buffer. After incubation for 10 min at ambient temperature, the surfaces were stored at 5 °C overnight. The samples were rinsed 3 times with PBS solution prior to *Salmonella* detection experiments.<sup>38</sup>

The freshly prepared NHS-terminated polySBMA-coated  $\text{Si}_x\text{N}_4$  surfaces were incubated with antibody solution at a concentration of  $1 \text{ mg.mL}^{-1}$  in  $0.5\times$  protein printing buffer at room temperature for 30 min. The samples were rinsed 3 times with PBS solution prior to *Salmonella* detection experiments.



## 2.11. Protein Adsorption

The adsorption of proteins onto zwitterionic polymer coated surfaces was evaluated by in-situ reflectometry, using fibrinogen (FIB) solution ( $0.1 \text{ g.L}^{-1}$  in PBS). All reflectometry experiments were performed at room temperature. Before measurements, surfaces were incubated 1 h in warm water ( $60 - 65 \text{ }^{\circ}\text{C}$ ) to sufficiently wet the coatings and subsequently in PBS solution for 1 h to avoid artifacts. After placing the samples in the reflectometer, PBS solution was injected until the output signal remained constant. Each experiment involved at least one adsorption phase, in which FIB solutions was added to the surface, and one desorption phase, in which only buffer was injected. Details on the preparation of FIB solution and the calculation of the amount of adsorbed protein were described in Chapter 2.

The second method to study the adsorption of proteins on modified surfaces was fluorescence imaging to observe adsorbed Alexa Fluor 488-labeled FIB. The modified surfaces were immersed in the solution of Alexa Fluor 488-labeled FIB ( $0.1 \text{ g.L}^{-1}$ ) for 1 h at room temperature. The samples were subsequently rinsed 3 times with PBS and dried under a stream of argon before fluorescence imaging.

## 2.12. Detection of *Salmonella* by Biofunctionalized Zwitterionic Surfaces

Antibody immobilized on  $\text{Si}_x\text{N}_4$  surfaces (polySBMA-coated and epoxide-coated  $\text{Si}_x\text{N}_4$  surfaces) and bare (uncoated) surfaces were incubated in SYTO®9-stained *Salmonella* solution in  $1\times$  PBS for 15 min. Subsequently, the surfaces were rinsed 5 times with  $1\times$  PBS then dried briefly with argon before CLSM measurements.

## 2.13. Detection of *Salmonella* by Biofunctionalized Zwitterionic Surfaces in a Mixture of FIB and *Salmonella*

Anti-*Salmonella* antibodies were attached onto polySBMA-coated and epoxide-coated  $\text{Si}_x\text{N}_4$  surfaces as described in Section 2.10, and these two types of surfaces were incubated in a mixture of Alexa Fluor 647-labeled FIB ( $0.2 \text{ g.L}^{-1}$ ) and *Salmonella* ( $10^7 \text{ cfu.ml}^{-1}$ ) for 15 min; uncoated  $\text{Si}_x\text{N}_4$  surfaces were similarly treated as reference samples. Subsequently, the surfaces were rinsed 5 times with  $1\times$  PBS and incubated with  $1\times$  PBS containing  $5 \text{ }\mu\text{g}$  FITC-labeled anti-*Salmonella* antibodies in the dark at room temperature for 15 min. After incubation, the surfaces were rinsed 5 times with  $1\times$  PBS and dried briefly with argon before CLSM measurements. For the comparison of fluorescence images, the same settings were used in all measurements.



### 3. Results and Discussion

#### 3.1. Surface-Initiated ATRP

Sulfobetaine methacrylate (SBMA) polymer brushes were grafted via controlled ATRP. To this purpose,  $\text{Si}_x\text{N}_4$  surfaces were covalently functionalized with an epoxide-terminated monolayer, which was reacted with ethylene diamine to yield an amine-terminated surface. Subsequently, ATRP initiators were attached via reaction with 2-bromoisobutyryl bromide, as described in detail earlier.<sup>27</sup> After polymerization with SBMA, the water contact angles of the polySBMA-modified surfaces were lower than  $20^\circ$ , indicating the presence of a highly polar coating on the surfaces. These results are in agreement with earlier observations for polySBMA coated on gold and silicon surfaces.<sup>39-41</sup> The wide-scan XPS spectrum of the polySBMA-grafted  $\text{Si}_x\text{N}_4$  surface showed a significant reduction of the  $\text{Si}_{2p}$  signal at 102 eV, demonstrating the presence of a thick polymer layer on the substrate (Figure 1, left). The narrow-scan XPS spectrum of the  $\text{N}_{1s}$  region revealed two distinct signals for nitrogen, one corresponding to the quaternary ammonium ions of the polySBMA polymer, and a signal stemming from the nitrogen atoms of the  $\text{Si}_x\text{N}_4$  substrate (Figure 1, right). Furthermore, the  $\text{Br}_{3d}$  narrow-scan spectrum revealed a signal at 70 eV, confirming retention of the bromide end groups after polymerization (Figure 2, left). These results demonstrate that polySBMA was grown in a controlled way from the Br initiator-coated  $\text{Si}_x\text{N}_4$  surface. However, the intensity of the bromide signal was found to decrease with increasing polymerization time (Figure 2, right). This may be attributed to steric hindrance between adjacent polymer chains during polymerization, particularly when grafting from dense initiator-coated surfaces, which causes some Br moieties to reside within the polymer brush rather than at the periphery, with a concomitant decrease in the  $\text{Br}_{3d}$  XPS signal. Moreover, growth of polymers via ATRP is determined by a complex interplay of a number of factors: solvent, catalyst, monomer, and ligand. Especially, controlled ATRP in water is often hampered by deactivation of the copper catalyst and the fast propagation rate of the polymerization in this medium.<sup>42-44</sup> Competing side reactions during polymerization may thus yield a diminishing fraction of living polymer chains with increasing reaction times.

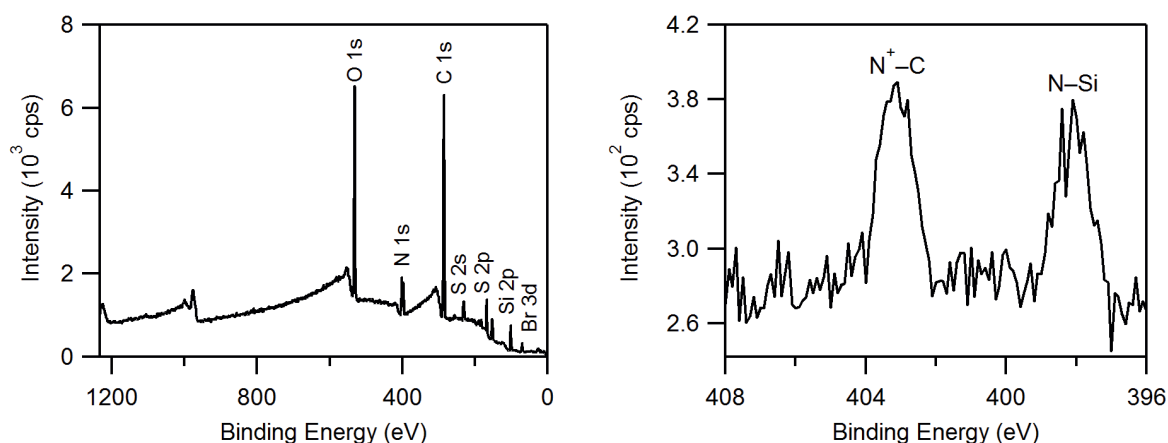


**Figure 1.** Wide-scan XPS spectrum of the polySBMA-grafted  $\text{Si}_3\text{N}_4$  surface (left) and narrow-scan XPS spectrum of  $\text{N}_{1s}$  region (right).

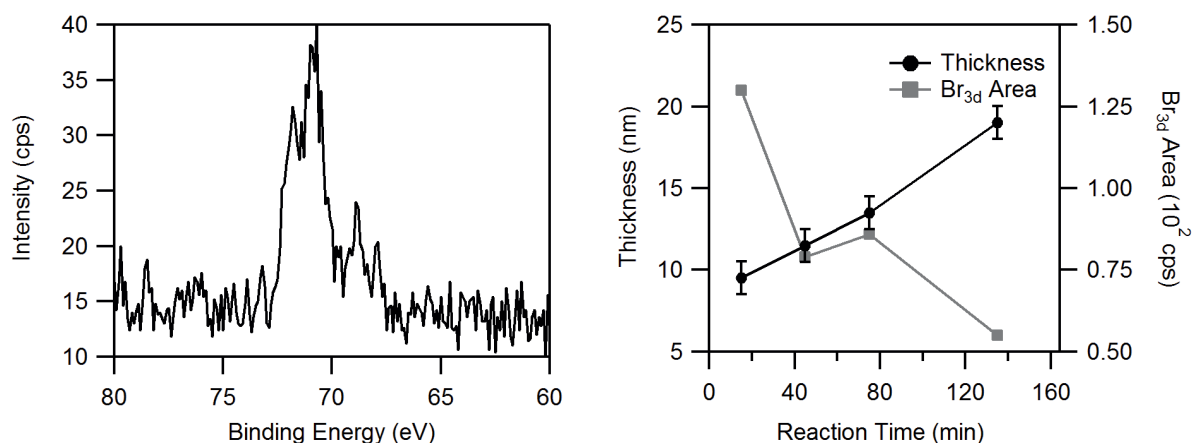


**Figure 2.** Narrow-scan XPS spectrum of  $\text{Br}_{3d}$  region (left) of a polySBMA-coated  $\text{Si}_3\text{N}_4$  surface and polySBMA film thickness and  $\text{Br}_{3d}$  signal intensity as function of polymerization time (right).

The thickness of zwitterionic polymer brushes of  $\sim 15$ – $20$  nm was earlier demonstrated to give best performance in protein repellence in blood solution.<sup>45</sup> Aiming for a similar range of polySBMA thicknesses, the intensity of retained bromides, the thicknesses of the polySBMA layer as well as their corresponding protein-repellent properties were investigated as a function of reaction time. The protein adsorption measured by in-situ reflectometry showed that a 7-nm thick polySBMA layer adsorbed  $1.4 \text{ mg.m}^{-2}$  of FIB, while 10-nm thickness of polySBMA allowed the adsorption of only  $0.5 \text{ mg.m}^{-2}$ , i.e., repelling 91% of FIB as compared to the hydrophobic surface<sup>27</sup> while the signal of  $\text{Br}_{3d}$  was still mostly retained. A further reduction of  $\text{Br}_{3d}$  intensity was found by XPS measurement for 19 nm thick polySBMA. A thickness of polySBMA of about 10 nm was, therefore, selected for further functionalization for simultaneous protein repellence and bioselective capture.

### 3.2. Amine- and NHS-Terminated polySBMA Brushes

The bromide moieties that were retained at the polymer chain ends may be used for further functionalization as described by Feng and coworkers.<sup>15</sup> The bromides were converted into amine moieties by reaction with neat tris(2-aminoethyl)amine. An additional nitrogen peak appears at 401 eV in the  $N_{1s}$  narrow-scan XPS spectrum (Figure 3, right), between the nitrogen peak stemming from the quaternary ammonium of SBMA and the inorganic nitrogen of the  $Si_xN_4$  substrate. In addition, the signal of  $Br_{3d}$  at 70 eV was no longer observed (Figure 3, left), while the water contact angle remained equally low. This indicates the successful attachment of tris(2-aminoethyl)amine onto the polySBMA-coated surfaces to give  $NH_2$ -polySBMA  $Si_xN_4$  surfaces.

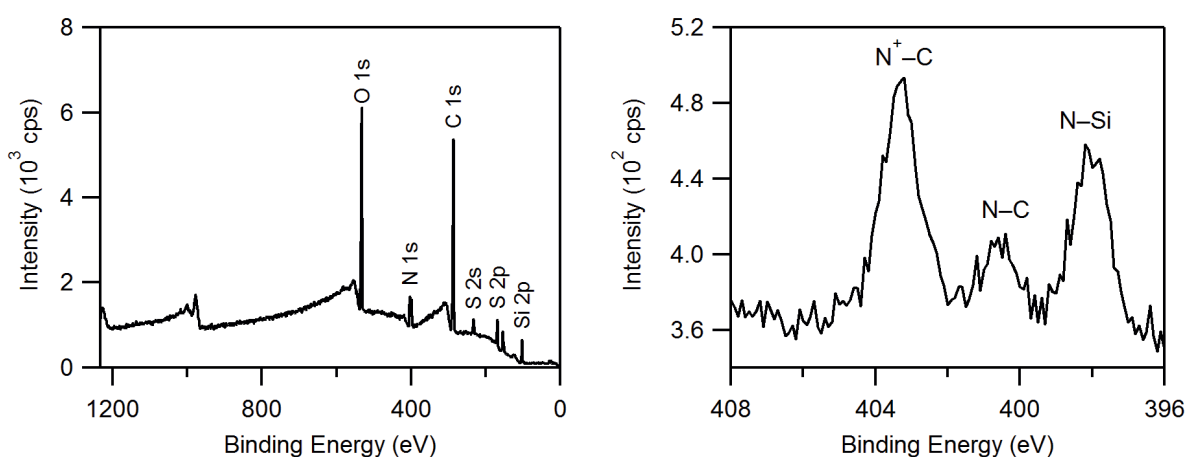


**Figure 3.** Wide-scan XPS spectrum(left) and narrow-scan XPS spectra of  $N_{1s}$  region (right) of  $NH_2$ -polySBMA coated  $Si_xN_4$  surface.

Following the tris(2-aminoethyl)amine attachment, these  $NH_2$ -polySBMA  $Si_xN_4$  surfaces were subsequently converted into *N*-hydroxysuccinimide (NHS) functionalized monolayers by reaction with the bifunctional suberic acid bis(*N*-hydroxysuccinimide ester). The water contact angle value still remained low (typically  $< 20^\circ$ ), indicating the persistence of the hydrophilic polySBMA brush. The integrity of the polymer brush was further confirmed by AFM measurements, which showed that the thickness of the polySBMA film remained constant at  $10 \pm 2$  nm after 2 consecutive reactions (Appendix 5). Unfortunately, XPS could not be used to follow the reaction progress, as the spectra display similar signals for the NHS-functionalized surface as compared to  $NH_2$ -polySBMA. Specifically, no significant change was found in the narrow-scan XPS spectrum of  $C_{1s}$  region, which can be attributed to overlap of the carbonyl signals of the NHS moieties with the signals of the underlying polySBMA, which are much larger.

### 3.3. Biofunctionalization on NHS-polySBMA

The attachment of FITC-labeled streptavidin was performed to test the reactivity of the NHS-functionalized surfaces. The fluorescence image displayed a strong signal of FITC from the coated area while the uncoated area (bare  $\text{Si}_x\text{N}_4$ ) gave virtually no signal (Figure 4). The fluorescence remained after washing with high ionic strength PBS, which shows that a homogeneous surface coverage was obtained of FITC-labeled streptavidin covalently bound to polySBMA-coated  $\text{Si}_x\text{N}_4$  surfaces. The successful attachment of streptavidin not only demonstrates a high immobilization efficiency of NHS-polySBMA  $\text{Si}_x\text{N}_4$  surfaces, but also opens the way to the immobilization of many biomolecules that have primary amine groups in the side chain onto these protein-repelling surfaces. This procedure was therefore also used for the immobilization of anti-*Salmonella* antibodies.

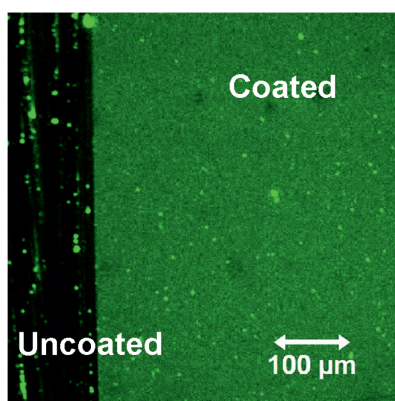


**Figure 4.** Fluorescence image of streptavidin-coated zwitterionic coating.

### 3.4. FIB Adsorption on AB-polySBMA Surfaces

The protein-repellent properties of polySBMA-coated  $\text{Si}_x\text{N}_4$  surfaces after antibody attachment were evaluated by exposure to an Alexa Fluor 488-labeled fibrinogen solution ( $0.1 \text{ g.L}^{-1}$ ) for 1 h at room temperature, and compared with  $\text{Si}_x\text{N}_4$  surfaces directly coated with antibodies via epoxide chemistry (AB-epoxide),<sup>38</sup> as well as with a bare  $\text{Si}_x\text{N}_4$  surface. Fluorescence images showed no signal of Alexa Fluor 488 on antibody-coated polySBMA surfaces as compared with background, while both AB-epoxide and bare  $\text{Si}_x\text{N}_4$  surfaces displayed strong signals (Figure 5). This observation indicates the near-complete reduction of nonspecific adsorption of FIB on AB-polySBMA surfaces, in comparison to the significant adsorption observed for both AB-epoxide  $\text{Si}_x\text{N}_4$  and bare  $\text{Si}_x\text{N}_4$  surfaces.

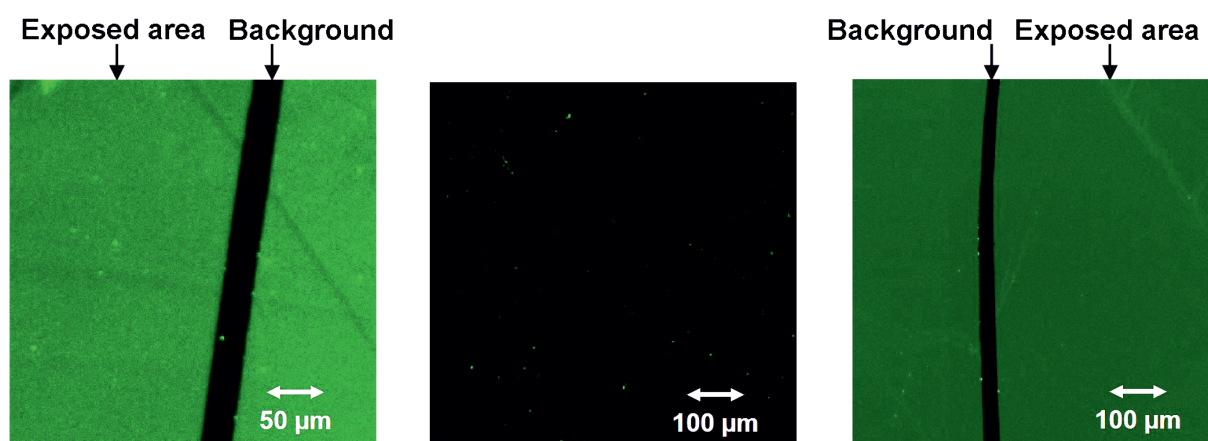


**Figure 5.** Alexa Fluor 488-labeled FIB adsorbed onto AB-epoxide (A), AB-polySBMA (B) and bare  $\text{Si}_3\text{N}_4$  surfaces (C).

### 3.5. Detection of *Salmonella* with AB-polySBMA Surfaces

The binding affinity of anti-*Salmonella* antibodies immobilized on polySBMA-coated  $\text{Si}_3\text{N}_4$  surfaces was further evaluated by exposure to *Salmonella* stained by SYTO®9 (green-fluorescent nucleic acid stain). The detection performance was compared with AB-epoxide and bare  $\text{Si}_3\text{N}_4$  surfaces, and for all these surfaces without prior use of a blocking solution that would typically contain agents such as bovine serum albumin and Tween-20. The surfaces were incubated with this stained *Salmonella* solution at a concentration of approximately  $10^7$  cfu. The fluorescence images showed almost no *Salmonella* was captured on uncoated  $\text{Si}_3\text{N}_4$  surfaces (Figure 6, left) whereas the AB-epoxide  $\text{Si}_3\text{N}_4$  surfaces (Figure 6, middle) and AB-polySBMA  $\text{Si}_3\text{N}_4$  surfaces (Figure 6, right) displayed significant binding of *Salmonella* with similar fluorescence intensities of the cells. However, the AB-polySBMA  $\text{Si}_3\text{N}_4$  surfaces showed much lower background signal (high signal-to-noise ratio) as compared to AB-epoxide  $\text{Si}_3\text{N}_4$  surfaces (Figure 6, middle and right). This difference is attributed to the nonspecific binding of either other microorganisms or free DNA present in *Salmonella* solutions, which are also stained by SYTO®9 dye as a nucleic acid stain. This attribution is further confirmed by the observation of a lower background for both of the antibody-coated surfaces in the case of using a blocking solution in order to minimize nonspecific adsorption. Interestingly, the amount of detected *Salmonella* on AB-polySBMA surfaces is comparable with that found on antibodies immobilized onto the epoxide-coated  $\text{Si}_3\text{N}_4$  surfaces. These results display that antibody-functionalized polySBMA surfaces combine excellent protein repellence with a highly efficient capture of *Salmonella*.



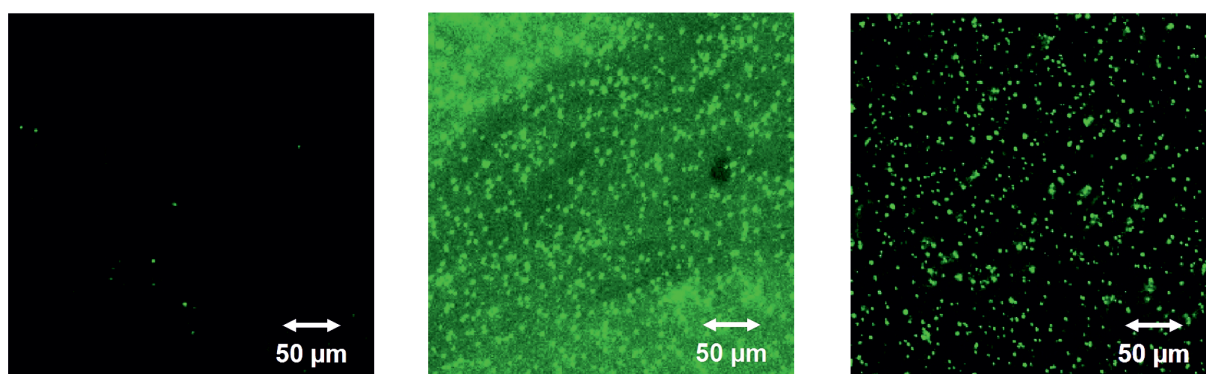


**Figure 6.** Fluorescence images of AB-epoxide (A), AB-polySBMA  $\text{Si}_3\text{N}_4$  (B) and bare  $\text{Si}_3\text{N}_4$  surfaces (C) exposed to *Salmonella* solution, without using blocking solution.

### 3.6. Detection of *Salmonella* in a Mixture of FIB and *Salmonella*

The protein-repellent and capturing properties of AB-polySBMA were further evaluated by exposing the surfaces to a mixture of Alexa Fluor 647-labeled FIB and *Salmonella* without prior use of a blocking solution. The detection performance and FIB adsorption of AB-polySBMA were compared with AB-epoxide surfaces that were treated with a blocking solution beforehand and with bare  $\text{Si}_3\text{N}_4$  surfaces without using blocking solution. After exposure to a mixture of the Alexa Fluor 647-labeled FIB and *Salmonella*, the surfaces were incubated with 100  $\mu\text{L}$  of  $1\times$  PBS solution containing 5  $\mu\text{g}$  FITC-labeled anti-*Salmonella* antibodies to visualize the captured *Salmonella* cells. The overlapped fluorescence images of FITC (green) and Alexa Fluor 647 (red) showed on bare  $\text{Si}_3\text{N}_4$  surfaces only little attachment of *Salmonella* and the significant adsorption of FIB (Figure 7, left). In contrast, both the AB-epoxide  $\text{Si}_3\text{N}_4$  surfaces (Figure 7, middle) and AB-polySBMA  $\text{Si}_3\text{N}_4$  surfaces (Figure 7, right) displayed binding of *Salmonella*, demonstrating that the attachment of *Salmonella* on these surfaces is specific, due to the presence of antibody. The AB-epoxide  $\text{Si}_3\text{N}_4$  surface still showed some uniform red fluorescence, indicating a moderate adsorption of FIB on the surfaces, although blocking solution was used. This can be attributed to the Vroman effect, i.e., FIB can displace earlier adsorbed proteins from the blocking solution, from the surface.<sup>46</sup> In case of not using the blocking solution, a similar image with a higher intensity of red fluorescence was obtained, indicating a major adsorption of FIB onto the surface, which is in agreement with the earlier observation (Section 3.4) that AB-epoxide surfaces adsorbed FIB. Interestingly, AB-polySBMA surfaces (Figure 7, right) showed almost no red fluorescence, indicating virtually no adsorption of FIB onto the surface. The result demonstrates that AB-polySBMA modified surfaces are superior to AB-epoxide modified surfaces, even when these surfaces are treated with blocking solution to prevent

nonspecific adsorption of proteins during the detection of bacteria in the complex matrices. This highly specific bacterial adsorption of AB-polySBMA in complex media clearly demonstrates the potential of zwitterionic polymer brushes for repelling proteins during bacterial detection.

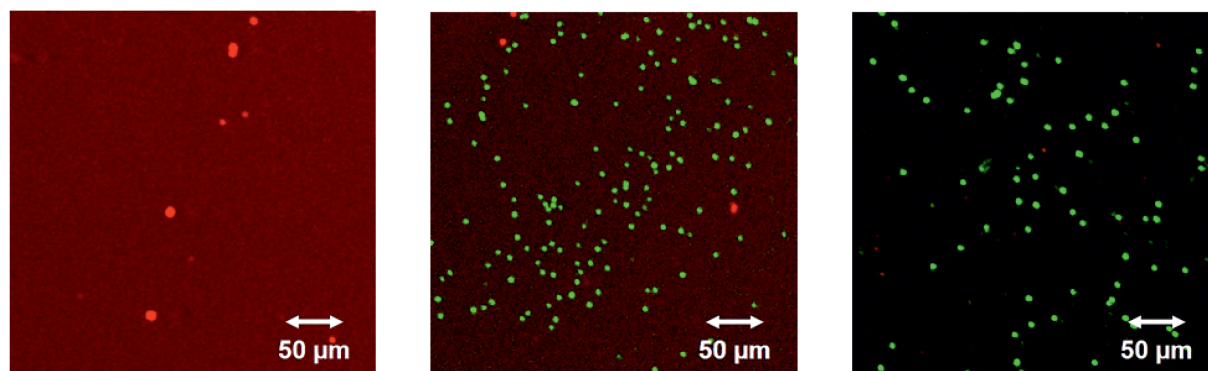


**Figure 7.** Fluorescence images of bare  $\text{Si}_3\text{N}_4$  (left), AB-epoxide surfaces with blocking solution (middle) and AB-polySBMA surfaces without using blocking solution (right) exposed to a mixture of FIB and *Salmonella* solution.

## 4. Conclusions

Coupling of anti-*Salmonella* antibodies to highly stable protein-repellent polySBMA brushes grafted onto  $\text{Si}_3\text{N}_4$  surfaces yields an antibody-coated surface with substantial capabilities for specific detection of *Salmonella*: even without blocking, solution *Salmonella* is detected specifically in complex media containing FIB proteins without any detectable FIB adsorption. Such modified surfaces thus present a highly useful platform for the detection of bacteria in crude biological samples. Furthermore, the chemistry involved (surface-initiated ATRP) allows for the attachment of a range of functional moieties to be used at the top of the polymeric layer, demonstrating the wide applicability of such modifiable polySBMA brushes.

## 5. Acknowledgment

The authors thank MicroNed (project 6163510587) for financial support, Hien Duy Tong (Nanosens B.V., Zutphen, The Netherlands) for his kind donation of  $\text{Si}_3\text{N}_4$  wafers, and Ronald van Doorn (Innosieve Diagnostics B.V., Vlijmen, The Netherlands) for assistance during microbial detection experiments.



## 6. References

- (1) North, J. R., Immunosensors: Antibody-based biosensors. *Trends Biotechnol.* **1985**, *3*, 180-186.
- (2) Kramer, S.; Joos, T. O.; Templin, M. F., Protein microarrays. *Curr. Protoc. Protein Sci.* **2005**, Chapter 23, Unit 23.5.
- (3) Barbee, K. D.; Hsiao, A. P.; Roller, E. E.; Huang, X. H., Multiplexed protein detection using antibody-conjugated microbead arrays in a microfabricated electrophoretic device. *Lab Chip* **2010**, *10*, 3084-3093.
- (4) Rusmini, F.; Zhong, Z.; Feijen, J., Protein Immobilization Strategies for Protein Biochips. *Biomacromolecules* **2007**, *8*, 1775-1789.
- (5) Angenendt, P.; Glökler, J.; Sobek, J.; Lehrach, H.; Cahill, D. J., Next generation of protein microarray support materials: Evaluation for protein and antibody microarray applications. *J. Chromatogr. A* **2003**, *1009*, 97-104.
- (6) Rebeski, D. E.; Winger, E. M.; Shin, Y.-K.; Lelenta, M.; Robinson, M. M.; Varecka, R.; Crowther, J. R., Identification of unacceptable background caused by non-specific protein adsorption to the plastic surface of 96-well immunoassay plates using a standardized enzyme-linked immunosorbent assay procedure. *J. Immunol. Meth.* **1999**, *226*, 85-92.
- (7) Seurnyck-Servoss, S. L.; White, A. M.; Baird, C. L.; Rodland, K. D.; Zangar, R. C., Evaluation of surface chemistries for antibody microarrays. *Anal. Biochem.* **2007**, *371*, 105-115.
- (8) Desai, T. A.; Hansford, D. J.; Leoni, L.; Essenpreis, M.; Ferrari, M., Nanoporous anti-fouling silicon membranes for biosensor applications. *Biosens. Bioelectron.* **2000**, *15*, 453-462.
- (9) Mandrusov, E.; Puszkin, E.; Vroman, L.; Leonard, E. F., Separated Flows in Artificial Organs: A Cause of Early Thrombogenesis? *ASAIO Journal* **1996**, *42*, M506-513.
- (10) Sampedro, M. F.; Patel, R., Infections Associated with Long-Term Prosthetic Devices. *Infect. Dis. Clin. North. Am.* **2007**, *21*, 785-819.
- (11) Turner, R. F. B.; Harrison, D. J.; Rojotte, R. V., Preliminary in vivo biocompatibility studies on perfluorosulphonic acid polymer membranes for biosensor applications. *Biomaterials* **1991**, *12*, 361-368.
- (12) Jonkheijm, P.; Weinrich, D.; Schröder, H.; Niemeyer, C. M.; Waldmann, H., Chemical Strategies for Generating Protein Biochips. *Angew. Chem. Int. Ed.* **2008**, *47*, 9618-9647.
- (13) Brault, N. D.; Gao, C.; Xue, H.; Pilarik, M.; Homola, J.; Jiang, S.; Yu, Q., Ultra-low fouling and functionalizable zwitterionic coatings grafted onto SiO<sub>2</sub> via a biomimetic adhesive group for sensing and detection in complex media. *Biosens. Bioelectron.* **2010**, *25*, 2276-2282.
- (14) Gao, C.; Li, G.; Xue, H.; Yang, W.; Zhang, F.; Jiang, S., Functionalizable and ultra-low fouling zwitterionic surfaces via adhesive mussel mimetic linkages. *Biomaterials* **2010**, *31*, 1486-1492.

- (15) Yao, Y.; Ma, Y.-Z.; Qin, M.; Ma, X.-J.; Wang, C.; Feng, X.-Z., NHS-ester functionalized poly(PEGMA) brushes on silicon surface for covalent protein immobilization. *Colloids Surf., B* **2008**, *66*, 233-239.
- (16) Wolter, A.; Niessner, R.; Seidel, M., Preparation and Characterization of Functional Poly(ethylene glycol) Surfaces for the Use of Antibody Microarrays. *Anal. Chem.* **2007**, *79*, 4529-4537.
- (17) Stavis, C.; Clare, T. L.; Butler, J. E.; Radadia, A. D.; Carr, R.; Zeng, H.; King, W. P.; Carlisle, J. A.; Aksimentiev, A.; Bashir, R.; Hamers, R. J., Surface functionalization of thin-film diamond for highly stable and selective biological interfaces. *Proc. Natl. Acad. Sci. U.S.A.* **2011**, *108*, 983-988.
- (18) Qin, G.; Cai, C., Oxidative degradation of oligo(ethylene glycol)-terminated monolayers. *Chem. Commun.* **2009**, 5112-4.
- (19) Leckband, D.; Sheth, S.; Halperin, A., Grafted poly(ethylene oxide) brushes as nonfouling surface coatings. *J. Biomater. Sci., Polym. Ed.* **1999**, *10*, 1125-1147.
- (20) Knop, K.; Hoogenboom, R.; Fischer, D.; Schubert, U. S., Poly(ethylene glycol) in Drug Delivery: Pros and Cons as Well as Potential Alternatives. *Angew. Chem. Int. Ed.* **2010**, *49*, 6288-6308.
- (21) Chang, Y.; Chen, W.-Y.; Yandi, W.; Shih, Y.-J.; Chu, W.-L.; Liu, Y.-L.; Chu, C.-W.; Ruaan, R.-C.; Higuchi, A., Dual-Thermoresponsive Phase Behavior of Blood Compatible Zwitterionic Copolymers Containing Nonionic Poly(*N*-isopropyl acrylamide). *Biomacromolecules* **2009**, *10*, 2092-2100.
- (22) Chang, Y.; Liao, S.-C.; Higuchi, A.; Ruaan, R.-C.; Chu, C.-W.; Chen, W.-Y., A Highly Stable Nonbiofouling Surface with Well-Packed Grafted Zwitterionic Polysulfobetaine for Plasma Protein Repulsion. *Langmuir* **2008**, *24*, 5453-5458.
- (23) Cho, W. K.; Kong, B.; Choi, I. S., Highly Efficient Non-Biofouling Coating of Zwitterionic Polymers: Poly((3-(methacryloylamino)propyl)-dimethyl(3-sulfopropyl)ammonium hydroxide). *Langmuir* **2007**, *23*, 5678-5682.
- (24) Holmlin, R. E.; Chen, X.; Chapman, R. G.; Takayama, S.; Whitesides, G. M., Zwitterionic SAMs that Resist Nonspecific Adsorption of Protein from Aqueous Buffer. *Langmuir* **2001**, *17*, 2841-2850.
- (25) Ladd, J.; Zhang, Z.; Chen, S.; Hower, J. C.; Jiang, S., Zwitterionic Polymers Exhibiting High Resistance to Nonspecific Protein Adsorption from Human Serum and Plasma. *Biomacromolecules* **2008**, *9*, 1357-1361.
- (26) Liu, P.-S.; Chen, Q.; Wu, S.-S.; Shen, J.; Lin, S.-C., Surface modification of cellulose membranes with zwitterionic polymers for resistance to protein adsorption and platelet adhesion. *J. Membr. Sci.* **2010**, *350*, 387-394.
- (27) Nguyen, A. T.; Baggerman, J.; Paulusse, J. M. J.; van Rijn, C. J. M.; Zuilhof, H., Stable Protein-Repellent Zwitterionic Polymer Brushes Grafted from Silicon Nitride. *Langmuir* **2011**, *27*, 2587-2594.

- (28) Estephan, Z. G.; Schlenoff, P. S.; Schlenoff, J. B., Zwitteration As an Alternative to PEGylation. *Langmuir* **2011**, *27*, 6794-6800.
- (29) Kitano, H.; Suzuki, H.; Matsuura, K.; Ohno, K., Molecular Recognition at the Exterior Surface of a Zwitterionic Telomer Brush. *Langmuir* **2010**, *26*, 6767-6774.
- (30) Menawat, A.; Jr, J. H.; Siriwardane, R., Control of surface energy of glass by surface reactions: Contact angle and stability. *J. Colloid Interface Sci.* **1984**, *101*, 110-119.
- (31) Sano, H.; Maeda, H.; Ichii, T.; Murase, K.; Noda, K.; Matsushige, K.; Sugimura, H., Alkyl and Alkoxy Monolayers Directly Attached to Silicon: Chemical Durability in Aqueous Solutions. *Langmuir* **2009**, *25*, 5516-5525.
- (32) Rivas, L. A.; García-Villadangos, M.; Moreno-Paz, M.; Cruz-Gil, P.; Gómez-Elvira, J.; Parro, V. c., A 200-Antibody Microarray Biochip for Environmental Monitoring: Searching for Universal Microbial Biomarkers through Immunoprofiling. *Anal. Chem.* **2008**, *80*, 7970-7979.
- (33) Skottrup, P. D.; Nicolaisen, M.; Justesen, A. F., Towards on-site pathogen detection using antibody-based sensors. *Biosens. Bioelectron.* **2008**, *24*, 339-348.
- (34) van Rijn, C. J. M., *Nano and Micro Engineered Membrane Technology*. Elsevier: Amsterdam, The Netherlands, 2004.
- (35) Scheres, L.; Arafat, A.; Zuilhof, H., Self-assembly of high-quality covalently bound organic monolayers onto silicon. *Langmuir* **2007**, *23*, 8343-8346.
- (36) Rosso, M.; Giesbers, M.; Schroën, K.; Zuilhof, H., Controlled Oxidation, Biofunctionalization, and Patterning of Alkyl Monolayers on Silicon and Silicon Nitride Surfaces using Plasma Treatment. *Langmuir* **2009**, *26*, 866-872.
- (37) Rosso, M.; Giesbers, M.; Arafat, A.; Schroën, K.; Zuilhof, H., Covalently Attached Organic Monolayers on SiC and Si<sub>3</sub>N<sub>4</sub> Surfaces: Formation Using UV Light at Room Temperature. *Langmuir* **2009**, *25*, 2172-2180.
- (38) Nguyen, A. T.; van Doorn, R.; Baggerman, J.; Paulusse, J. M. J.; Zuilhof, H.; Klerks, M.; van Rijn, C. J. M., Rapid Microsieve-Based Microbial Diagnostics. (*in preparation*) **2011**.
- (39) Cheng, N.; Brown, A. A.; Azzaroni, O.; Huck, W. T. S., Thickness-Dependent Properties of Polyzwitterionic Brushes. *Macromolecules* **2008**, *41*, 6317-6321.
- (40) Omar, A.; Andrew, A. B.; Huck, W. T. S., UCST Wetting Transitions of Polyzwitterionic Brushes Driven by Self-Association. *Angew. Chem. Int. Ed.* **2006**, *45*, 1770-1774.
- (41) Rodriguez Emmenegger, C.; Brynda, E.; Riedel, T.; Sedlakova, Z.; Houska, M.; Alles, A. B., Interaction of Blood Plasma with Antifouling Surfaces. *Langmuir* **2009**, *25*, 6328-6333.
- (42) Bergenudd, H.; Coullerez, G.; Jonsson, M.; Malmström, E., Solvent Effects on ATRP of Oligo(ethylene glycol) Methacrylate. Exploring the Limits of Control. *Macromolecules* **2009**, *42*, 3302-3308.

- (43) Terayama, Y.; Kikuchi, M.; Kobayashi, M.; Takahara, A., Well-Defined Poly(sulfobetaine) Brushes Prepared by Surface-Initiated ATRP Using a Fluoroalcohol and Ionic Liquids as the Solvents. *Macromolecules* **2011**, *44*, 104-111.
- (44) Tsarevsky, N. V.; Matyjaszewski, K., "Green" Atom Transfer Radical Polymerization: From Process Design to Preparation of Well-Defined Environmentally Friendly Polymeric Materials. *Chem. Rev.* **2007**, *107*, 2270-2299.
- (45) Yang, W.; Xue, H.; Li, W.; Zhang, J.; Jiang, S., Pursuing "Zero" Protein Adsorption of Poly(carboxybetaine) from Undiluted Blood Serum and Plasma. *Langmuir* **2009**, *25*, 11911-11916.
- (46) Bamford, C. H.; Cooper, S. L.; Tsurutta, T.; Vroman, L., *The Vroman effect : Festschrift in honor of the 75th birthday of dr. Leo Vroman*. VSP: Utrecht, 1992.



## General Discussion

This chapter gives an overview of the most important findings presented in this thesis and discusses several remaining questions as well as recommendations for further research.

## General Discussion

In this thesis, a number of surface functionalization approaches of silicon nitride ( $\text{Si}_x\text{N}_4$ ) surfaces and microsieves was explored to show the potential of protein-repellent and/or bioselective capture coatings. The pioneered methods and new findings obtained during the course of this project are described in detail. The most important achievement is the development of surface functionalization of  $\text{Si}_x\text{N}_4$  microsieves for biological applications. Many successful functionalizations of  $\text{Si}_x\text{N}_4$  surfaces have been achieved. Yet we were unable to answer all the related questions, as new results also generate new questions. In this chapter, remaining questions, additional ideas and recommendations are discussed to place this work into a broader context, including practical applications.

UV-induced modification of hydrogen-terminated silicon nitride ( $\text{Si}_x\text{N}_4$ ) surfaces with alkenes was employed as a reliable and reproducible surface functionalization technique that gives access to an avenue of new application. The obtained Si-C and N-C chemical linkages between the substrate and the coatings are considered to be a solid foundation for making the functional organic layer on top of the substrate, because of their superior stability in comparison with Si-O-Si-C<sup>1</sup> or Si-O-C<sup>2</sup> linkages obtained by silanization and thermal activation of alkenes, respectively.

Well-defined monolayers of short oligoethylene oxide chains, with three ( $\text{EO}_3$ ) and six ( $\text{EO}_6$ ) ethylene oxide units, were successfully grafted onto  $\text{Si}_x\text{N}_4$  surfaces by using a one-step UV-induced reaction as described in Chapter 2. For the  $\text{EO}_6$ -coated surfaces, efficient protein-repellence in bovine serum albumin (BSA) solution was observed (> 94% repellence as compared to  $\text{C}_{16}$ -modified surfaces). However, the protein repellence of these modified surfaces in fibrinogen (FIB) solution was only moderate (~80% repellence). This was attributed to differences in the Van der Waals interactions between the surface and the proteins, i.e., BSA and FIB. The Van der Waals interactions between FIB and the modified surfaces are approximately eight times larger than that of BSA and the modified surfaces (based on DLVO theoretical calculations). Adsorption of proteins onto solid surfaces is a complex phenomenon, depending on many factors such as surface properties (charges and chemical composition), characteristics of the proteins (size, pI, intermolecular cohesion, and conformation) and the nature of the aqueous buffered solution (ionic strength, pH, and temperature).

Beside that, topography of solid surface, e.g., roughness and crystal lattice of the substrate, was shown to also play a significant role in protein adsorption processes.<sup>3</sup> Grunze and co-workers<sup>4</sup> showed that the packing density of  $\text{EO}_6$  monolayers on gold and silver surfaces is of importance to the protein repellence thereof. The packing density of EO monolayers on silver is higher than on gold surfaces, originating from a different



interatomic distance. The obtained conformation of EO<sub>6</sub> is therefore also different: on gold surfaces they display a helical structure with excellent protein-repellent properties, while on silver an all-*trans* conformation was found, rendering a less effective repellence.<sup>5</sup> Hamers and co-workers have reported that smooth EO<sub>6</sub>-coated diamond surfaces (RMS < 0.2 nm) exhibit lower adsorption of proteins than rougher surfaces (RMS > 1 nm).<sup>6</sup> This effect could contribute to explaining the difference in the observed protein repellence of EO<sub>6</sub> coated on Si<sub>x</sub>N<sub>4</sub> surfaces (RMS > 0.5 nm) as compared with similar monolayers on silicon carbide,<sup>7</sup> gold or silver.<sup>4, 5</sup>

Interestingly, it was observed that the adsorption of FIB on EO<sub>6</sub>-coated surfaces is strongly dependent on the method of protein dissolution. A vigorously shaken FIB solution showed no adsorption on EO<sub>6</sub>-coated Si<sub>x</sub>N<sub>4</sub> surfaces, while a gently dissolved solution yielded ~1 mg.m<sup>-2</sup> of FIB on the surface. An appropriate method was obtained to dissolve FIB with low-solubility properties in PBS solution. The method was found to be of great help in order to obtain a reproducible adsorption of this protein on modified surfaces (Chapter 2).

EO<sub>6</sub>-monolayers coated on Si<sub>x</sub>N<sub>4</sub> surfaces in PBS and alkaline (pH = 10) solution at room temperature were found to degrade after 1 week, while the Si<sub>x</sub>N<sub>4</sub> substrates itself remained oxide-free. This observation reveals that the surface linkage is stable, but that the ethylene oxide chains are auto-oxidized in aqueous solution, which is in agreement with similar findings reported by Cai and co-workers.<sup>8</sup>

The protein-repellent performance of antifouling coatings, as well as their stability was explored with zwitterionic polymer brushes in Chapter 3. For the first time, a method was presented to grow zwitterionic polymer brushes by atom transfer radical polymerization (ATRP) from initiators attached onto Si<sub>x</sub>N<sub>4</sub> surfaces via stable Si-C and N-C linkages. The initiator layers were derived from highly stable and well-defined monolayers of epoxides coated on Si<sub>x</sub>N<sub>4</sub> surfaces. The monolayers of epoxide obtained by an one-step photochemical reaction were found to be versatile precursor layers for subsequent (bio-)functionalization. For example, in this thesis, the attachment of ethylene diamine, streptavidin and even antibodies onto epoxide-coated surfaces was achieved. A new chemical route to amine-terminated surfaces by reacting epoxide-coated surfaces with ethylene diamine was introduced. The method does not require cumbersome chemical syntheses or additional protective group chemistry, thereby offering a simple way to access many types of  $\omega$ -functionalization of the surfaces.

Zwitterionic polymers grafted from Si<sub>x</sub>N<sub>4</sub> surfaces via the developed method exhibited an excellent protein repellence in FIB solution (> 99% as compared to C<sub>16</sub>-modified surfaces). The superior performance of zwitterionic polymers as compared to monolayer

EO<sub>6</sub>-coated surfaces was attributed to the highly polar nature of the zwitterionic brushes: the tight solvation of the charges yields a thicker and more tightly bound water layer. The zwitterionic polymer was demonstrated to be highly stable as compared to EO<sub>6</sub>-modified surfaces, i.e., the polymer thickness did not change and protein-repellence remained constant after 1 week in PBS solution. However, the stability of the zwitterionic polymers in alkaline and acidic media was not examined. Thus, it would be worthwhile to test the stability of zwitterionic coatings in these media to broaden their application potential. Besides that, the actual effect of zwitterionic coatings on the filtration performance of Si<sub>x</sub>N<sub>4</sub> microsieves was not investigated so far. Therefore, additional tests with coated microsieves are strongly recommended to bring this work to completion. In addition, the effect of protein-repellent surfaces may be further enhanced by combination with mechanical antifouling methods as reported by Lammertink and co-workers.<sup>9</sup> Therefore, it would be valuable to invest in a study on a combination of stable zwitterionic polymer and mechanical antifouling methods.

As mentioned in Chapter 1, microfiltration processes are often operated in combination with dynamic controls – such as ultrasound, back-pulsing and vibration – to enhance flux. In this respect, membrane surfaces not only need to be protein repellent (hydrophilic), but should also exhibit good fouling-release (hydrophobic) properties. Therefore, amphiphilic coatings, having both good protein-resistance and fouling-release properties may form an ultimate solution for long term use of microsieves in microfiltration processes. Recently, amphiphilic coatings, known as controlled hybrid hydrophilic-hydrophobic coatings, for bio-antifouling have been studied.<sup>10-15</sup> The target application of these studies is marine anti-fouling, which mainly focuses on anti-adhesion of cells and microorganisms.<sup>10-12, 14</sup> Expansion of this work to Si<sub>x</sub>N<sub>4</sub> microsieves could be a promising way to achieve long-term operation of microsieve-based filtrations.

Bio-selective functionalization of microsieves to enhance microbial detection devices was explored in Chapter 4. A simple approach to attach antibodies covalently onto the microsieve via epoxide monolayers was employed. The simplicity of the method and superior stability of epoxide coatings, offer the possibility for easy and reproducible scale-up of this concept. Immobilization of antibodies onto epoxide-coated surfaces was achieved via reaction of epoxide moieties with primary amines and thiol groups that are available on the amino acid residues at the outside of the antibodies. This results in immobilization of antibodies on the surface with a random orientation. As consequence, not all binding sites are available for biorecognition, because some may face downwards, which to a certain extent may influence in the capture efficiency of antibody coatings. Therefore, attachment of antibodies on the surface with a uniform upward orientation<sup>16, 17</sup>

may improve the sensitivity of the system. Furthermore, a more sophisticated detection system may be further pursued by creating multiplex microarrays with many different antibody spots on the microsieve surface.

An anti-*Salmonella* antibody layer coated on a microsieve exhibited good capture efficiencies, even when the pore size was much larger than the size of *Salmonella*. The developed approach allows for straightforward analysis of larger volumes of crude biological samples with less fouling issues, signifying a substantial improvement for the development and use of microsieves for new rapid diagnostic methods. With the aid of antibody coatings on the microsieves *Salmonella* was captured with an efficiency between 30% for 5- $\mu\text{m}$  microsieves up to 40% 2- $\mu\text{m}$  microsieves, as compared to 100% for 0.45- $\mu\text{m}$  microsieves (through which no bacteria should pass) and agar plating. The developed protocol shows reproducible capture efficiencies. Hence, for enumeration purposes the system can be calibrated by determining an efficiency factor for different matrices. However, in order to bring the current platform into practical application, further investigation is highly recommended. For instance, a study on the influence of the flow-rate at low concentrations of *Salmonella* is crucial. The capture efficiency of *Salmonella* in crude milk samples was found to be lower than that obtained in buffered solution. This is most likely due to nonspecific adsorption of milk proteins onto antibody-coated microsieves.<sup>18</sup>

With the ambition to create a microbial detection platform with high sensitivity and high selectivity, the incorporation of antibodies on protein-repellent zwitterionic layers coated on  $\text{Si}_x\text{N}_4$  surfaces was studied (Chapter 5). The antibody-conjugated zwitterionic brushes yielded a significant reduction of background noise, while maintaining a selective detection of *Salmonella* as compared to a dense antibody-coated epoxide monolayer under identical conditions. The results demonstrate a novel approach that enables rapid detection of bacteria while minimizing nonspecific adsorption of proteins that are not of interest. This shows its potential for the development of a new generation of biosensors with high selectivity and a low limit of detection for direct detection in crude biological samples. However, further studies towards practical application in detection devices still need to be performed. Additional experiments that determine the sensitivity and selectivity of such modified microsieve surfaces in complex media are necessary.

In summary, a range of (bio)functionalized  $\text{Si}_x\text{N}_4$  surfaces and  $\text{Si}_x\text{N}_4$  microsieves has been investigated. This study shows the versatility of surface functionalization for the further improvement of microsieves for biological applications via 1) significant protein repellence, 2) effective capturing of microorganisms, and 3) the selectively capturing of microorganisms while repelling other components. These achievements thus contribute

substantially to the future application of biological microfilters, microreactors and biosensors. Surface functionalization is the next wave in microfluidics: turn on the taps, and let it flow!

## References

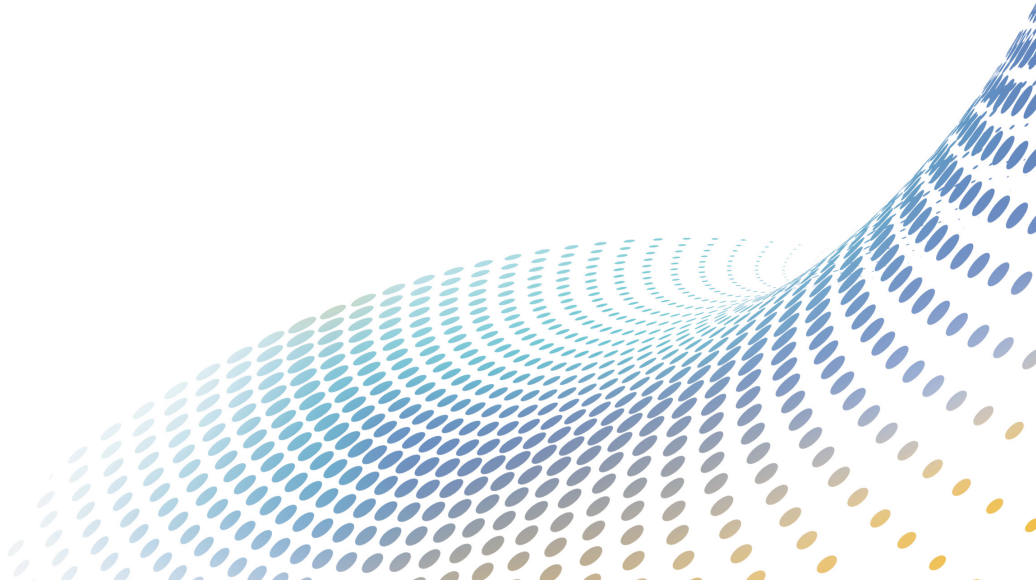
- (1) Menawat, A.; Jr, J. H.; Siriwardane, R., Control of surface energy of glass by surface reactions: Contact angle and stability. *J. Colloid Interface Sci.* **1984**, *101*, 110-119.
- (2) Sano, H.; Maeda, H.; Ichii, T.; Murase, K.; Noda, K.; Matsushige, K.; Sugimura, H., Alkyl and Alkoxy Monolayers Directly Attached to Silicon: Chemical Durability in Aqueous Solutions. *Langmuir* **2009**, *25*, 5516-5525.
- (3) Banerjee, I.; Pangule, R. C.; Kane, R. S., Antifouling Coatings: Recent Developments in the Design of Surfaces That Prevent Fouling by Proteins, Bacteria, and Marine Organisms. *Adv. Mater.* **2011**, *23*, 690-718.
- (4) Herrwerth, S.; Eck, W.; Reinhardt, S.; Grunze, M., Factors that determine the protein resistance of oligoether self-assembled monolayers - Internal hydrophilicity, terminal hydrophilicity, and lateral packing density. *J. Am. Chem. Soc.* **2003**, *125*, 9359-9366.
- (5) Pertsin, A. J.; Grunze, M.; Garbuzova, I. A., Low-Energy Configurations of Methoxy Triethylene Glycol Terminated Alkanethiol Self-Assembled Monolayers and Their Relevance to Protein Adsorption. *J. Phys. Chem. B* **1998**, *102*, 4918-4926.
- (6) Stavis, C.; Clare, T. L.; Butler, J. E.; Radadia, A. D.; Carr, R.; Zeng, H.; King, W. P.; Carlisle, J. A.; Aksimentiev, A.; Bashir, R.; Hamers, R. J., Surface functionalization of thin-film diamond for highly stable and selective biological interfaces. *Proc. Natl. Acad. Sci. U.S.A.* **2011**, *108*, 983-988.
- (7) Qin, G.; Zhang, R.; Makarenko, B.; Kumar, A.; Rabalais, W.; Lopez Romero, J. M.; Rico, R.; Cai, C., Highly stable, protein resistant thin films on SiC-modified silicon substrates. *Chem. Comm.* **2010**, *46*, 3289-3291.
- (8) Qin, G.; Cai, C., Oxidative degradation of oligo(ethylene glycol)-terminated monolayers. *Chem. Comm.* **2009**, 5112-4.
- (9) Girones, M.; Bolhuis-Versteeg, L.; Lammertink, R.; Wessling, M., Flux stabilization of silicon nitride microsieves by backpulsing and surface modification with PEG moieties. *J. Colloid Interface Sci.* **2006**, *299*, 831-840.
- (10) Chen, Y.; Thayumanavan, S., Amphiphilicity in Homopolymer Surfaces Reduces Nonspecific Protein Adsorption. *Langmuir* **2009**, *25*, 13795-13799.
- (11) Gudipati, C. S.; Finlay, J. A.; Callow, J. A.; Callow, M. E.; Wooley, K. L., The Antifouling and Fouling-Release Performance of Hyperbranched Fluoropolymer (HBFP)-Poly(ethylene glycol) (PEG) Composite Coatings Evaluated by Adsorption of Biomacromolecules and the Green Fouling Alga *Ulva*. *Langmuir* **2005**, *21*, 3044-3053.

- (12) Krishnan, S.; Ayothi, R.; Hexemer, A.; Finlay, J. A.; Sohn, K. E.; Perry, R.; Ober, C. K.; Kramer, E. J.; Callow, M. E.; Callow, J. A.; Fischer, D. A., Anti-Biofouling Properties of Comblike Block Copolymers with Amphiphilic Side Chains. *Langmuir* **2006**, *22*, 5075-5086.
- (13) Krishnan, S.; Weinman, C. J.; Ober, C. K., Advances in polymers for anti-biofouling surfaces. *J. Mater. Chem.* **2008**, *18*, 3405-3413.
- (14) Park, D.; Weinman, C. J.; Finlay, J. A.; Fletcher, B. R.; Paik, M. Y.; Sundaram, H. S.; Dimitriou, M. D.; Sohn, K. E.; Callow, M. E.; Callow, J. A.; Handlin, D. L.; Willis, C. L.; Fischer, D. A.; Kramer, E. J.; Ober, C. K., Amphiphilic Surface Active Triblock Copolymers with Mixed Hydrophobic and Hydrophilic Side Chains for Tuned Marine Fouling-Release Properties. *Langmuir* **2010**, *26*, 9772-9781.
- (15) Finlay, J. A.; Krishnan, S.; Callow, M. E.; Callow, J. A.; Dong, R.; Asgill, N.; Wong, K.; Kramer, E. J.; Ober, C. K., Settlement of Ulva Zoospores on Patterned Fluorinated and PEGylated Monolayer Surfaces. *Langmuir* **2007**, *24*, 503-510.
- (16) Franco, E. J.; Hofstetter, H.; Hofstetter, O., A comparative evaluation of random and site-specific immobilization techniques for the preparation of antibody-based chiral stationary phases. *J. Sep. Sci.* **2006**, *29*, 1458-1469.
- (17) Jung, Y.; Jeong, J. Y.; Chung, B. H., Recent advances in immobilization methods of antibodies on solid supports. *Analyst* **2008**, *133*, 697-701.
- (18) Prakash, B. S.; Meyer, H. H. D.; Van De Wiel, D. F. M., Sensitive enzyme immunoassay of progesterone in skim milk using second-antibody technique. *Anim. Reprod. Sci.* **1988**, *16*, 225-235.



# APPENDICES

Supporting information for previous chapters is presented in this section.



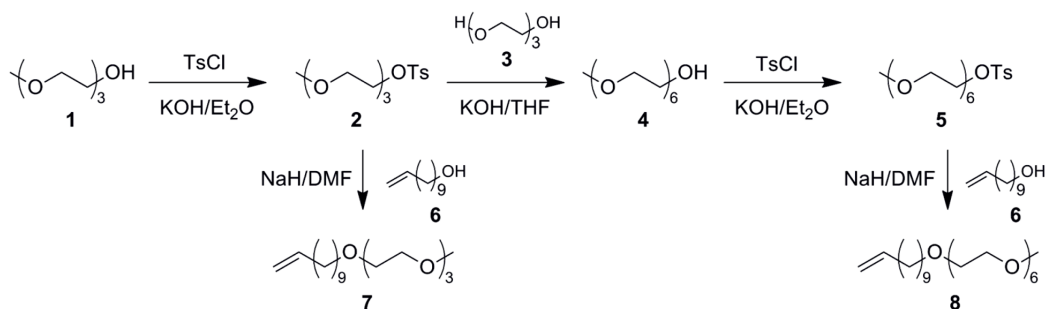




## Appendix 1

### Synthesis of Tri- and Hexaethylene glycol methyl $\omega$ -undecenyl ether (EO<sub>3</sub> and EO<sub>6</sub>)

Triethylene glycol (>99%), triethylene glycol monomethyl ether (>97%) and anhydrous DMF (99.5%) were purchased from Fluka. 11-Undecen-1-ol (98%), tosyl chloride (98%), sodium hydride (60% dispersion in mineral oil) were purchased from Aldrich. All solvents were distilled before use.



**Scheme 1.** Synthetic route to EO<sub>3</sub> and EO<sub>6</sub>.

*Triethylene glycol methyl ether ω-methylbenzenesulfonate (2).* Triethylene glycol monomethyl ether (**1**, 34.14 g, 208 mmol) and *p*-toluenesulfonyl chloride (43.80 g, 230 mmol) were dissolved in diethyl ether (100 mL). Freshly ground KOH (46.70 g, 830 mmol) was then added in several portions to the ice-cooled solution, keeping the temperature below 5 °C. After 3 hours of reaction, 75 mL of ice and water were added, the organic phase was extracted 3 times with diethyl ether. The combined organic fractions were dried on Na<sub>2</sub>SO<sub>4</sub>, filtered, and the solvent was evaporated under reduced pressure to give **2** as a colorless oil (63.5 g, 96%). <sup>1</sup>H-NMR (300 MHz, CDCl<sub>3</sub>, δ): 2.45 (s, 3H), 3.38 (s, 3H), 3.53 (t, 2H), 3.61 (m, 6H), 3.70 (t, *J* = 6, 2H); 4.17 (t, *J* = 6, 2H), 7.35 (d, *J* = 7.5, 2H), 7.80 (d, *J* = 7.5, 2H); <sup>13</sup>C-NMR (300 MHz, CDCl<sub>3</sub>): δ 21.58, 58.95, 68.64, 69.23, 70.51, 70.71, 71.88, 127.93, 129.80, 133.06, 144.77.

*Hexaethylene glycol monomethyl ether (4).* Under argon atmosphere, triethylene glycol (**3**, 42 g, 283 mmol) was dissolved in anhydrous THF (40 mL), and the resulting solution was brought to reflux. Freshly ground KOH (3 g, 52 mmol) was added in small portions. After complete dissolution, the solution was cooled to room temperature, and **2** (15 g, 47 mmol) in THF (20 mL) was added drop by drop. The solution was then refluxed under argon overnight. After evaporation of THF under vacuum, water was added to the resulting mixture, and the solution was extracted with dichloromethane until no product was detected by TLC (eluent: ethyl acetate). **4** was obtained as a pale yellow oil (11.3 g,

81%). **<sup>1</sup>H-NMR** (300 MHz, CDCl<sub>3</sub>, δ): 2.70 (m, 1H), 3.32 (s, 3H), 3.47-3.62 (m, 24H); **<sup>13</sup>C-NMR** (300 MHz, CDCl<sub>3</sub>): δ 60.96, 69.99, 70.04, 70.15, 71.61, 72.34.

*Hexaethylene glycol methyl ether ω-methylbenzenesulfonate (5)*. The synthesis was carried out as for **2**. After evaporation of solvents, **5** was obtained as colorless oil (11.15 g, 89%). **<sup>1</sup>H-NMR** (300 MHz, CDCl<sub>3</sub>, δ): 2.45 (s, 3H), 3.38 (s, 3H), 3.53-3.71 (m, 22H), 4.16 (t, 2H), 7.35 (d, J = 6, 2H), 7.81 (d, J = 6, 2H); **<sup>13</sup>C-NMR** (300 MHz, CDCl<sub>3</sub>): δ 21.63, 59.01, 68.67, 69.23, 70.51, 70.55, 70.60, 70.74, 71.93, 127.97, 129.81, 133.03, 144.77.

*EO<sub>3</sub>: Triethylene glycol methyl ω-undecenyl ether (7)*. In a dry vessel, under argon atmosphere, NaH (2.0 g of 60% dispersion in mineral oil, 28 mmol) was cleaned three times with pentane, and dry DMF (20 mL) were eventually added. The vessel being kept at 0 °C in an ice bath, 10-undecen-1-ol (**6**, 4.71 g, 27.7 mmol) in THF was added dropwise. After 4 h, hydrogen evolution being finished, **2** (8 g, 25.1 mmol) was added dropwise. The reaction was left stirring overnight under argon. After quenching with water, the mixture was extracted 3 times with ether. The combined organic phases were washed with brine, dried over Na<sub>2</sub>SO<sub>4</sub>, and the solvent was evaporated to give a pale yellow oil. After purification with silica gel column chromatography, with a 2/1 mixture of ethyl acetate/petroleum ether (40/60), 6.1 g (73%) of **7** were obtained as a colorless oil. **<sup>1</sup>H-NMR** (300 MHz, CDCl<sub>3</sub>, δ): 1.25-1.4 (br, 14H), 1.58 (t, J = 6, 2H), 2.06 (m, 2H), 3.39 (s, 3H), 3.46 (t, J = 6, 2H), 3.55-3.68 (m, 10H), 4.97 (m, 2H), 5.82 (m, 1H). **<sup>13</sup>C-NMR** (300 MHz, CDCl<sub>3</sub>): δ 26.08, 28.92, 29.11, 29.42, 29.46, 29.53, 29.63, 33.80, 59.03, 70.05, 70.53, 70.60, 70.64, 71.53, 70.95, 114.09, 139.22.

*EO<sub>6</sub>: Hexaethylene glycol methyl ω-undecenyl ether (8)*. The synthesis was carried out as for **7**. After evaporation of the solvents, **8** was obtained as pale yellow oil. After purification on column chromatography (eluent: ethyl acetate), 4.52 g (65%) of colorless oil was obtained. **<sup>1</sup>H-NMR** (300 MHz, CDCl<sub>3</sub>, δ): 1.3-1.45 (m, 14H), 1.58 (t, J = 6, 2H), 2.05 (m, 2H), 3.39 (s, 3H), 3.46 (t, J = 6, 2H), 3.55-3.75 (m, 22H), 4.95 (m, 2H), 5.82 (m, 1H). **<sup>13</sup>C-NMR** (300 MHz, CDCl<sub>3</sub>): δ 26.08, 28.92, 29.12, 29.43, 29.46, 29.53, 29.63, 33.80, 59.03, 70.06, 70.53, 70.59, 71.54, 71.95, 114.09, 139.23.

## Appendix 2

### Reflectometry

#### Calculation of the adsorbed amounts

The adsorbed amounts were calculated from Equation 1, where  $\Gamma$  = adsorbed amount ( $\text{mg.m}^{-2}$ ),  $Q_f$  = sensitivity factor ( $\text{mg.m}^{-2}$ ),  $S_0$  (mV) = signal given by the reflectometer before introducing protein solutions, and  $\Delta S$  (mV) = recorded difference in signal before and after introduction of the protein solutions:

$$\Gamma = Q_f \cdot \frac{\Delta S}{S_0} \quad (1)$$

$Q_f$  was determined for each measurement with Prof. Huygens software ([www.dullware.nl](http://www.dullware.nl)).  $Q_f$  depends on the signal change ( $\Delta S$ ) and the system parameters: laser incident angle, thicknesses, real and imaginary refractive indexes of solid substrates and monolayers, refractive index of solutions, and differential refractive index of protein solutions ( $dn/dC$ ) (see values in Table S1). The values of  $0.185 \text{ L.kg}^{-1}$  were chosen for  $dn/dC$  of both proteins; the possible variations encountered in the literature about these values ( $\pm 0.003 \text{ L.kg}^{-1}$ ) didn't have a significant influence on our calculations. The same Prof. Huygens software was used to determine the optimal angle of incidence ( $66^\circ$ ) at the solvent/substrate interface and to minimize the error in the calculation of  $Q_f$  due to the angular position of each sample. The thickness of the adsorbed protein layer was shown to be unimportant for regular adsorption (calculated variation of  $\pm 2\%$  in  $Q_f$  for values of 3 to 10 nm). However, it is difficult to calculate  $Q_f$  accurately for low adsorbed amounts ( $d_3 < 2 \text{ nm}$ ; see discussion of the experimental results).

**Table 1.** Parameter values for the calculation of adsorbed amounts of protein.

Parameter	Value
Si100 real ref. index ( $n_1$ )	3.85
Si100 im. ref. index ( $k_1$ )	0.02
Si <sub>3</sub> N <sub>4</sub> real ref. index ( $n_2$ )	2.15
Si <sub>3</sub> N <sub>4</sub> layer thickness ( $d_2$ )	147 nm
Assumed protein layer thickness ( $d_3$ )	5 nm
Solution ref. index ( $n_4$ )	1.33
BSA diff. ref. index ( $dn_{bsa}/dC$ ) [a]	$0.185 \pm 0.003 \text{ L.kg}^{-1}$
Fibrinogen diff. ref. index ( $dn_{fib}/dC$ ) [a]	$0.185 \pm 0.003 \text{ L.kg}^{-1}$
Laser incident angle on the surface ( $\theta$ )	$66^\circ$
Laser wavelength ( $\lambda$ )	632.8 nm

[a] De Feijter, J. A.; Benjamins, J.; Veer, F. A., *Biopolymers* **1978**, 17, 1759-1772.



## Appendix 3

### Calculation of Van der Waals Interactions of FIB and BSA with Monolayer-Modified Si<sub>x</sub>N<sub>4</sub> Surfaces Based on DLVO Theory

As FIB has a fibrous structure with dimension of 9×9×45 nm<sup>3</sup> and BSA has an elliptical structure with dimension of 4×4×14 nm<sup>3</sup>, a disc-model calculation was chosen to calculate the Van der Waals interaction or Gibbs energy between these proteins and the monolayer-modified surfaces. The Gibbs energy for a two-disc interaction with distance  $h$ :

$$\Delta G_{disp}(h) = -\frac{A}{12\pi h^2}$$

Wherein:  $A$  is the Hamaker constant. Approximate values of Hamaker constants for individual materials and the detailed calculation thereof can be found on pages 316-317 of “Colloids and Interfaces in Life Sciences”, by Willem Norde. In this calculation,  $A$  was chosen to be  $1 \times 10^{-20}$  J.  $h$  is the distance between two disc objects. In case of monolayer-modified surfaces,  $h$  reflects the thickness of the monolayer (approximately 2-3 nm derived from X-ray reflectivity). In this calculation,  $h$  was selected to be ~2.5 nm as the mean monolayer thickness.

Each FIB molecule occupies  $45 \times 9 \times 10^{-18}$  (m<sup>2</sup>/molecule), the number of FIB molecules per squared meter is defined as:  $B = \frac{10^{18}}{45 \times 9}$  (molecules/m<sup>2</sup>)

The Van der Waals interaction between FIB and the modified surface is:

$$\Delta G_{disp}(h) = -\frac{A \times N_A}{12\pi h^2 \times B}$$

In which,  $N_A$  is Avogadro constant ( $\sim 6.0 \times 10^{23}$  molecules per mole)

$$\Delta G_{disp}(h) = -\frac{10^{-20} \times 6.0 \times 10^{23} \times 45 \times 9}{12 \times 3.14 \times (2.5 \times 10^{-9})^2 \times 10^{18}} = -10.3 \text{ (kJ/mol)}$$

The Van der Waals interaction between BSA and the modified surface was calculated following the same procedure. The resultant interaction between BSA and the modified surface is:

$$\Delta G_{disp}(h) = -\frac{10^{-20} \times 6.0 \times 10^{23} \times 14 \times 4}{12 \times 3.14 \times (2.5 \times 10^{-9})^2 \times 10^{18}} = -1.2 \text{ (kJ/mol)}$$

The energy of thermal motion at 25 °C is:  $E = R \times T = 8.13 \times 298 = 2.4$  (kJ/mol)

Wherein:  $R$ : Gas constant (8.13 J K<sup>-1</sup> mol<sup>-1</sup>) and  $T$ : Temperature (K)





## Appendix 4

### 1. Conversion of Epoxy-Coated Surface into Amine-Terminated Surface

The  $C_{1s}$  region of the XPS data measured on amine-terminated surfaces (Figure 1) displays two characteristic peaks corresponding to the carbons of the hydrocarbon chains (C-C at 285.0 eV) and the carbons bound to nitrogen and oxygen (C-O&C-N at 286.3 eV). After fitting the high-resolution spectra, the measured (C-C)/(C-O&C-N) ratios of 2.1 are very close to the theoretical value of 2.0, corresponding to the attachment of 1,2-ethylenediamine onto the epoxide-terminated surface via a single amine moiety. While the bridged conformation, in which both amines of a single 1,2-ethylenediamine molecule are coupled to epoxide moieties, should result in a significantly higher ratio of 2.6. The presence of either bridged conformation (ratio of (C-C)/(C-O&C-N) is 2.6) or unreacted epoxide moiety (ratio of (C-C)/(C-O) is 4.0) will lead to a higher ratio. Assumed that the difference between theoretical and experimental ratio of 0.1 corresponds to the epoxide moieties which did not react with ethylenediamine molecules, the actual conversion of epoxide into amine-terminated surface therefore is 95%.

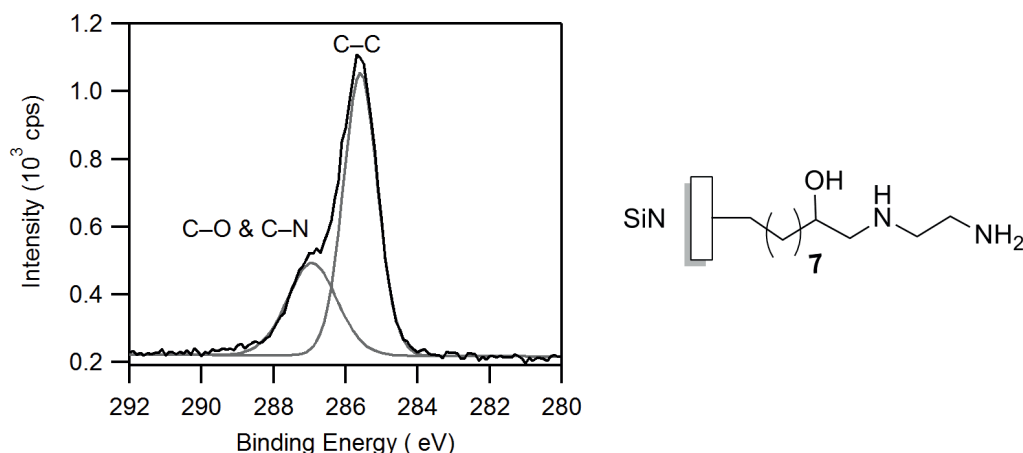


**Figure 1.** Narrow-scan XPS spectrum of  $C_{1s}$  region of amine-terminated surface  $Si_xN_4$ .

### 2. Conversion of Epoxy-Coated Surface into *n*-Propyl Amine-Terminated Surface

A static water contact angle of  $74^\circ$  was observed for the *n*-propyl amine-terminated surface. The narrow-scan XPS of  $C_{1s}$  region measured on amine-terminated surfaces display two characteristic peaks corresponding to carbon of the hydrocarbon chains (C-C at 285.0 eV) and carbons bound to nitrogen and oxygen (C-O&C-N at 286.3 eV) (Figure 2). After fitting the high-resolution spectrum, the measured (C-C)/(C-O&C-N) ratio of 3.4 is very close to the theoretical value of 3.3. The theoretical ratio of 3.3 was

estimated for 100% conversion of the epoxide into *n*-propyl amine-terminated surface. The presence of unreacted epoxide moieties will lead to a higher (C-C)/(C-O&C-N) ratio of 4.0. The difference between theoretical and experimental ratio (0.1), corresponds to 15% of unreacted epoxide moieties. Therefore, the actual conversion of epoxide into *n*-propyl amine groups is 85%.

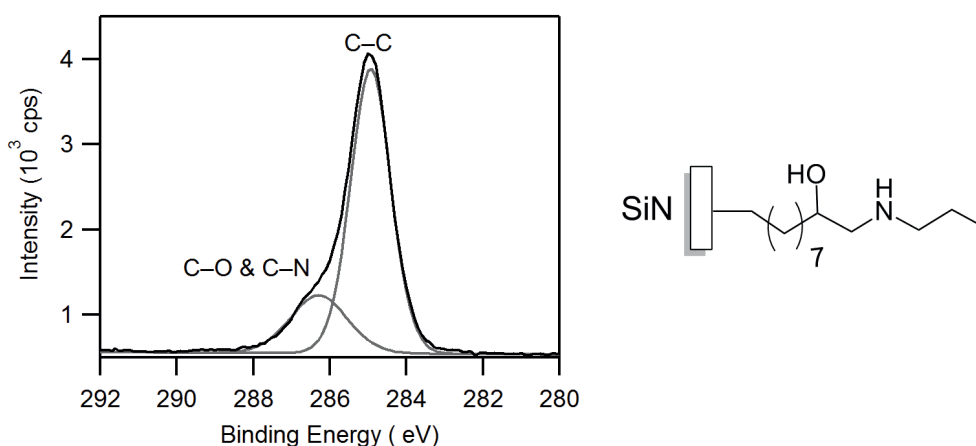


**Figure 2.** Narrow-scan XPS spectrum of  $C_{1s}$  region of *n*-propyl-terminated  $Si_3N_4$  surface.

### 3. Conversion of Br-Initiators Attachment onto *n*-Propyl-Terminated Surface

The narrow-scan XPS spectrum of  $C_{1s}$  region measured on the Br-initiator attached surface indicates from reaction of epoxide-terminated surface and *n*-propylamine (Figure 3) as was divided into three characteristic components. The peak at 285.0 eV corresponds to carbon of the hydrocarbon chains (C-C). The broad peak at 286.5 eV is attributed to overlapping C-N, C-Br. The appearance of the peak at 287.9 eV can be attributed to either epoxide moieties or secondary amide-carbonyl moieties in the resultant monolayer. The peak at 289.5 eV corresponds to the ester-carbonyl moiety (Figure 3). The experimental and theoretical ratios of the analytical peaks obtained by fitting are shown in Table 1.

**Table 1.** Theoretical and experimental ratio of analytical peaks of XPS spectra of Br-initiators attached on  $Si_3N_4$  surface.

Components	Theoretical ratio		Experimental ratio
	Ester*	Amide**	
C-C	12	12	12
C-N&C-Br	3	4	3.4
C-O(C=O) or C=O(N-C)	1	1	0.7
C=O(O-C)	1	0	0.4

\*: 2-bromoisobutyryl bromide attaches only to secondary alcohol

\*\*.: 2-bromoisobutyryl bromide attaches only to secondary amine

The experimental ratio between C-C and C=O(O-C) is 12:0.4 which shows that conversion is less than 100%. Theoretically, the ratio between C-O(C=O) and C=O(O-C) should be 1:1, however the fitting of the experimental data shows a ratio of 0.7:0.4. This indicates the formation of both ester and amide groups in the monolayer. Calculation of the exact conversion is difficult in this case because the reaction results in a mixture of ester and secondary amide moieties. It is assumed that 2-bromoisobutyryl bromide attaches to either the secondary alcohol or the secondary amine in a molecular chain. The experimental data shows approximately 40% conversion of secondary alcohol into ester moieties and 30% conversion of secondary amine into secondary amide. The attachment of more than a single 2-bromoisobutyryl bromide molecule in the same chain is unlikely to occur due to steric hindrance.

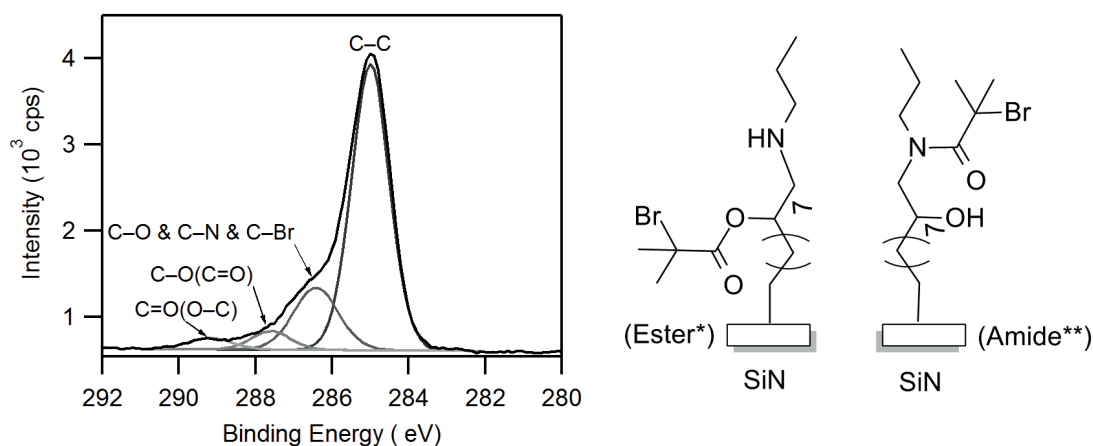


**Figure 3.** Narrow-scan XPS spectrum of C<sub>1s</sub> region of Br-initiators terminated Si<sub>x</sub>N<sub>4</sub> surface via propylamine reaction

#### 4. Conversion of Br-Initiators Attachment onto Amine-Terminated Surface

The C<sub>1s</sub> regions of the XPS data measured on Br-initiator attached surfaces that stemmed from reaction of epoxide-terminated surface with ethylenediamine (Figure 4) was divided into three main components. The peak at 285.0 eV corresponds to carbon of the hydrocarbon chains (C-C). The broad peak at 286.5 eV is attributed to overlapping C-N, C-Br and C-O(C=O). The appearance of a peak at 288.3 eV can be attributed to primary and secondary amide-carbonyl moieties. The peak at 289.5 eV corresponds to the ester-carbonyl moiety. The experimental and theoretical ratios of the analytical peaks obtained by fitting are shown in Table 2. Calculation of the conversion is difficult because the reaction results in a complex mixture of ester, primary amide and secondary amide moieties. It is assumed that 2-bromoisobutyryl bromide attaches to only the secondary alcohol, the secondary amine or primary amine in a single chain. The secondary amine is unlikely to react with 2-bromoisobutyryl bromide more than once due to steric hindrance.

However, the actual participation and conversion of secondary amines into amides based on XPS spectra is unlikely but cannot be exclusive due to similarity of primary and second amides in term of binding energy. The experimental data shows roughly 30% conversion of secondary alcohol into ester moieties and 70% conversion of primary or secondary amine into amide.

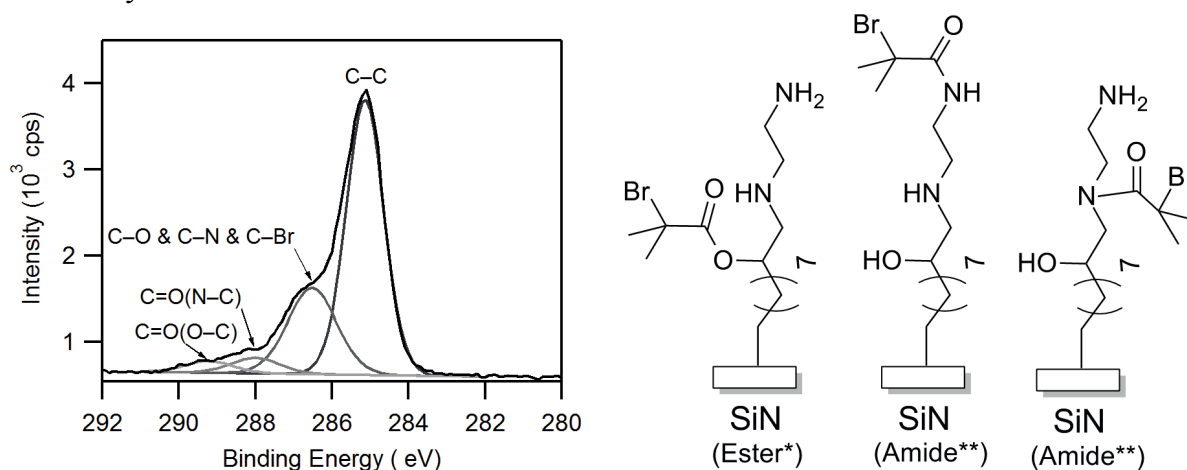


**Figure 4.** Narrow-scan XPS spectrum of C<sub>1s</sub> region of Br-initiators terminated Si<sub>x</sub>N<sub>4</sub> surface via ethylenediamine reaction.

**Table 2.** Theoretical and experimental ratio of analytical peaks of XPS spectra of Br-initiators attached on Si<sub>x</sub>N<sub>4</sub> surface via propylamine reaction.

Components	Theoretical ratio		Experimental ratio
	Ester*	Amide**	
C-C	10	10	10
C-N&C-Br & C-O(C=O)	5	5	4.5
C=O(N-C)	0	1	0.7
C=O(O-C)	1	0	0.3

\*: 2-bromoisobutyl bromide attaches only to secondary alcohol

\*\*: 2-bromoisobutyl bromide attaches only to either primary or secondary amine

## Appendix 5

### AFM Images

Top-view and cross-section AFM images of the polySBMA films after reaction with trifunctional tris(2-aminoethyl)amine linkers and bifunctional suberic acid bis(*N*-hydroxysuccinimide ester), respectively.

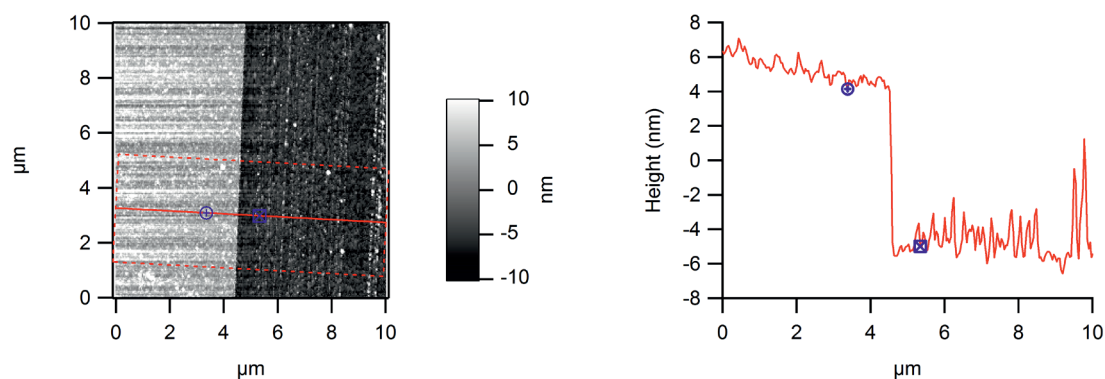


**Figure 1.** Top-view (left) and cross-section (right) AFM images of polySBMA.

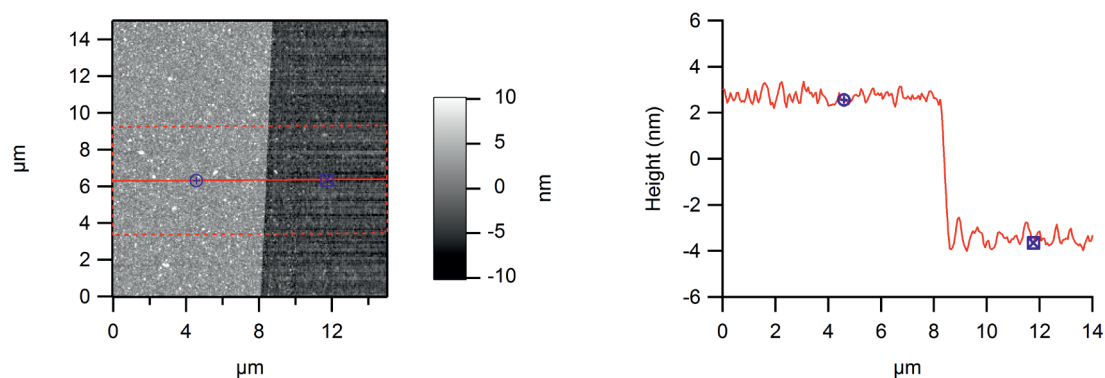


**Figure 2.** Top-view (left) and cross-section (right) AFM images of  $\text{NH}_2$ -polySBMA.

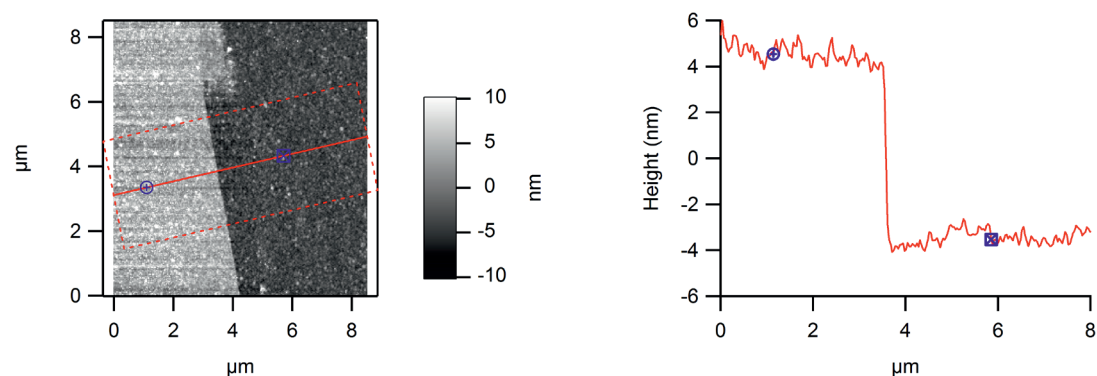


**Figure 3.** Top-view (left) and cross-section (right) AFM images of NHS-polySBMA.



## Summary

Microsieves – microengineered membranes – have been introduced in microfiltration technology as a new generation of inorganic membranes. The thin membranes are made of silicon nitride ( $\text{Si}_x\text{N}_4$ ), which gives the membranes outstanding features, such as chemical inertness and high mechanical strength. Microsieves have very well-defined pore size and pore shape, with an extremely homogeneous size distribution and high porosity. As a result, high-flux performance and excellent selectivity may be achieved. However, biofouling issues exert limitations on the application of microsieves in filtration and diagnostics. Surface functionalization was found to be a feasible way to minimize biofouling, but also to achieve biorecognition in microbiological applications. The aim of this thesis is to improve microsieve performance in biological applications by means of surface functionalization with organic coatings for protein repellence and selective capture of microorganisms.

In this thesis,  $\text{Si}_x\text{N}_4$  surfaces were functionalized with organic monolayers via stable Si-C and N-C linkages. Coatings to render  $\text{Si}_x\text{N}_4$  surfaces protein repellent were studied in depth by two approaches: grafting of ethylene oxide monolayers onto the surface (*Chapter 2*); and grafting of zwitterionic polymers from the surface (*Chapter 3*). UV-induced surface modification with oligo(ethylene oxide) chains with three ( $\text{EO}_3$ ) and six ( $\text{EO}_6$ ) units and the detailed characterization of these modified surfaces are described in *Chapter 2*. Successful attachment of  $\text{EO}_3$  and  $\text{EO}_6$  on  $\text{Si}_x\text{N}_4$  surfaces was achieved. The modified surfaces exhibit excellent protein repellence in bovine serum albumin (BSA) solution ( $\sim 94\%$ ), but only moderate ( $\sim 80\%$ ) protein repulsion was observed in fibrinogen (FIB) solution. This observation motivated the study towards grafting zwitterionic polymer brushes from  $\text{Si}_x\text{N}_4$  surfaces for improved protein repellence. A new method to grow zwitterionic polymers from monolayers containing tertiary bromides, via atom transfer radical polymerization (ATRP) was developed. The zwitterionic polymer coated surfaces showed excellent protein repellence in FIB solution ( $> 99\%$ ), while exhibiting very stable performance in PBS during one week, i.e., unchanged thickness, no hydrolysis of the polymers occurred and protein repellence in FIB solution remained constant.

The use of microsieves as detection platform for microorganisms was explored in *Chapter 4*. Microorganisms can be caught by microsieves whose pore sizes are smaller than the microorganisms while allowing an easy flow-through of other components. However, detection capacity of microsieves is severely hampered by fouling issues. To avoid this problem, the use of microsieves with pore sizes larger than the microorganisms, in combination with immobilized antibodies was investigated in *Chapter 4*.



Anti-*Salmonella* antibodies were immobilized onto epoxide monolayers on microsieive surfaces by reaction with the primary amines present in the antibody. The antibody-coated microsieves showed excellent detection of *Salmonella* with high sensitivity and selectivity, significantly improving detection efficiency in crude biological samples, and reducing analysis times.

The capture efficiency of *Salmonella* in milk samples was, however, found to be lower than that achieved in buffered solution. Most likely, this is due to nonspecific adsorption of milk proteins on the antibody-coated microsieves. In addition, the use of a blocking solution before incubation with microorganism solution remained an essential step in order to avoid the occurrence of interfering background fluorescence. In order to minimize these problems, the incorporation of antibodies on top of protein-repellent zwitterionic polymers coated on  $\text{Si}_x\text{N}_4$  surfaces was studied in *Chapter 5*. Anti-*Salmonella* antibodies were immobilized on zwitterionic polymer brushes coated  $\text{Si}_x\text{N}_4$  surfaces through the bromide moieties retained at the end of the polymer chain after ATRP. Antibody-functionalized zwitterionic polymers adsorbed only minimal amounts of FIB, indicating excellent protein repellence of the modified surfaces. Moreover, anti-*Salmonella* antibodies immobilized onto zwitterionic surfaces exhibit highly selective capture and improved sensitivity, as compared to antibodies on epoxide coated surfaces. This achievement offers a new approach that enables highly sensitive and selective detection of microorganism, while minimizing nonspecific adsorption of proteins that are not of interest.

In *Chapter 6*, an overview is given of the most important findings presented in the thesis. Recommendations, as well as additional ideas on how to bring this research into industrial application are discussed.

## Samenvatting

Microzeven – microgefabriceerde membranen – zijn geïntroduceerd in de microfiltratie-technologie als een nieuwe generatie anorganische precisie membranen. De dunne membranen zijn gemaakt van silicium nitride ( $\text{Si}_x\text{N}_4$ ), wat de membranen buitengewone eigenschappen geeft, zoals chemische resistentie en mechanische sterkte. Microzeven hebben poriën met een zeer goed gedefinieerde grootte en vorm, een extreem homogene poriegrootte verdeling en een hoge porositeit. Dit maakt filtratie met een hoge flux en excellente scheiding op deeltjesgrootte mogelijk. Echter, biofouling zorgt voor een beperking van de toepasbaarheid van microzeven voor filtratie en diagnostiek. Oppervlaktemodificatie is een bekende methode om biofouling te minimaliseren, maar ook om biologische herkenning te bewerkstelligen in microbiologische applicaties.

Het doel van dit proefschrift is het verbeteren van de prestaties van microzeven in biologische toepassingen door middel van oppervlaktemodificatie met organische coatings voor eiwitafstoting en selectieve invang van micro-organismen.

In dit proefschrift zijn  $\text{Si}_x\text{N}_4$  oppervlakken gefunctionaliseerd met organische monolagen via stabiele Si-C en N-C koppelingen. Eiwitafstotende coatings op  $\text{Si}_x\text{N}_4$  zijn in detail bestudeerd door middel van twee verschillende technieken: 1) aanbrengen van ethyleenoxide monolagen op het oppervlak (*Hoofdstuk 2*) en 2) groeien van zwitterionische polymeren vanaf het oppervlak (*Hoofdstuk 3*). UV geïnduceerde oppervlaktemodificatie met oligo(ethyleenoxide) ketens, met drie ( $\text{EO}_3$ ) en zes ( $\text{EO}_6$ ) eenheden, en de gedetailleerde karakterisatie van deze gemodificeerde oppervlakken zijn beschreven in *Hoofdstuk 2*. De aanhechting van  $\text{EO}_3$  en  $\text{EO}_6$  op  $\text{Si}_x\text{N}_4$  oppervlakken is met succes gedaan. De gemodificeerde oppervlakken vertonen excellente eiwitafstoting in bovien serum albumine (BSA) oplossing (~ 94%), maar slechts matige eiwitafstoting (~ 80%) werd waargenomen in fibrinogeen (FIB) oplossing. Deze observatie was de motivatie voor het bestuderen van het groeien van zwitterionische polymere borstels van  $\text{Si}_x\text{N}_4$  oppervlakken voor verbeterde eiwitafstoting. Een nieuwe methode is ontwikkeld voor het groeien van zwitterionische polymeren vanaf monolagen die tertiäre bromides bevatten, via atoomtransfer radicaalpolymerisatie (ATRP). De met zwitterionische polymeren gecoate oppervlakken vertonen excellente eiwitafstoting in FIB oplossing (> 99%), en geven tegelijkertijd erg stabiele prestaties in PBS buffer gedurende een week, dat wil zeggen: onveranderde dikte, geen hydrolyse van de polymeren en lage eiwitadsorptie in FIB oplossing.

Het gebruik van microzeven als detectieplatform voor micro-organismen is beschreven in *Hoofdstuk 4*. Micro-organismen kunnen worden ingevangen met microzeven waarvan

de poriën kleiner zijn dan de micro-organismen, terwijl doorstroming van andere componenten eenvoudig is. Echter, de detectiecapaciteit wordt sterk gereduceerd door fouling problemen. Om deze problemen te voorkomen zijn microzeven onderzocht met poriën groter dan micro-organismen in combinatie met immobilisatie van antilichamen om deze in te vangen (*Hoofdstuk 4*). Anti-*Salmonella* antilichamen zijn geïmmobiliseerd via epoxide monolagen op microzeefoppervlakken door middel van reactie met de primaire amines aanwezig in de antilichamen. De met antilichamen gecoate microzeven vertoonden excellente detectie van *Salmonella* met hoge gevoeligheid en selectiviteit, dit is een aanzienlijke verbetering voor de detectie-efficiëntie in ruwe biologische monsters en verkort de analyse tijd sterk.

De detectie-efficiëntie van *Salmonella* in melk monsters bleek echter lager dan die gevonden in gebufferde oplossingen. Waarschijnlijk komt dit door niet-specifieke binding van melkeiwitten op de met antilichamen gecoate microzeven. Daarnaast was het gebruik van een blokkeeroplossing voor incubatie met micro-organisme oplossing een essentiële stap voor het vermijden van interfererende achtergrond fluorescentie. Om deze problemen te minimaliseren is het aanbrengen van antilichamen bovenop eiwitafstotende zwitterionische polymeren gecoat op  $\text{Si}_x\text{N}_4$  oppervlakken bestudeerd in *Hoofdstuk 5*. Anti-*Salmonella* antilichamen werden geïmmobiliseerd op met zwitterionische polymere borstels gecoate  $\text{Si}_x\text{N}_4$  oppervlakken via de overgebleven bromide atomen aan het uiteinde van de polymeerketen na ATRP. Met antilichaam gefunctionaliseerde zwitterionische polymeren adsorbeerden slechts minimale hoeveelheden FIB, wat de excellente eiwitafstoting van de gemodificeerde oppervlakken aangeeft. Anti-*Salmonella* antilichamen geïmmobiliseerd op zwitterionische oppervlakken vertonen bovendien uitermate goede selectieve invanging en een verbeterde selectiviteit in vergelijking met antilichamen aangebracht op epoxide gecoate oppervlakken. Deze resultaten bieden perspectief op een nieuwe methode die uitermate gevoelige en selectieve detectie van micro-organismen mogelijk maakt, terwijl niet-specifieke adsorptie van ongewenste eiwitten wordt geminimaliseerd.

In *Hoofdstuk 6* wordt een overzicht gegeven van de meest belangwekkende vindingen gepresenteerd in dit proefschrift. Zowel aanbevelingen als aanvullende ideeën over mogelijke industriële toepassing van dit onderzoek worden besproken.

## Tóm tắt

Màng vi lọc (microsieve), chế tạo bằng công nghệ vi cơ điện tử, đã và đang được sử dụng trong công nghệ vi lọc như một thể hệ mới của màng vi lọc vô cơ. Các màng lọc microsieve được chế tạo từ vật liệu bán dẫn silicon nitride ( $\text{Si}_x\text{N}_4$ ), với các tính chất ưu việt như trơ hóa học và độ bền cơ học cao. Độ dày của màng lọc siêu mỏng (150 nm), các lỗ lọc có kích thước và hình dạng đồng nhất, được phân bố đồng đều với độ xốp cao. Do đó, màng lọc có khả năng đạt được hiệu suất và độ chọn lọc cao. Hiện nay, màng vi lọc microsieve được ứng dụng rộng rãi trong các lĩnh vực vi lọc sinh học và chẩn đoán sinh học. Tuy nhiên, vấn đề tắc nghẽn màng lọc do sự tích tụ của các phân tử sinh học như protein, chất béo và vi khuẩn trong quá trình lọc đã ảnh hưởng nghiêm trọng đến các ứng dụng của màng vi lọc, như gây gián đoạn hệ thống và hạn chế quá trình phân tích mẫu sinh học. Một trong những giải pháp được đánh giá có tính khả thi cao nhất hiện nay là ứng dụng công nghệ xử lý hóa bề mặt trên màng lọc nhằm tối thiểu hóa sự tích tụ của các phân tử sinh học và tăng cường tính năng chọn lọc sinh học của bề mặt. Mục tiêu của luận văn này là nghiên cứu các phương pháp xử lý bề mặt vi lọc microsieve theo phương thức phủ hữu cơ để nâng cao khả năng chống hấp thụ protein và khả năng phát hiện vi khuẩn một cách chọn lọc của màng vi lọc microsieve trong các ứng dụng sinh học.

Luận văn tập trung nghiên cứu các lớp phủ hữu cơ được gắn trên bề mặt  $\text{Si}_x\text{N}_4$  thông qua các liên kết cộng hóa trị Si-C và N-C bằng phản ứng quang học. Các lớp phủ hữu cơ có tính năng chống hấp phụ protein được chế tạo theo hai hướng: gắn những phân tử ethylene oxide, bao gồm ba ( $\text{EO}_3$ ) và sáu ( $\text{EO}_6$ ) đơn vị ethylene oxide, lên bề mặt dưới dạng đơn phân tử (*Chương 2*) và phát triển những phân tử cao phân tử (polymer) có chứa điện tích dương và điện tích âm (zwitterion) từ bề mặt  $\text{Si}_x\text{N}_4$  (*Chương 3*). Kết quả thu được ở *Chương 2* cho thấy chiều dài của những phân tử ethylene oxide ảnh hưởng lớn đến khả năng đẩy lùi protein của bề mặt: các phân tử ethylene oxide càng dài, khả năng đẩy lùi protein càng cao. Cụ thể là, các bề mặt được gắn lớp đơn phân tử  $\text{EO}_6$  đẩy lùi protein tốt hơn các bề mặt được gắn các phân tử  $\text{EO}_3$ . Các bề mặt được gắn lớp đơn phân tử  $\text{EO}_6$  có khả năng đẩy lùi khoảng 94% albumin huyết thanh bò (BSA) và khoảng 80% dung dịch tơ huyết (Fibrinogen). *Chương 3* nghiên cứu về sự phát triển các phân tử zwitterion từ bề mặt  $\text{Si}_x\text{N}_4$  bằng phương pháp polymer hóa nguyên tử gốc tự do - atom transfer radical polymerization (ATRP). Bề mặt được phủ polymer zwitterion thể hiện khả năng chống protein cực tốt trong dung dịch Fibrinogen, đẩy lùi hơn 99% protein so với các bề mặt kỵ nước. Ngoài ra, các lớp phủ zwitterion còn thể hiện tính năng bền hóa học trong dung dịch đệm photphat (PBS). Cụ thể hơn, độ dày của lớp phủ không thay đổi, không xảy ra hiện

tượng thủy phân của các polymer và tính năng chống protein của bề mặt không suy giảm sau một tuần ngâm trong dung dịch PBS ở nhiệt độ phòng.

Ngoài khả năng tách lọc các phân tử sinh học, màng vi lọc microsieve còn được sử dụng như một công cụ xét nghiệm vi khuẩn. Về nguyên tắc, các màng lọc có kích thước lỗ lọc nhỏ hơn kích thước của vi khuẩn có thể được sử dụng để phát hiện các vi khuẩn trong dung dịch sinh học, trong khi cho phép lọc bỏ các thành phần khác của dung dịch một cách dễ dàng. Tuy nhiên, màng vi lọc bị tắc nghẽn khá nhanh do sự tích tụ của các phân tử sinh học có kích thước lớn hơn kích thước lỗ lọc. Hiện tượng này có thể dẫn đến sai lệch trong kết quả xét nghiệm. Do đó, trong *Chương 4*, các màng vi lọc với kích thước các lỗ lọc hơi lớn hơn kích thước của vi khuẩn tích hợp với lớp phủ kháng thể trên bề mặt màng lọc được nghiên cứu để giải quyết vấn đề tắc nghẽn trong quá trình xét nghiệm. Vi khuẩn *Salmonella* được sử dụng để đánh giá và tối ưu hóa hệ thống. Kháng thể chống vi khuẩn *Salmonella* được gắn trực tiếp lên bề mặt màng lọc nhờ lớp phủ đơn phân tử epoxide thông qua phản ứng hóa học giữa các nhóm amin bậc 1 xung quanh kháng thể và nhóm epoxide trên bề mặt. Màng lọc được gắn các kháng thể chống *Salmonella* có khả năng phát hiện vi khuẩn *Salmonella* với độ nhạy và độ chọn lọc cao, tăng cường hiệu quả xét nghiệm vi khuẩn trong dung dịch sinh học. Đồng thời, màng lọc tạo điều kiện dễ dàng cho các thành phần khác trong dung dịch sinh học đi qua, góp phần nâng cao tính chọn lọc của hệ thống và giảm thiểu thời gian phân tích mẫu so với các phương pháp xét nghiệm thông dụng khác như phương pháp xét nghiệm vi khuẩn trong môi trường thạch trắng (agar).

Tuy nhiên, hiệu quả xét nghiệm *Salmonella* trong dung dịch sữa thấp hơn so với trong dung dịch đệm. Hiện tượng này rất có khả năng là do sự hấp phụ của các phân tử protein trong dung dịch sữa lên các kháng thể gắn trên bề mặt màng vi lọc, làm che khuất các nhóm nhận biết của kháng thể với vi khuẩn *Salmonella*. Thêm vào đó, việc sử dụng dung dịch đầy cho bề mặt trước khi xét nghiệm là một bước không thể thiếu để tối thiểu hóa hiện tượng nhiễu huỳnh quang. Do đó, trong *Chương 5*, phương pháp gắn các kháng thể chống vi khuẩn *Salmonella* lên lớp phủ polymer zwitterion chống hấp phụ protein trên màng vi lọc được nghiên cứu. Thử nghiệm cho thấy, hệ thống lớp phủ này có khả năng phát hiện vi khuẩn *Salmonella* với độ nhạy cao, ngang bằng với lớp phủ kháng thể được gắn trực tiếp lên màng lọc. Đồng thời, hệ thống lớp phủ còn có khả năng chống hấp phụ protein trong các mẫu sinh học thô, hứa hẹn một công cụ xét nghiệm nhanh chóng và hiệu quả trong tương lai gần.

*Chương 6* trình bày tổng quan về các kết quả quan trọng đạt được trong luận văn. Kiến nghị cũng như các ý tưởng, đặt đề tài nghiên cứu này trong bối cảnh ứng dụng thực tế được thảo luận.

## Curriculum Vitae



Ai Thuy Nguyen was born on January 11<sup>th</sup> 1980 in Ho Chi Minh City, Vietnam. She obtained her bachelor degree in Electrochemistry in 2003 and master degree in Material Science and Technology in 2005 at Ho Chi Minh City University of Technology in Vietnam.

After a internship at University of California Santa Barbara in USA about nanoporous alumina templates, she started her PhD in Wageningen University in the Laboratory of Organic Chemistry under supervision of Prof. Cees van Rijn and Prof. Han Zuilhof. The most important results of her PhD research are described in this thesis. Currently she is working for Aquamarijn Company in The Netherlands as researcher on surface modification.





## List of Publications

Nguyen, A. T.; Baggerman, J.; Paulusse, J. M. J.; Van Rijn, C. J. M.; Zuilhof, H., Stable Protein-Repellent Zwitterionic Polymer Brushes Grafted from Silicon Nitride. *Langmuir* **2011**, 27, 2587-2594.

Rosso, M.; Nguyen, A. T.; de Jong, E.; Baggerman, J.; Paulusse, J. M. J.; Giesbers, M.; Fokkink, R. G.; Norde, W.; Schroën, K.; Van Rijn, C. J. M.; Zuilhof, H., Protein-Repellent Silicon Nitride Surfaces: UV-Induced Formation of Oligoethylene Oxide Monolayers. *ACS Appl. Mater. Interfaces* **2011**, 3, 697-704.

Nguyen, A. T.; Baggerman, J.; Paulusse, J. M. J.; Zuilhof, H.; Van Rijn, C. J. M., Bioconjugation of Protein-Repellent Zwitterionic Polymer Brushes Grafted from Silicon Nitride Surface. (*submitted*) **2011**.

Nguyen, A. T.; Doorn, R. v.; Baggerman, J.; Paulusse, J.; Zuilhof, H.; Klerks, M.; Van Rijn, C. J. M., Rapid Microsieve-Based Microbial Diagnostics. (*in preparation*) **2011**.



## Overview of Completed Training Activities

Graduate School VLAG	Year
<b>Discipline specific activities</b>	
<i>Courses</i>	
Analytical methods in Organic Chemistry	2009
Advanced organic chemistry	2009-2010
C.S. Membrane Technology	2010
<i>Meetings</i>	
First International Workshop on Nanotechnology and Applications, Vietnam	2007
Euromembrane conference, Montpellier, France	2009
ESAO, winter school, Semmering, Austria	2011
Annual NWO Conference, Lunteren, The Netherlands	2007-2011
Annual MicroNed-MinacNed conference, The Netherlands	2007-2011
Wageningen Symposium of Organic Chemistry, WUR	2010-2011
<b>General courses</b>	
Academic Writing, Centa, Wageningen	2010
Techniques for writing and presenting scientific papers, Wageningen	2009
Organizing and supervising MSc thesis project, Wageningen	2010
System membrane-complex roadmaps toward functional devices, France	2009
PhD week, organized by VLAG school	2007
<b>Optionals</b>	
Group meetings (Laboratory of Organic Chemistry), Wageningen	2007-2011
Colloquia (Laboratory of Organic Chemistry), Wageningen	2007-2011
PhD study trip, organized by Laboratory of Organic Chemistry, China	2009
Preparing PhD research proposal	2007



## Acknowledgement

The road to success is never smooth, this does not exclude my four-year journey to a PhD. For me, The Netherlands was just like another planet compared to my home town. Studying in this country on a topic which I did not have much background, was not an easy job, yet it has been an incredible journey. During these four years, I have received a lot of help, support and encouragement from friends, colleagues and my family. Without them this thesis could not have been done.

First of all, I like to thank Prof. Cees van Rijn for the opportunity to do research in The Netherlands. It was a great start for my scientific adventure. Cees, you are not always the best finisher, but you have been a great initiator with all extraordinary ideas for my research. You did not always give me answers to my questions but many times you raised the right questions, which lead me to fantastic answers. Cees, thanks for all thoughtful and great support during the past four years.

I particularly thank Prof. Han Zuilhof for all the inspiration and guidance in surface chemistry. Han, thank you for all the time you spent reading and correcting my texts. Special appreciation for many working hours, no matter how late in the evening or at weekend, for correcting my thesis. You were a great support for my research. You definitely knew when to put me in the spot light and when to keep me behind. Step by step you knew how to train me to become an independent researcher. You motivated me to achieve great things in research. From you I did not only learn how to do research, but also how to keep things simple and explicit to go through them.

My special thanks to Dr. Jos Paulusse for his great assistance in my project and for being such a stimulating supervisor. Jos, without you I do not think that I would have had enough motivation to finish the EO<sub>6</sub> paper. You brought inspiration and vitality into my research. And big thanks for giving me deadlines for almost everything ☺. Frankly, I felt stressed with deadlines in the beginning but eventually it turned out to be the enjoyable “set-and-run” things. This greatly helped me to get a lot of work done in a short time.

I am grateful to Prof. Willem Norde for helpful discussions about protein adsorption. Willem, you are kind and respectful. You amazed me with your vast knowledge about proteins and you gave me the feeling that you even could communicate with them. I liked it very much whenever you told me about your “art meets science” life. In you, I found the true nature of a scholar.

I would like to thank Prof. Lina Sarro for the useful project meetings in the early stage of my project. Thanks for your kindness and welcome collaboration. I hope that we can have a further collaboration in research in the near future.

I would like to thank Dr. Đặng Mậu Chiến for giving me kind supports to study abroad. This greatly helped me to go further in my scientific career. My special thanks to all the friends and colleagues at the Material Science and Technology department of the University of Technology in Ho Chi Minh City for all the support and friendship.

For the technical assistance, I would like to thank Marcel Giesbers, Barend van Lagen, Remco Fokkink, Jasper van der Gucht, and Hans de Jong. Thanks to all of you for making it possible for me to use and learn a lot about many different techniques. I would like to thank Michel Rosso for his kind assistance for the first lesson on UV-induced surface modification. My big thank to Willem-Jan and staff members at Laboratory of Aero & Hydrodynamics of TU Delft for their kind assistance and support during the time I was working on the topic of ultrasound.

I would like to thank Ronald van Doorn and Michel Klerks at Innosieve company for the exciting collaboration on diagnostic devices. Thanks for all the microbiological input in my thesis and for all interesting discussions. Ronald, you amazed me with your interest in beer. I feel like for you, drinking beer is not just entertainment but also a science. Sorry that it took so long to arrange a “biertje” with you. But for sure, we will do it very soon.

My very special thanks to Dr. Tổng Duy Hiền for all beautiful  $\text{Si}_x\text{N}_4$  wafers. Anh Hiền, thanks for picking me up at Schiphol when I arrived in the Netherlands for the first time. Without you guiding me on that day, perhaps it would have taken me another day to get to Wageningen ☺.

I would like to thank all colleagues in Organic Chemistry laboratory. Special thanks to Ton, Maurice and Carel for all the organic chemistry lessons during the courses and for additional answers to my questions during the project. A big thank to Teris for welcome trips around The Netherlands when I arrived. Special thanks to Mabel and Hamilton for useful discussion about ATRP polymerization and surface chemistry. Thanks to Jaime, Willem, and Tom for spending time reading and checking my thesis. Special thanks to Willem for being such a good friend during past four years. Thanks to Ronald for all daily doses of humor and of course for sending all the orders ☺.

To all PhD-student friends, thanks to all you guys for sharing and helping me during my PhD. Thanks for all the good fun we had together during and after working hours. It gave me such a huge amount of energy to keep on working. I loved playing volleyball with you guys in the backyard very much. It was the most awesome game I ever had.

A big hug to Jacinthe for lending me  $\text{EO}_6$  compound many times. Later, it turned out to be a small business between us. You were selling the  $\text{EO}_6$  for some Vietnamese dinner ☺. Thanks for being such a big fan of my cooking. Many many thanks to Rokus for all the laughter we had together. It was amazing how our perspectives in life have many things in

common. I enjoyed very much sharing with you all the thoughts. I very much appreciated your friendship. A warm thank to Alexandre and Dani for their friendship and for all the interesting discussions about nature.

A lot of hugs to my Vietnamese friends in Wageningen, especially to Dr. Lê Thanh Phong, family of chú Thanh & cô Thủy and family of anh Kê & chị Quyên. Thanks for all the help and fun together. Thanks for all friendship and delicious Vietnamese food.

To Tin, thanks for all thoughtful care, for fixing my bike many times and for all the cookies you left on my desk when you knew that I was going to work late on that day. Tin, thank you very much for being such a great friend. I truly wish you a bright future!

To Jacob, thanks for the fact that we found each other to do not only inspiring research at work, but also exciting things in life. Your great competence in literature study was a perfect supplementation to my “crazy” creativity in practical work, which made us an awesome team. Thanks for being such a patient tutor, explaining for me all little details about basic organic chemistry. Your love, friendship and your kind, gentle spirit made my stay in this country warmer. Thanks for being by my side for whatever I do. People say: “Each life has its own journey”, I hope our journeys will meet each other in the end.

Special thanks to Tike for designing the super awesome cover and for staying up many nights to work on my thesis design. Thanks for taking special care for mom and dad when I am away, even though you are extremely busy at work. I’m proud to call you my brother.

Being away from home, up to now, has been more than 6 years, travelling to many places, meeting many people, nevertheless perhaps the warmest and happiest place in the world is still my family. Great thanks to my parents and other members in the family (grandma, aunt 2, aunt 4, aunt 5, and brother) for giving me such a great family where I began and where I always have been meant for.

Wageningen, August 2011



Nguyễn Thúy Ái



The research described in this thesis was financially supported by MicroNed, funded by the Dutch Ministry of Economic Affairs (Project no. 6163510587).

Design & Layout: Nguyễn An Hòa, Jacob Baggerman  
Printed by: De Budelse BV, Budel, The Netherlands

